Durham University

Durham E-Theses

An Investigation into Ruthenium-based Carbene- and Sandwich Complexes as Potential Histone Deacetylase Inhibitors

CHRISTOPHER SAMUEL JENNINGS

How to cite:

JENNINGS, CHRISTOPHER SAMUEL (2016) An Investigation into Ruthenium-based Carbene- and Sandwich Complexes as Potential Histone Deacetylase Inhibitors. Masters thesis, Durham University.

Use policy

The full-text may be used and/or reproduced, and given to third parties in any format or medium, without prior permission or charge, for personal research or study, educational, or not-for-profit purposes provided that:

- a full bibliographic reference is made to the original source
- a https://etheses.durham.ac.uk/id/eprint/11846/ is made to the metadata record in Durham E-Theses
- the full-text is not changed in any way

The full-text must not be sold in any format or medium without the formal permission of the copyright holders.

Please consult the full Durham E-Theses policy for further details.

Academic Support Office, The Palatine Centre, Durham University, Stockton Road, Durham, DH1 3LE
e-mail: e-theses.admin@durham.ac.uk Tel: +44 0191 334 6107
https://etheses.durham.ac.uk

Durham University
Department of Chemistry

An Investigation into Ruthenium-based Carbene- and Sandwich Complexes as Potential Histone Deacetylase Inhibitors

MSc in Research Project Report

Christopher S. Jennings

Supervisor – Dr. James W. Walton

October 2016

Abstract

A novel, ruthenium(II)-based, *p*-cymene-capped sandwich complex with a hydroxamic acid functionality, designed as an organometallic variation of known effective HDAC inhibitors, was synthesised. Additionally, the pharmacological activity of this complex was assessed in both an MTT assay with the H460 non-small cell lung carcinoma cell line and a fluorometric HDAC assay, which yielded IC_{50} values of 7.4 ± 4.8 μM and between 0.1 and 1 μM respectively. These results provide the groundwork for extensive exploration into the optimisation and development of a novel class of anticancer agents. The synthesis of the benzene-capped analogue of this complex was attempted, but not achieved. However, insights are provided into why the synthesis was unsuccessful, thereby providing a basis for its synthesis in future work.

Furthermore, several synthetic routes towards a novel, *N*-heterocyclic carbene-containing ruthenium(II) piano stool complex - also a candidate HDAC inhibiting anticancer agent - were attempted. Though the complex was not successfully isolated through any of the explored routes, a thorough investigation into carbene chemistry in both organometallic and purely organic contexts has been undertaken. This work not only contributes to a general understanding of an emerging branch of synthetic chemistry, but also establishes a basis from which the synthesis of such candidates can be more readily realised.

Acknowledgements

First and foremost, I'd like to express my gratitude to my parents and grandparents, for following me keenly with love and support along my academic journey in its entirety. It has been, and continues to be, a privilege to be their boy.

My gratitude is extended to my supervisor Dr. James Walton, for not only his guidance and helpful discourse at every stage of the project, but also for tolerating my questionable sense of humour, which was on many occasions at his expense. I am also grateful towards my co-supervisor Dr. Paul M^{c}Gonigal, as well as Dr. Alyssa Avestro for their additional support, in particular in the stressful weeks leading to submission.

It would be completely amiss to not fully acknowledge the Walton, M^{c}Gonigal and Avestro groups, as well as a select few members of the Whiting group for making the year so entirely memorable and shaping me as a chemist through the year. I like to think that this report contains influences of everyone in these groups who have been a part of the journey, and reflects what has, purely because of the people surrounding me, been an extraordinary year. Special mentions must go to the demanding little princess Aisha Bismillah, for holding me together and keeping me in the right direction during the lowest points of the year, while providing some unforgettable highlights as well, and Archie McNeillis, whose limitless creativity constantly inspired new ideas, both in and beyond of the context of chemistry.

A final thank you goes to #TeamFiveOaks for seeing me over the finish line.

Table of Contents

Abbreviations

ATCC – American type culture collection

CML – Chronic myelogenous leukaemia

COSY – Correlation spectroscopy

Cp – Cyclopentadienyl

d - Doublet

DBU – 1,8-Diazabicyclo[5.4.0]undec-7-ene

DCM – Dichloromethane

DIPEA – *N*,*N*-Diisopropylethylamine

DMF – Dimethylformamide

DMPU – *N*,*N*'-dimethyl-*N*,*N*'-propylene urea

DMSO – Dimethyl sulfoxide

DNA – Deoxyribonucleic acid

ESI – Electrospray ionisation

EtOH – Ethanol

Fc JAHA – Ferrocene Jay Amin hydroxamic acid

FT-IR – Fourier transform infra-red (spectroscopy)

HATs – Histone acelyslases

HATU – (1-[Bis(dimethylamino)methylene]-1H-1,2,3-triazolo[4,5-b]pyridinium 3-oxid hexafluorophosphate)

HBSS – Hank's balanced salt solution

HDAC – Histone deacetylase

HDLP – Histone deacetylase-like protein

HMBC – Heteronuclear multiple-bond correlation spectroscopy

HMPT – Hexamethylphosphoramide

HPLC – High performance liquid chromatography

HRMS – High resolution mass spectrometry

HSQC – Heteronuclear single-quantum correlation spectroscopy

IC_{50} – Half maximal inhibitory concentration

IC_{90} – 90^{th} percentile maximal inhibitory concentration

IR – Infra-red (spectroscopy)

JAHA – Jay Amin hydroxamic acid

KHMDS – Potassium bis(trimethylsilil) amide

LCMS – Liquid chromatography mass spectroscopy

m - Multiplet

m – Meta substituted

Me – Methyl

MeOH – Methanol

MS – Mass spectrometry

MTT - 3-(4,5-dimethylthiazol-2-yl)-2,5-diphenyltetrazolium bromide

NHC – *N*-Heterocyclic carbene

NMR – Nuclear magnetic resonance

NOESY – Nuclear Overhauser effect spectroscopy

NSCLC – Non-small cell lung cancer

o – Ortho substituted

p – Para substituted

Ppm – Parts per million

PTA – 1,3,5-triaza-7-phosphatadamantane

q – Quartet

quin. - Quintet

R,R-dach – (1*R*,2*R*)-*Trans*-diaminocyclohexane

RPMI – Roswell Park Memorial Institute

s – Singlet

SAHA – Suberanilohydroxamic acid

SCLC – Small cell lung cancer

t - Triplet

THF – Tetrahydrofuran

TLC – Thin layer chromatography

TOF – Time of flight

TSA – Trichostatin A

UVA – Ultraviolet A

δ – Chemical shift

η - Hapticity

1. Introduction

1.1. Cancer – A General Overview

In 2012, over 14 million cases of cancer worldwide were reported, and it was the cause of over 8 million deaths in that year alone.[1] Consequently, the search for effectual preventative measures in the form of earlier detection and diagnoses as well as more effective treatments is currently a focal point within medicinal chemistry. The forms of cancer treatment used at present can be categorised into three separate methodologies: surgical treatment, radiotherapy and chemotherapy. Chemotherapeutic drugs themselves are typically divided into broad categories including alkylating agents and antimetabolites.[2] In many cases, chemotherapeutic agents are designed to selectively kill rapidly proliferating cells; an essential property of most cancer cells. The use of cytotoxic drugs remains extensive despite their well-known adverse side effects as well as problems associated with the development of resistance. However, despite the concerted effort worldwide to address the leading global cause of death, the number of cancer-related deaths has been steadily increasing. This is primarily due to longer lifespans and lifestyle changes in the developing world.[3] The most significant risk factor for developing cancer is age.[4] Although it is possible for anyone of any age to develop cancer, most patients with invasive cancer are over 65.[4] Some of the association between aging and cancer is attributed to immunosenescence,[5] errors accumulated in DNA over a lifetime and age-related changes[6] in the endocrine system.[7] In order to address the unmet needs for new ways to treat and moderate cancer, a wide variety of anticancer therapeutics with novel modes of action are constantly being devised and brought through to clinical testing.

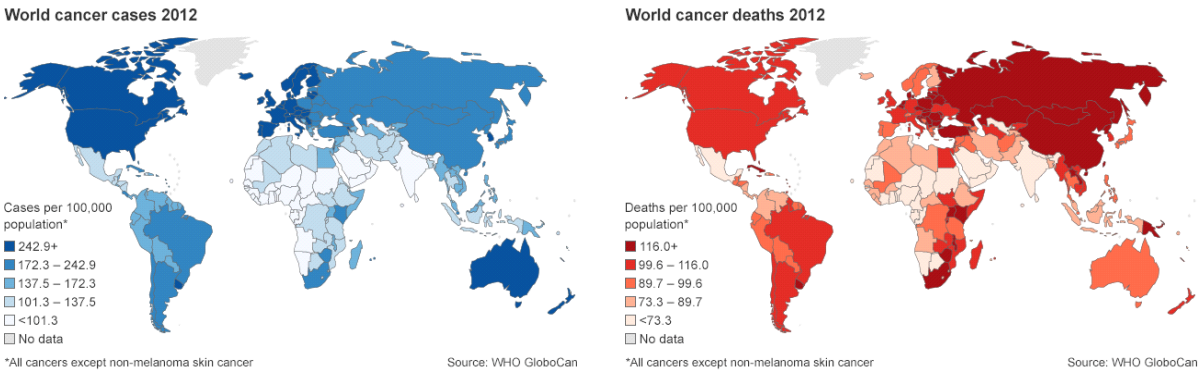

Figure 1.1 - Reported cases (left) of cancer and cancer-related deaths (right) worldwide[8]

1.2. Metals in Cancer Therapy

Metal complexes play a key role in a wide array of medical therapeutics. Figure 1.2 highlights the versatility of such compounds in a therapeutic context.

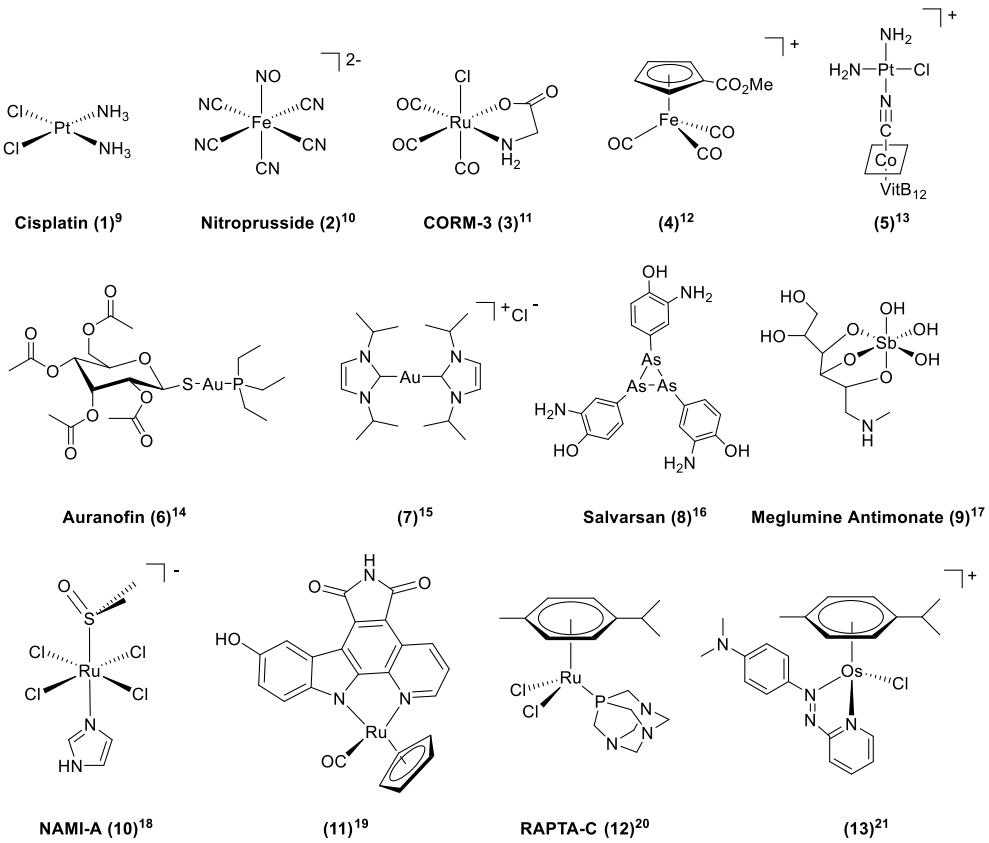

Figure 1.2 - A selection of metal complexes used in therapeutics[22]

The selected examples range from gas-releasing molecules (**2, 3, 4**), to the antirheumatic and anticancer agents of gold (**6, 7**), to organometallic drugs used to treat diseases such as syphilis (**8**) and leishmaniasis (**9**), to a few of the extensive assortment of complexes used to treat cancer (**1, 5, 10, 11, 12, 13**). Given the fact that effective therapeutics operate via specific binding interactions with disease-relevant substrates, metal complexes carry several advantages over their organic, small-molecule counterparts. Firstly, the manipulation of three-dimensional space about varying molecular structures that confer a wide number of coordination numbers and geometries is of paramount importance in order to fully exploit interactions of the complex with active sites within biological systems.[23,24] An additional advantage is the presence of redox potentials within organometallic complexes - the oxidation state of a metal is an important tool to permit the participation in biological redox chemistry, as well as to control the bioavailability of the agent.[25] Furthermore, the partially filled *d* orbitals in transition metals can impart certain electronic properties within the complex that can act as suitable probes in the design and action of anticancer agents.[26] The ability of metal complexes to undergo ligand exchange reactions also opens up a wide range of opportunities to fine-tune a drug's properties via a modular mix-and-match approach, leading to improved interactions and coordination to biological substrates, as demonstrated by the archetypal anticancer drug cisplatin (**1**).[23] A final and often overlooked advantage of organometallic drugs is their modular syntheses, which often entail fewer steps and allow some degree of synthetic flexibility over organic counterparts.

1.3. Cisplatin – The Canonical Chemotherapeutic

The introduction of cisplatin (**1**) as the leading chemotherapeutic agent for the treatment of testicular cancer has seen survival rates of over 90% for a previously untreatable and acutely deadly disease. To date, very few agents match the clinical efficacy of cisplatin; a drug approved in the UK as early as 1979.[27] The drug has since been employed to treat a variety of tumours including ovarian, cervical, head and neck, non-small cell lung carcinoma and is regularly used in combination regimens.[28,29] However, cisplatin has several affiliated side-effects such as nephrotoxicity, neurotoxicity and myelosuppression which limit its viability as a safe and reliable form of anticancer treatment. Further, the severity of the side-effects means that sub-lethal doses are often administered, thereby allowing the cancer cells to develop a resistance to the drug. These side-effects arise from the nature of chemotherapeutics, which rely on the unregulated proliferation of cancerous cells in regard to that of healthy cells - the higher metabolic activity of cancerous cells leads to a larger uptake of the cytotoxic drug, and resultantly the cancerous cells are selectively killed. However, it is unavoidable that some degree of the agent is also taken up by healthy cells. It is its relatively high toxicity paired with the appearance of intrinsic and developed resistance that hampered its continued widespread use and sparked the search for alternatives.[30,31]

1.3.1. Analogues of Cisplatin

In order to address the innate shortcomings of cisplatin, analogous compounds featuring the square planar Pt^{II} scaffold have been designed. Two further antineoplastic agents of this type are now in routine clinical practise: carboplatin and oxaliplatin, and an additional three see clinical use in single markets in Asia: nedaplatin, lobaplatin and heptaplatin (Fig. 1.3).

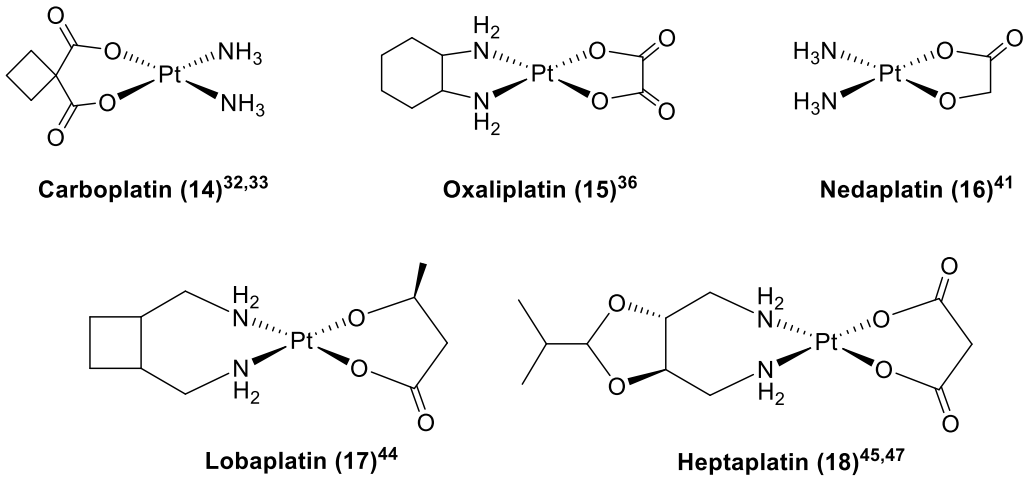

Figure 1.3 - Clinically approved 2nd and 3rd generation cisplatin analogues[32]

These 2nd and 3rd generation platinum anticancer drugs successfully maintain a more manageable toxicity profile than that of cisplatin, and can target a wider range of cancers than cisplatin (**1**) alone. Carboplatin (**14**) exhibits particular efficacy in the treatment of ovarian carcinoma, lung cancer as well as head and neck cancers.[33] Carboplatin was specifically designed in order to reduce the side-effects associated with cisplatin treatment.[32] Platinum complexes with highly labile ligands, such as water or nitrate, are observed to show acute biotoxicity whereas slowly-aquating ligands such as bis-carboxylates lead to inherently lower toxicities for a specific complex. While cisplatin aquates with a rate constant of 10^{-5} s^{-1}, replacing the chloride ligands of cisplatin with the 1,1-cyclobutanedicarboxylate ligand in carboplatin reduces the rate of aquation to 10^{-8} s^{-1}.[34] As a result of its lower kinetic reactivity, carboplatin can be administered in significantly higher doses (300-450 mg m^{-2}) than cisplatin (20-120 mg m^{-2}).[35] Aquated carboplatin yields the same complex as when cisplatin is aquated and the complexes form the same DNA adducts, meaning that it is only clinically relevant to the same strains of cancer that cisplatin is used to treat. For the same reason, resistance remains a pertinent issue when carboplatin is used as a cisplatin alternative.

On the other hand, oxaliplatin (**15**) was the first approved drug observed to overcome cisplatin resistance.[36] Oxaliplatin features lowered kinetic reactivity through the replacement of cisplatin's chloride ligands with an oxalate moiety, but also replaces the two ammine ligands seen in cisplatin and carboplatin with a single bidentate diamine ligand (1*R*,2*R*)-trans-diaminocyclohexane, or *R*,*R*-dach). It is reported that oxaliplatin overcomes cisplatin resistance through the different adducts it forms when bound to DNA.[37] The bulky, hydrophobic dach ligand prevents the binding of the DNA repair proteins responsible for the build-up of resistance.[38] Oxaliplatin is clinically approved for the treatment of colorectal cancer, which shows high resistance towards cisplatin.[39] It is also currently in clinical trials to examine its viability as a therapeutic agent for gastric, fallopian tube and ovarian, breast, non-small cell lung cancer (NSCLC), pancreatic cancers, acute myeloid leukaemia, indolent non-Hodgkin's lymphoma and hepatoma.[40]

Three further analogues of cisplatin have achieved marketing approval for human use in the treatment of cancer. However, unlike the commercially dominant carboplatin and oxaliplatin, nedaplatin (**16**), lobaplatin (**17**) and heptaplatin (**18**) have not gained worldwide approval, but have gained clearance in the single markets of Japan, China and the Republic of Korea respectively.[32]

Since its approval in Japan in 1995, nedaplatin has been used in the treatment of NSCLC, small cell lung cancer (SCLC), oesophageal cancer and head and neck cancers.[41] Promising results have also been shown when nedaplatin is used in combination therapies. It is reported that lobaplatin (**17**) doesn't induce alopecia, renal, neuro- or ototoxic side effects when administered through either IV bolus injection or infusion.[42,43] Lobaplatin is currently approved for the treatment of chronic myelogenous leukaemia (CML), certain strains of breast cancer as well as SCLC.[44] Heptaplatin (**18**) showed similar

in vitro and *in vivo* cytotoxicity to cisplatin in certain cell lines, and as such, was selected for clinical trials. It also showed a significantly lower toxicity profile than its precursors,[45,46,47] as well as remarkable anticancer activity towards cisplatin-resistant cells.[45,47] Heptaplatin sees use in the treatment of gastric cancer.[48,49]

1.4. Mechanism of DNA Interaction

The mechanism through which cisplatin and related cis-diammine platinum agents operate has been the subject of several decades of investigation. The two ammine ligands can either be chelating or nonchelating, but remain bound to the Pt^{II} centre during intracellular transformations. In contrast to this, the "leaving group" ligands (chloride ligands in cisplatin and typically a chelating dianionic fragment in analogous complexes) leave the coordination sphere and facilitate the formation of DNA adducts.[50] A widely reported mechanism of action of cisplatin is generalised in Figure 1.4.

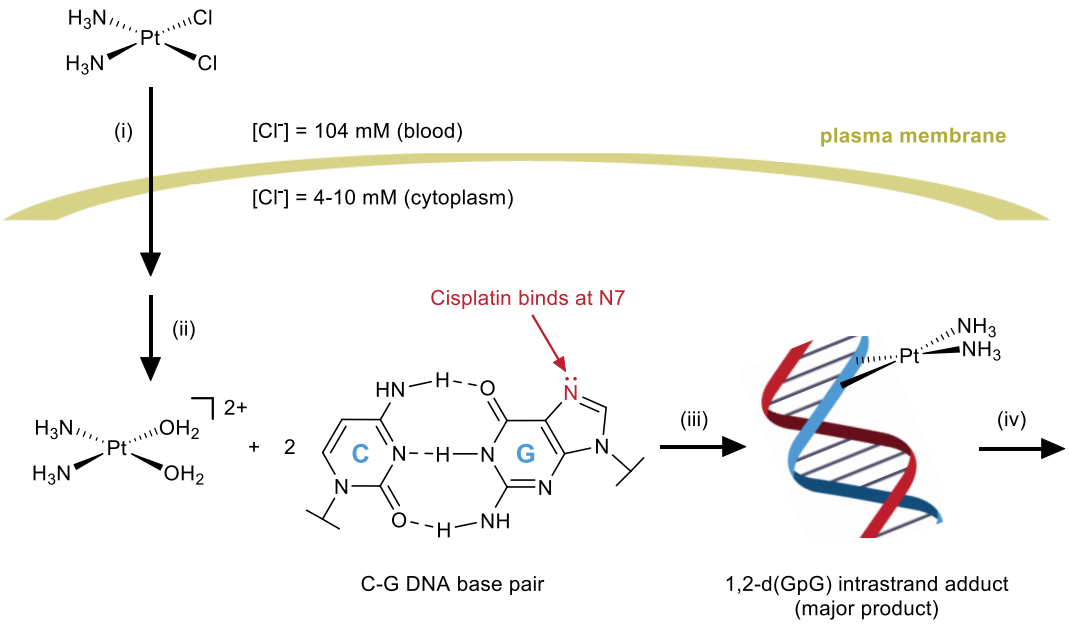

Figure 1.4 - Mechanism of action of cisplatin comprising (i) cellular uptake, (ii) aquation/activation, (iii) DNA platination, and (iv) cellular processing leading to apoptosis. Reproduced / modified from ref. 50

Firstly the drug is taken up into a cell, which is believed to occur through one of two pathways: either passive diffusion through the cell's lipid membrane or active transport mediated by membrane proteins. The small molecular size and planar geometry of cisplatin and cisplatin analogues have long been cited as the reasoning behind its passive diffusion into a cell. Further, it was found by Gale *et al.*[51] that a double reciprocal (Lineweaver-Burk) plot of platinum accumulation vs drug concentration yielded a straight line that passes through the origin, suggesting that the rate limiting factor for the uptake of the drug was its concentration. These findings were corroborated by a separate study nearly two decades later.[52] Further evidence for the passive diffusion of square planar diammino-Pt(II) complexes into

cells is that its uptake is found to not be saturable. It is also reported by Gale *et* al.[51] that the uptake of *cis*-diammine(dipyridine) platinum(II) into transplanted carcinoma cells in mice was linear up to the levels of its solubility in DMSO. This lack of saturability has since been confirmed by a number of studies conducted by other groups using either atomic absorption[53] or NMR studies of ^{195}Pt-cisplatin.[54]

Despite the large amount of evidence for passive and unmediated diffusion of cisplatin and related complexes into a cell being the relevant pathway, there is an ever-increasing body of data suggesting that at least a part of the uptake of these complexes is mediated in some way by some type of transport mechanism. Results were surfacing as early as 1981 that indicated this mediated pathway.[55] The toxicity of cisplatin towards both resting and cycling human T lymphocytes was investigated and observed to be different for the two cell types. Such a toxicity profile mirrors that of alkylating agents with known carriers (melphalan and nitrogen mustard) and is not observed in agents that enter the cell through passive diffusion (mitomycin C and various nitrosoureas).[55,56] It is also reported that the protein synthesis inhibitor benzaldehyde significantly reduced the cytotoxicity of cisplatin when the two were administered in tandem to human cervix carcinoma cells (NHIK-3025 cell line). It did not have the same effect when paired with a nitrosourea derivative or nitrogen mustard. It was suspected that the benzene ring may play some role in the observed reduction of cisplatin's efficacy, and so other simple, monosubstituted aromatics were tested in the same manner. Neither benzoic acid nor phenol exhibited the same effect on cisplatin's toxicity. It was concluded that the rationale behind benzaldehyde's hindering of cisplatin's potency was a result of reaction between the aldehyde and the membrane proteins responsible for internalising cisplatin, in turn leading to inhibition of the intracellular accumulation of platinum.[57] The same research group later discovered that benzaldehyde and other aldehyde derivatives act at the cell membrane by means of formation of Schiff base adducts. This occurs through bonding to amino groups on the cell membrane, which leads to the proposed reduction of uptake of platinum. This was confirmed by relevant measurements of the downwards shift in absorbance maxima of the aldehydes once imine formation has occurred.[58] A series of aldehydes were measured to inhibit cisplatin toxicity by up to 50%.[59] A combination of both passive and mediated transport best describes the pathway of cisplatin and analogous complexes into a cell in order to fit the seemingly conflicting data acquired. However, the relative importance of the two means and the exact extent to which they influence each other remains to be determined.

The square planar geometry of cisplatin and other platinum(II) analogues enables ligand substitution chemistry, which is at the core of its mode of action through the adducts they form with DNA. Cisplatin undergoes a ligand substitution reaction prior to its interaction with DNA, through which one of its two labile chloride ligands is replaced by a molecule of water. The reaction of hydrolysis of cisplatin to form *cis*-$[Pt(NH_3)_2Cl(H_2O)]^+$ is reported to have a half-life of approximately 2 h.[60] Conversely, the bidentate ligands opposite the kinetically inert amine ligands on carboplatin and oxaliplatin lead to a

hydrolysis that is observed to be much slower. The two complexes are reported to be stable to aquation over a period of weeks to months.[61,62]

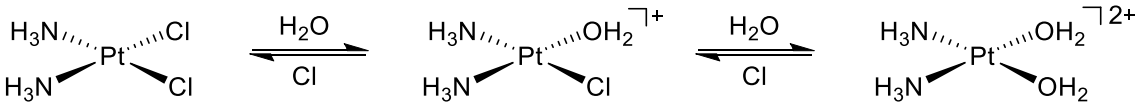

Figure 1.5 - First and second hydrolyses of cisplatin

Hydrolysed cisplatin can enter the cell, which is in part due to the positive charge generated on the hydrolysed products drawing the cation close to the negatively charged nuclear DNA. Furthermore, the more kinetically labile water ligands facilitate effective substitution about the platinum centre with the nucleophilic sites of DNA. The nitrogen atoms in the N7 positions (shown in Fig. 1.4) of the two purine bases of DNA: adenine and guanine, and these are the sites that are preferentially platinated. Cisplatin can bind to form DNA lesions in a number of ways (Fig. 1.6).

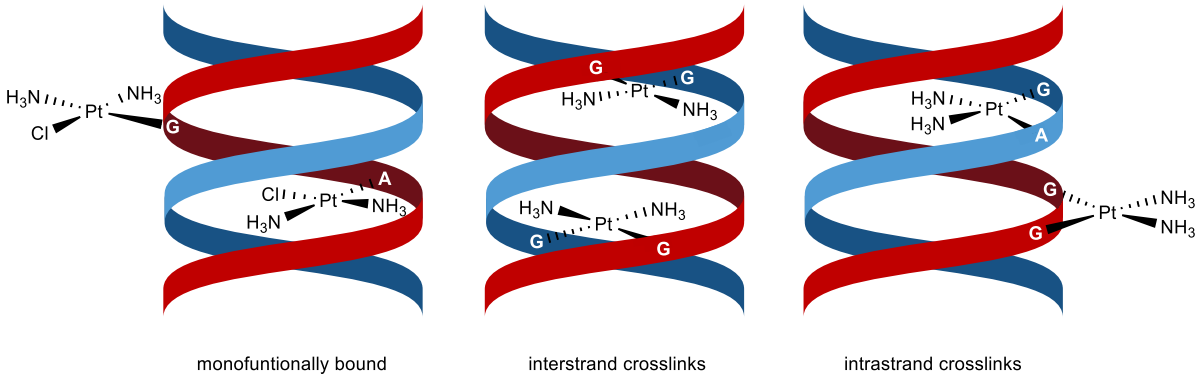

Figure 1.6 - Schematic representation of the known adducts formed between DNA and cisplatin. Reproduced / adapted from ref. 63

Time dependent ^{195}Pt studies have shown that monofunctionally-bound adducts are initially formed via the nucleophilic displacement of a molecule of water by an imidazole nitrogen on the relevant DNA bases.[63] Then, subsequent crosslinks are formed by the substitution of the second chloride ligand with a nearby guanine base on the same strand or on a different strand, which leads to either interstrand or intrastrand crosslinks, respectively. There are a variety of intra- and interstrand crosslinks that can be formed between square planar Pt^{II} drugs and DNA, which have been identified *in vivo* as well as *in vitro*. The major lesion formed by cisplatin is a *cis*-1,2-[$Pt(NH_3)_2^{2+}$]-d(GpG) intratrand crosslink (shown in Figs. 1.4 and 1.6). This adduct comprises ~65 % of the total products. The remaining 35% includes *cis*-1,2-[$Pt(NH_3)_2^{2+}$]-d(ApG) (~25 %) and *cis*-1,3-[$Pt(NH_3)_2^{2+}$]-d(GpNpG) (5-10 %) intrastrand adducts as well as a minority of interstrand crosslinks and monodentate lesions. Carboplatin and oxaliplatin form similar lesions, but in differing proportions.[64,65] Resolved X-ray crystallographic data of some of the DNA adducts of cisplatin (a-c) as well as a number of adducts formed with analogues oxaliplatin (d), satraplatin (e) and pyriplatin (f) are shown in Figure 1.7.[66] Sartraplatin represents an example of a platinum(IV) drug; an octahedral, more kinetically inert analogue of platinum(II) therapeutic agents.

The advantages afforded by platinum(IV) complexes, in particular the freedom afforded by the two extra ligands to explore and fine-tune desired pharmacological properties, such as lipophilicity, favourable manipulation of three-dimensional space, stability towards redox conditions and improved cellular uptake, have led to a relatively recent surge of interest.[49]

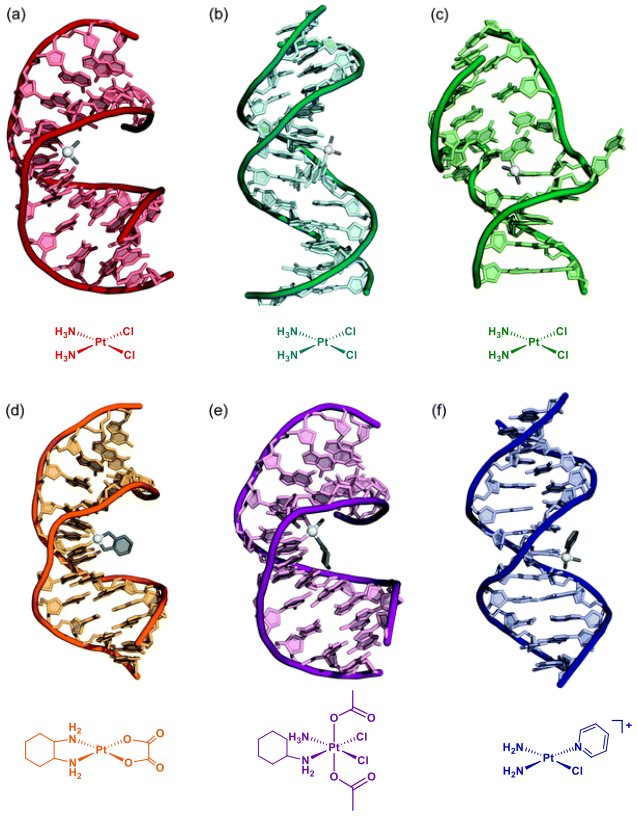

Figure 1.7 - Structures of double-stranded DNA adducts of different platinum anticancer. (a) Cisplatin 1,2-d(GpG) intrastrand cross-link. (b) Cisplatin 1,3-d(GpTpG) intrastrand cross-link. (c) Cisplatin interstrand cross-link. (d) Oxaliplatin 1,2-d(GpG) intrastrand cross-link. (e) Satraplatin 1,2-d(GpG) intrastrand cross-link. (f) cDPCP monofunctional adduct. Modified from ref. 66

The twisting, bending and unwinding of DNA observed in Figure 1.7 is the core of how platinum(II) drugs and many analogues operate. The induced structural distortion to a cell's DNA inhibits processes such as transcription and replication and consequently leads to cell death pathways.[67] DNA repair mechanisms are induced once the chelation to DNA is made and the structure distorted, which in turn activate programmed cell death, or apoptosis, when the repair proves impossible.[68] It has also been shown that in certain cell lines, particularly those with resistance to the drug, cisplatin kills the cells via necrosis: unprogrammed death caused by external factors such as toxins or trauma.[69] Furthermore, cases have been reported where both necrotic and apoptotic cell death occur in the same population of cisplatin-treated cells.[70] Depending on the cell line, the exact mechanism of cell death could feasibly be apoptosis, necrosis or a combination of the two.

1.5. Ruthenium-based Anticancer Agents

Following the success of cisplatin and related platinum based anticancer drugs, ruthenium complexes quickly attracted a lot of attention as well-suited alternatives for transition-metal-based anticancer agents. There is a large amount of potential in the application of ruthenium in particular to diversifying the organometallic drugs currently used as anticancer agents: markedly reduced toxicity and novel mechanisms of action. Further, in differing physiological conditions within the body, ruthenium shows the unique property of being stable across the oxidation states II, III and IV.[71] The accessibility of different ruthenium oxidation states enables the body to catalyse redox reactions of an agent, thereby adding another dimension to their mechanisms of action. Ruthenium(III) complexes have an octahedral geometry, but exhibit similar ligand kinetics as complexes of platinum(II). The influence of the two additional coordination sites in ruthenium(III) complexes leads to a higher degree of tunability in the synthesis of organometallic agents with a similar mode of action as cisplatin. Such relatively slow ligand exchange rates, which are close to those of cellular processes such as cellular reproduction, mean that once bound, a ruthenium or platinum complex is likely to remain bound for the remainder of the cell's lifetime (Fig. 1.8). This is a crucial feature of complexes to be used in biological applications.[72]

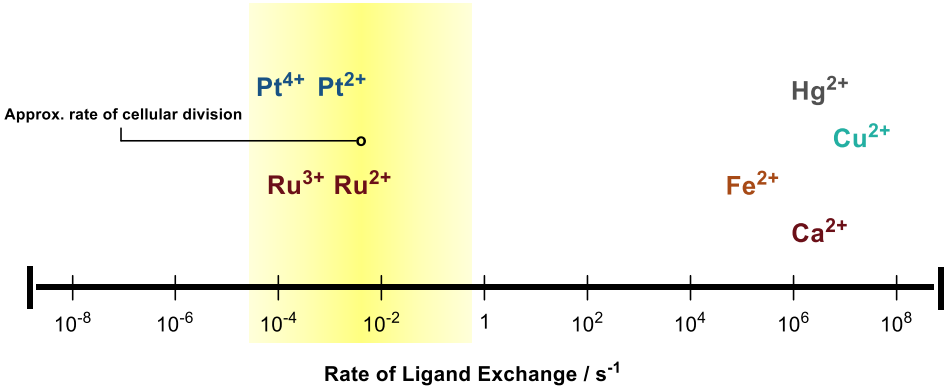

Figure 1.8 - Ligand exchange rates for a selection of transition-metal cations (reproduced from ref. 73)

A further advantage of such agents is the ability of ruthenium to mimic iron in binding to certain biological molecules, which is also an important facet to exploit in order to optimise drug delivery, uptake and a given complex's mode of action.[74] The chelating nitrogen and sulphur sites of proteins such as albumin and transferrin, both of which display high affinities for binding to iron, become useful tools in the transport of ruthenium agents around the body.[75] Complexes of ruthenium(III) can bind to the iron(III) sites of transferrin and are taken up by the cell via receptor-mediated endocytosis.[76] As rapidly dividing cells have an increased demand for iron, such cells also feature a larger amount of transferrin receptors. Cancerous cells have been reported to feature between two to twelve times as many transferrin receptors as the corresponding healthy cells.[77] This results in a significantly increased selectivity of the ruthenium drug, which, for the most part, bypasses healthy cells and is sequestered in cancerous tissues. This effect is a large contributor to the notably lower toxicities displayed by ruthenium complexes in comparison to those of platinum.[78]

It was hypothesised by Clark *et al.*[79,80,81] that ruthenium(III) complexes serve as prodrugs, that are reduced *in vivo* to their more active ruthenium(II) forms. This idea was formed on the basis that ruthenium(II) complexes are generally more biologically active than complexes of ruthenium(III). Furthermore, tumours utilise oxygen at an increased rate, such that the development of new blood vessels often fails to keep pace, generating a hypoxic environment within tumour cells. As a consequence, there is a larger dependence on glycolysis for energy, which generates lactic acid, thus lowering the pH in tumour cells. These metabolic differences lead to cancerous cells featuring a more chemically reducing environment, which would typically favour the production of ruthenium(II) complexes. For this reason, alongside the high degree of mobility of such drugs in the bloodstream, complexes of ruthenium can be administered in the III oxidation state; corresponding to a relatively inert drug which doesn't interact with healthy cells, and are activated to the II oxidation state solely at the site of cancerous cells. This mechanism is known as "activation by reduction" and is a main contributing factor to the rapid onset of ruthenium(III) induced apoptosis within cancer cells, but also the significantly lowered toxicity towards healthy cells that is observed for such complexes.[82] Furthermore, ruthenium(II) complexes are postulated to be able to be oxidised and deactivated when out of the cancerous environment. Activation by reduction for drugs of ruthenium(III) has been demonstrated thoroughly *in vitro* but has so far been difficult to prove experimentally *in vivo*.[75]

It is also proposed that ruthenium can substitute iron in Fenton-like redox processes,[83] which induce intracellular radicals that would result in major cell damage and subsequently, programmed cell death. The oxidative stress of the variable intra- and intercellular conditions of the body could facilitate the radical-generating redox processes (Eqn. 1.1) of a ruthenium complex, thus enabling selective and rapid damage to the DNA of cancerous cells through exposure to radical species.

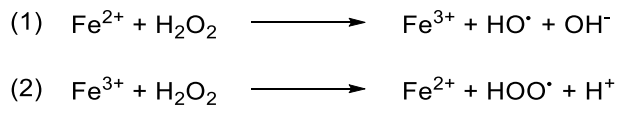

Equation 1.1 - Disproportionation of hydrogen peroxide by Fenton's reagent, with radical generation[84]

These inherent advantages of ruthenium have been actualised, as several ruthenium based agents have been developed within the last 30 years; two of which having passed Phase I human clinical trials.[85]

1.5.1. Dimethyl Sulfoxide (DMSO) Ruthenium Complexes

Ruthenium complexes that are designed as anticancer agents are often deliberately designed in order to mimic the aforementioned DNA-targeting drugs of platinum. Perhaps the closest resemblance between a class of ruthenium-based antineoplastic complexes and cisplatin and its analogues is that of ruthenium-DMSO complexes. DMSO containing complexes of both ruthenium(II) and ruthenium(III)

have been shown to exhibit comparable antitumour activity to that of cisplatin at equitoxic doses. Further, *in vivo* modelling of metastatic tumours also showed significantly less severe side effects than the platinum congener.[86] The two stereoisomers of $[Ru(DMSO)_4Cl_2]$ were identified as potential anticancer agents as far back as the early 1980s.[87] Since then, a series of complexes whose parent molecules are *cis*- and *trans*-$[Ru(DMSO)_4Cl_2]$ (complexes **19** and **20**, Fig. 1.9) have been extensively studied as alternatives for cisplatin.[88]

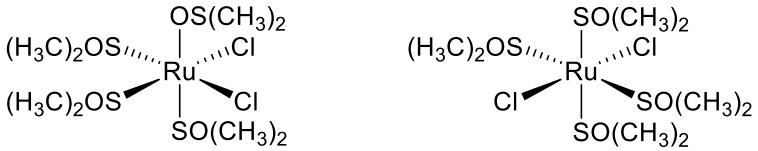

(19) **(20)**

Figure 1.9 - Structures of *cis*- and t*rans*-$[Ru(DMSO)_4Cl_2]$[88]

Investigations into the two stereoisomers were initially carried out on complex **19** because of its structural similarity to cisplatin. However, comparative studies of *cis*- and *trans*-$[Ru(DMSO)_4Cl_2]$ revealed the latter to be the more effective agent.[89] *Cis*-$[Ru(DMSO)_4Cl_2]$ is a complex which displays linkage isomerism. Of the DMSO ligands of *cis*-$[Ru(DMSO)_4Cl_2]$, three are S-bound DMSO molecules and the fourth ligand is bound through oxygen, whereas the DMSO ligands of the *trans* isomer are all bound through sulphur. It has been shown that upon aquation, the O-bound DMSO ligand of **19** is readily substituted, whereas **20** will dissociate two adjacent DMSO ligands yielding the *cis*-diaqua species. Both hydrolysed isomers then undergo a much slower, reversible chloride dissociation to form the multiply aquated, monocationic complexes that are active in DNA-binding.[89] At this point, the *trans* complex features three kinetically labile water ligands while the *cis* isomer only presents two reactive sites. Moreover, the increased steric bulk induced by the additional DMSO ligand remaining on the *cis* isomer is proposed to contribute to the markedly lower anticancer activity observed of this isomer.[90]

The photocytotoxicity profiles of both isomers of $[Ru(DMSO)_4Cl_2]$ were investigated by Brindell *et al.*[91] in two cell lines of melanomia; human (SK-MEL 188) and mouse (S91). *Trans*-$[Ru(DMSO)_4Cl_2]$ was observed to show higher toxicity than the *cis* isomer both in the presence and absence of illumination. The antiproliferative activity of both isomers were significantly enhanced when exposed to UVA light (Fig. 1.10). IC_{50} incubation times for *cis*-$[Ru(DMSO)_4Cl_2]$ when added to S91 melanomia cells with and without UVA irradiation were measured to be 51 ± 10 and 26 ± 5 minutes respectively. These values for the *trans* isomer were calculated to be 35 ± 4 and 14 ± 5 minutes. The study not only corroborates the increased efficacy of *trans*-$[Ru(DMSO)_4Cl_2]$ over the *cis* isomer, but also serves as a pertinent example of photoactive drugs; a new approach in chemotherapy that has been extensively studied over the last decade.[92]

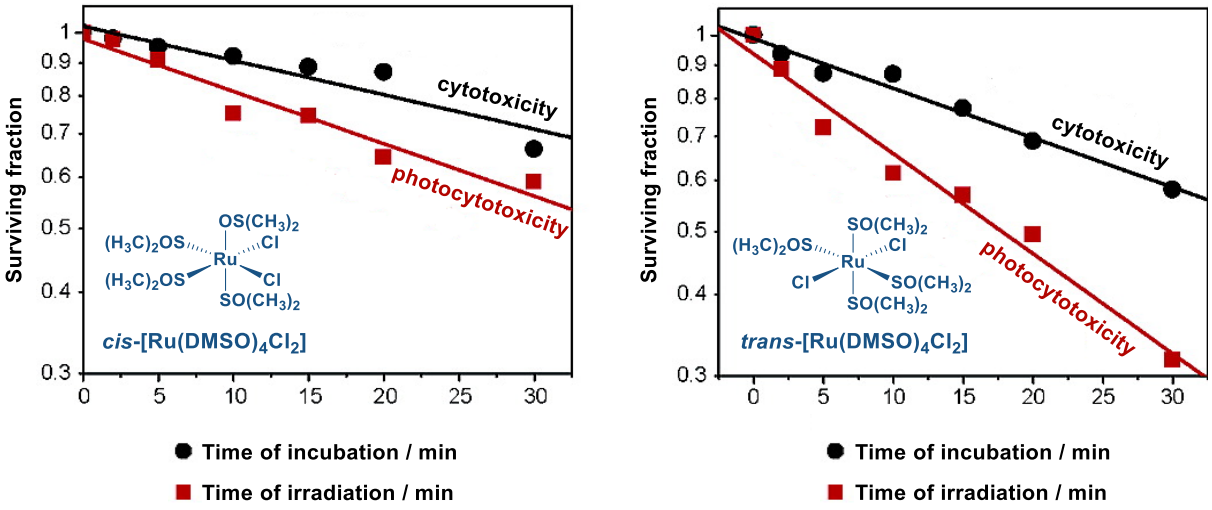

Figure 1.10 - Cytotoxicity and photocytotoxicity profiles for *cis*- and *trans*-[Ru(DMSO)$_4$Cl$_2$] with mouse (S91) melanoma cells. Reproduced / adapted from ref. 91

1.5.2. Heterocyclic Ruthenium(III) Complexes

Complexes of ruthenium(III) featuring a coordinated heterocyclic base such as imidazole (Im) or indazole (Ind) represent a relatively new class of organometallic anticancer compounds (Fig. 11).[93,94] Such complexes have been shown to exhibit activity in a number of tumour models and are particularly effective against cisplatin-resistant colorectal tumours.[93]

KP1019, or *trans*-[tetrachlorobis(1H-Ind)ruthenate(III)] (**21**), is an example of a heterocyclic ruthenium(III) complex which shows particular efficacy against colorectal cancer that is resistant to cisplatin both *in vivo* and *in vitro*.[95] At therapeutically relevant doses it exhibits no serious adverse side effects.[95] Because of its poor water solubility, which leads to inherent difficulties in its transport in the bloodstream, KP1019 is typically prepared and administered as its sodium salt, KP1339 (**22**). Such agents exhibit such therapeutic relevance and efficacy as they are specifically designed to mirror the mode of action of cisplatin while featuring additional advantages, such as activation by reduction and transferrin-based transportation, as well as inherently lowered systemic toxicity. Replacement of the indazole ligands and indazolium counterion of KP1019 with imidazole and imidazolium, respectively, yields the derivative KP418 (**23**). The structures of KP1019 and three derivatives are shown in Figure 1.11. KP418 exhibits slower cellular uptake and slower protein binding, and because of its lower therapeutic index is yet to complete Phase I clinical testing.[96]

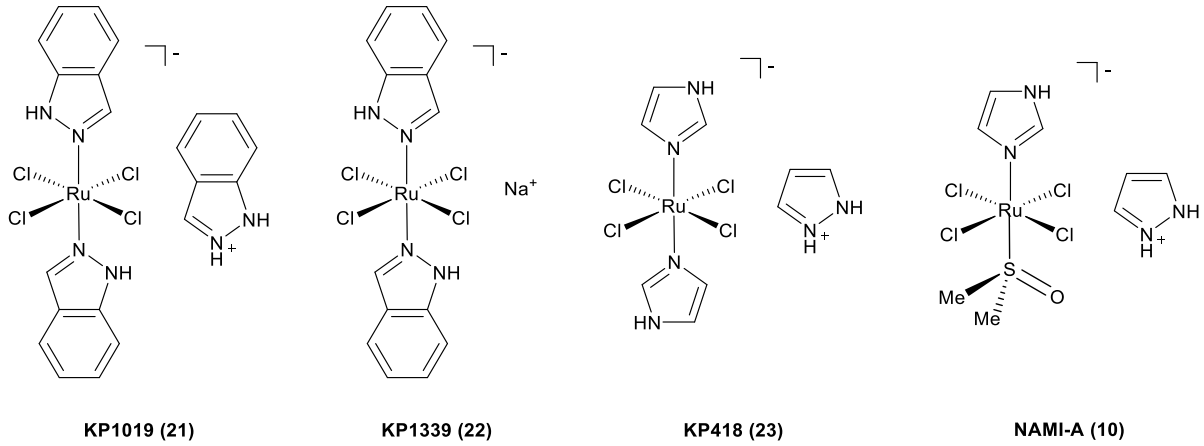

Figure 1.11 - Structures of KP1019 and derivatives NKP1339, KP418 and NAMI-A[93,95]

Two subsequent analogues of these complexes, which feature both DMSO ligands as well as an *N*-bound heterocycle, were developed. Na[*trans*-Ru(DMSO)Cl_4(Im)] (NAMI) and more recently the corresponding imidazolium salt NAMI-A (**10**) were synthesised with the aim of creating an agent with similar efficacy to the precursory heterocyclic ruthenium complexes, while maintaining a higher degree of stability in the solid-state.[97] In a comparative study between the DNA-binding effects of cisplatin (**1**) and **10** across a number of different cell lines, the latter was observed to be on average over three orders of magnitude less cytotoxic than the former, at the same effective dose.[98] Results of other studies have indicated that DNA-binding is not the most significant process in the mode of action of **10**, but rather that other processes such as the lysis of various proteins may be the main contributors to its cell-killing ability.[89] Sava *et al.*[99] conducted both *in vitro* and *in vivo* studies of **10**; the latter involving the administering of the drug into CBA mice carrying MCa mammary carcinoma. It was shown that while **10** exhibits a small amount of toxicity, it effectively decreases the metastasis of the cancerous cells. Even more impressively, the complex remained operative over a wide range of changes to environment, including changes in pH as well as exposure to the following biological reductants: ascorbic acid, glutathione and cysteine. **10** and KP1339 (**22**) are currently the only two ruthenium-based anticancer drugs to have passed Phase I clinical trials.

1.5.3. Ruthenium(II) Piano Stool Complexes

Piano stool complexes of ruthenium(II) represent an emerging class of ruthenium-based antitumour drug. Such complexes feature an η^6-bound arene, which stabilises the ruthenium(II) oxidation state, as well as three further sites to occupy with ligands of any hapticity. Typically, it is complexes with two of these sites occupied by a bidentate ligand and the third by a monofunctional leaving group that exhibit the highest activity. Complexes of this group do not follow the "activation by reduction" mechanism, since they are active and stable in the ruthenium(II) oxidation state. With a single reactive coordination site and lower oxidation state, it is suggested that ruthenium(II) piano stool complexes operate through

a differing, or modified mechanism than those of the ruthenium(III) complexes NAMI-A (**10**) and KP1339 (**22**).[100]

RM175, [(η^6-C_6H_5Ph)Ru(en)Cl](PF_6) (en = ethylenediamine, **24**, Fig. 1.12) is one of the leading complexes of this class, and displays *in vitro* a cytotoxicity comparable to that of cisplatin, as well as high cytotoxicity towards cisplatin-resistant colorectal cancer cells.[101] RM175 belongs to a class of complexes designed with the principal aim of engineering strong DNA-binding interactions through bifunctional effects; standard metal-DNA intercalation as well as hydrogen-bonding interactions through the *N*-heteroatoms of the en ligand. The types and extent of adducts formed between an organometallic antitumour drug and DNA, and the resultant degree of DNA distortion are believed to be responsible for their biological effects.[102,103] Therefore, the targeting of multifaceted complexes, which can exploit a larger degree of DNA distortion and thus reduce their susceptibility to DNA repair mechanisms, remains a very attractive tool for the development of metal-based anticancer agents.

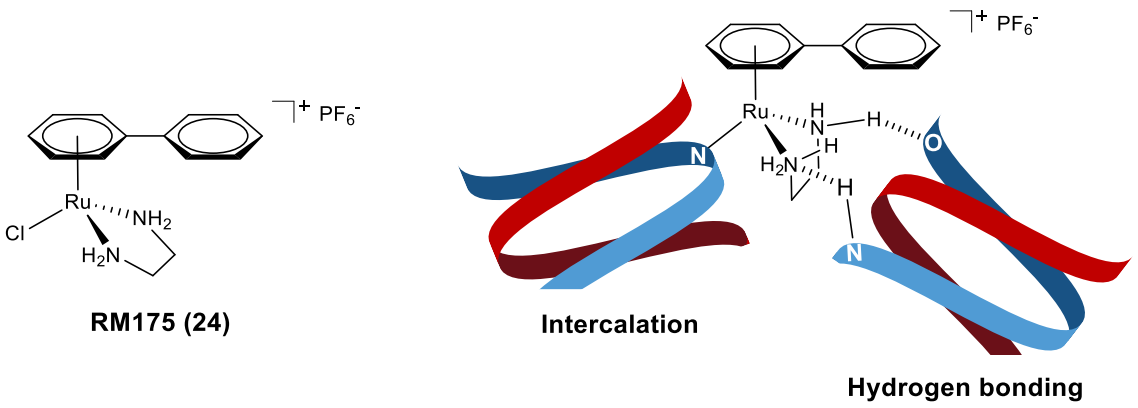

Figure 1.12 - Structure of RM175 and a schematic of the bifunctional DNA-binding features of the complex[104,105]

RAPTA complexes are arene-capped ruthenium(II) complexes bearing the 1,3,5-triaza-7-phosphatricyclo[3.3.1.1]decane (PTA) ligand. The PTA ligand confers an increased solubility in water to the complex, which is bio-functionalised through two labile chloride ligands or a bidentate chelator (Fig. 1.13). Whether the active sites feature chloride ligands or a bridging carboxylate ligand allows for tuning of the aquation characteristics of a complex. While an increase in water solubility, and resultantly drug uptake, is observed in the latter class of complexes, this is at the cost of drug selectivity towards cancer cells.[20]

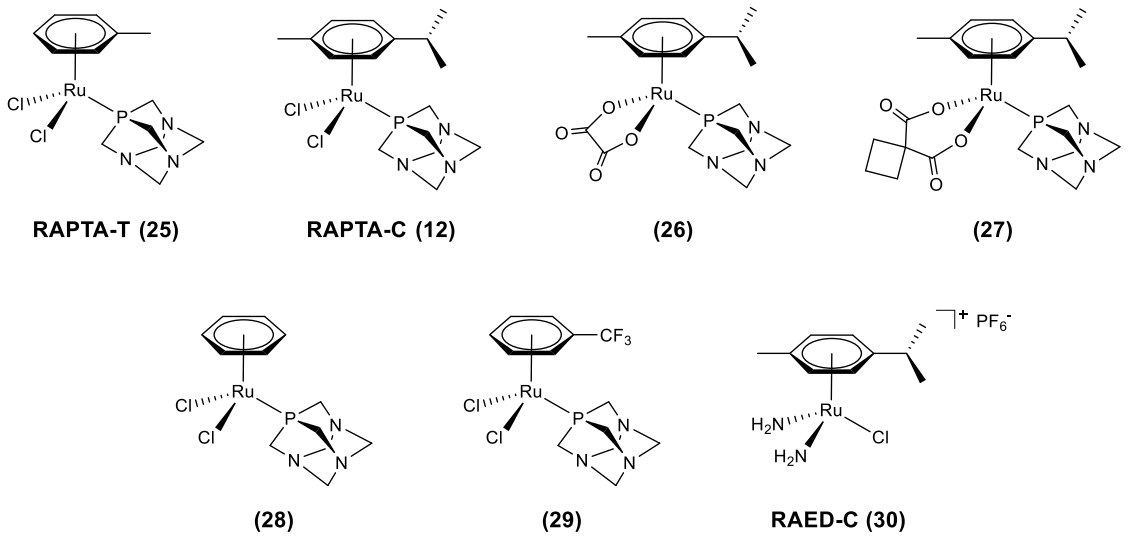

Figure 1.13 - A selection of RAPTA complexes evaluated for anticancer activity, and RM175 analogue RAED-C[20]

Generally, ruthenium–arene complexes show promising cytotoxic activity, particularly against human ovarian cancer cell lines, with some complexes being as potent as cisplatin and carboplatin. Despite the innate chemical and structural differences between piano-stool complexes and NAMI-A (**10**) and RAPTA-T (**25**) among other RAPTA complexes have been shown to exhibit remarkably similar *in vitro* and *in vivo* effects to this class of complexes, in particular selectivity to metastatic tumours over the localised sites of primary tumours.[20] Bergamo *et al*.[107] compiled a comparative review of some of the different classes of ruthenium anticancer complexes, namely their antitumour and antimetastatic activity towards a mammary carcinoma model and a lung carcinoma model, both carried in mice (Fig. 1.14). RM175 (**24**), like KP1019 (**21**) exhibited non-selective cytotoxicity, i.e. the compound primary tumour and lung metastasis growth inhibits in a similar way. However, the toluene-capped RAPTA complex RAPTA-T (**25**) showed the same impressive selectivity for anti-metastatic effects as demonstrated by NAMI-A (**10**). The strongly inhibiting effect towards lung metastases with no or marginal effects on primary tumour growth remains an important and attractive asset for future anticancer drugs. As moderating agents of the spread of cancer; such agents do not endanger healthy cells through high cytotoxic effects. These effects of RAPTA complexes on spontaneously metastasizing tumours are important in that this is the first evidence for another ruthenium-based compound to show some degree of selectivity of anti-tumour activity towards metastases, following the novel results of **10**. Cellular studies of **25** in tumour cells suggest the possibility for this compound to modulate cell cytoskeleton of the treated cells leading to a cell with characteristics which lead to a lower ability to migrate and metastasize.[106] While the exact nature of the mechanism followed by RAPTA complexes and **10** remains uncertain, it is clear that it is somewhat different to, or alongside additional effects of, the cisplatin-like DNA-binding proposed for early ruthenium anticancer agents.

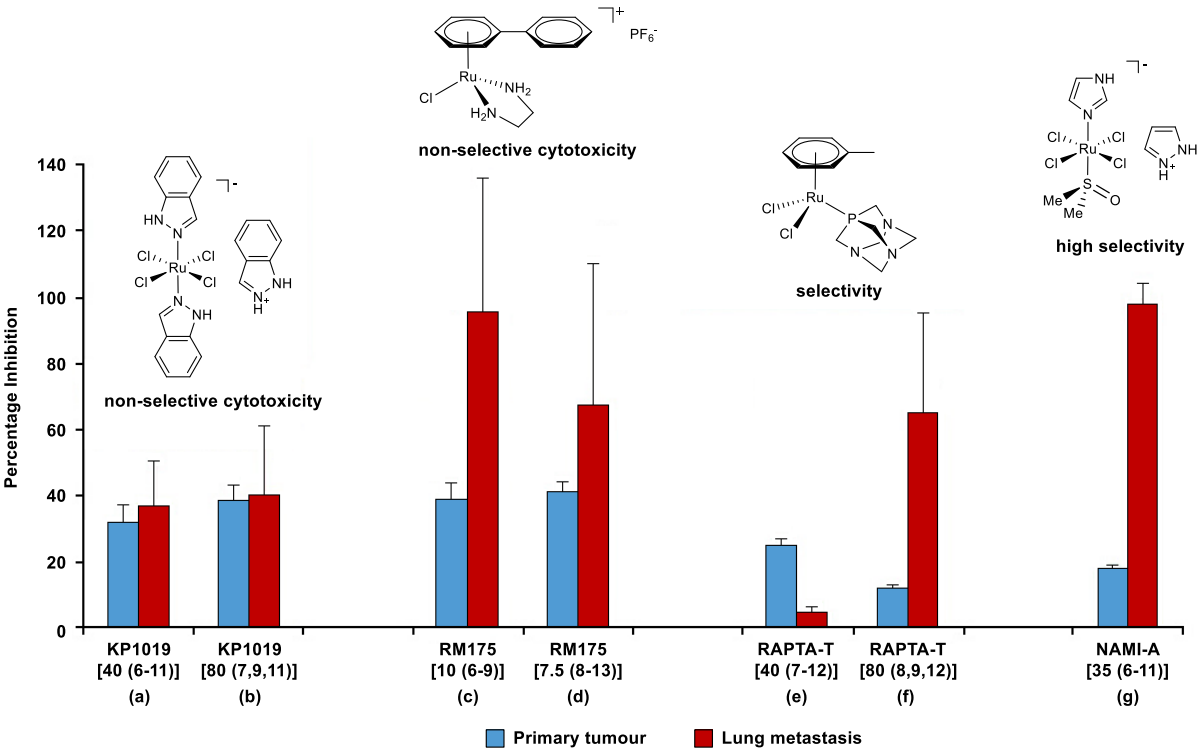

Figure 1.14 - Comparison of the selectivity of the anti-metastatic effects of ruthenium anticancer agents KP1019, RM175, RAPTA-T and NAMI-A in the mammary carcinoma model. Groups of at least 10 CBA mice, implanted i.m. with 106-MCA tumour cells on day 0 were treated with KP1019 via intraperitoneal injection at 40 mg/kg/day on days 6–11 (a), or at 80 mg/kg/day on days 7, 9, and 11 (b) after tumour implant; with RM175 at 10 mg/kg/day on days 6–9 (c), or at 7.5 mg/kg/day on days 8–13 after tumour implant (d); with RAPTA-T at 40 mg/kg/day on days 7–12 (e), or at 80 mg/kg/day on days 8, 9 and 12 after tumour implant (f); and with 35 mg/kg/day NAMI-A on days 6–11 after tumour implant (g). Lung metastases (right red bar) and primary tumour growth (left blue bar) were determined on day 20 after tumour implant. Reproduced / adapted from ref. 107

RAED-C (**30**), alongside RAPTA-C (**12**), was the subject of cellular impact experiments in comparison to cisplatin in order to further ascertain the underlying mechanistic causes of the pharmacological distinctions between the therapeutic agents of ruthenium (Table 1.1)[108]. Compared with the 14-fold increase in cisplatin resistance of the crA2780 cells relative to the A2780 cells, **30** and **12** display only a minor degree of cross-resistance, i.e. 1.5-fold and 2.1-fold, respectively. This suggests a notable, but yet unascertained, difference in the exact cell-killing mechanism of the ruthenium drugs. In addition to the pronounced distinctions relative to cisplatin, differences in cellular impact between **30** and **12** are also apparent. In particular, **12** is more effective than **30** at rapidly killing cells at a markedly lower dose. The stark differences observed in the IC_{50} values between the structurally similar complexes have recently been tentatively attributed to the different preferential binding sites of the complexes. It has been reported that **12** favourably binds directly to DNA alone, while the latter forms complimentary adducts with protein components of a cell, going some way to dilute the cell-killing effects of direct DNA-binding.[108]

Table 1.1 - Cell growth inhibition values (μM) of cisplatin (1), RAED-C (30) and RAPTA-C (12) in human ovarian cancer lines A2780 and cisplatin resistant A2780, (crA2780). Reproduced from ref. 108

	Cisplatin	RAED-C	RAPTA-C
A2780			
IC_{50} / μM	1.00 ± 0.05	4.53 ± 0.93	247 ± 15
IC_{90} / μM	9.17 ± 1.85	17.6 ± 1.2	772 ± 35
crA2780			
IC_{50} / μM	14.0 ± 0.3	6.8 ± 0.3	507 ± 38
IC_{90} / μM	26.4 ± 0.6	17.9 ± 0.3	933 ± 58

Further probing was conducted in the same paper, looking at quantifying the extent of DNA adducts at varying concentrations of RAPTA-C (**12**), RAED-C (**30**) and cisplatin (**1**, Fig. 1.15). This is of particular note, as DNA–metal levels are closely linked to the respective cell growth inhibiting power of the different agents. In particular, the amount of DNA adducts measured for the three complexes are approximately equal at their respective IC_{90} concentrations. This implies that the effect of all three agents on cell killing and growth inhibition arises primarily from the adducts formed on DNA, and that any further non-DNA binding effects are complementary to the primary mode of action.[108]

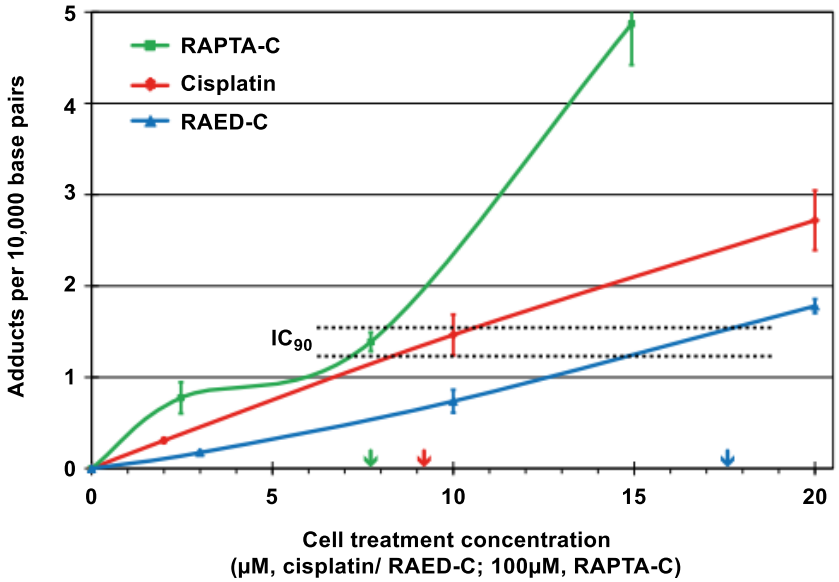

Figure 1.15 - DNA-metal adduct levels in treated A2780 cancer cells. Arrows indicate IC_{90} values for RAPTA-C (green; 7.2 μM), cisplatin (red; 9.2 μM) and RAED-C (blue;17.6 μM). Reproduced from ref. 108

1.5.4. Polypyridyl Complexes of Ruthenium

A fourth class of antitumour ruthenium complexes discussed herein are complexes of ruthenium which feature polypyridyl ligands. These complexes can exist as chiral species that have been shown to undergo enantioselective recognition of DNA. Prior to polypyridyl ruthenium complexes gaining attention as a class of anticancer compounds, the DNA binding and cleaving properties of such complexes, stemming from their chirality, had already been extensively studied. They were investigated as potential probes of the conformation of DNA as well as agents to cleave DNA in studies by Barton *et al.*[109] and Thorp *et al.*[110,111] respectively.

The chloropyridyl complexes [RuCl(bpy)(terpy)]Cl (**31**), *cis*-[Ru(bpy)$_2$Cl$_2$] (**32**) and *mer*-[RuCl$_3$(terpy)] (**33**) (bpy = 2,2'-bipyridyl, terpy = 2,2':6',2''-terpyridine) (Fig. 1.16) have been demonstrated to exhibit cytotoxicity towards murine and human tumour cell lines.[112] Of the three complexes, *mer*-[RuCl$_3$(terpy)] (**33**) showed the highest degree of antitumour activity. All three ruthenium complexes were shown to coordinate to DNA residues in much the same way as cisplatin. *In vitro* studies have demonstrated that it is the metal-DNA adducts that halt DNA synthesis.[113] Corroborative to its enhanced anticancer activity, complex **33** showed a significantly higher degree of DNA crosslinking. This suggests that, as observed with NAMI-A (**10**), the *trans*-functionality of a ruthenium(III) agent is a key component for the formation of relevant crosslinks that inhibit the metastasis of a tumour. Consequently, *trans*-dichloro polypyridyl complexes of ruthenium(III) are presumed to be operative through a cisplatin-like mechanism, and display stark potential as alternatives for platinum(II) anticancer complexes.

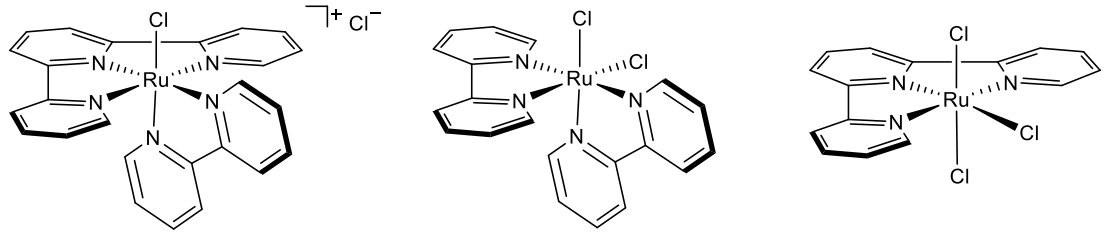

(31) **(32)** **(33)**

Figure 1.16 - Structures of chloropolypyridyl ruthenium complexes [RuCl(bpy)(terpy)]Cl, *cis*-[Ru(bpy)$_2$Cl$_2$] and *mer*-[RuCl$_3$(terpy)][112]

The α-, β- and γ- isomers of [Ru(azpy)$_2$Cl$_2$] (azpy = 2-phenylazopyridine) (**34**, **35** and **36** respectively, Fig. 1.17) were investigated for their cytotoxic properties against a series of tumour cell lines.[114] Interestingly, complex **34** exhibited a high degree of cytotoxicity (observed as even higher than cisplatin), in comparison to the much lower cytotoxicity shown by the β-*cis*-confomer **35** and the *trans*-analogue **36**. The binding of complex **34** to monomeric 9-ethylguanine and guanosine was investigated and compared to previous data obtained of the *cis*-[Ru(bipy)$_2$Cl$_2$] analogue, **32**. The guanine derivatives in the complexes formed from **34** have more orientations than found in the corresponding bipy-

containing analogue **32**. It is suggested that this versatility is a key factor for the ability of a complex to bind to DNA and that it is also related to the cytotoxicity of an agent.[114]

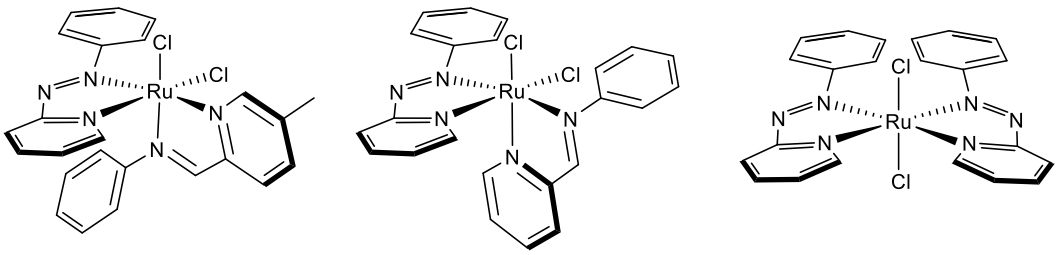

(34) **(35)** **(36)**

Figure 1.17 - Structures of α-, β- and γ-[Ru(azpy)$_2$Cl$_2$][114]

In the same study, the complexes [Ru(azpy)$_3$](PF$_6$)$_2$ (**37**), [Ru(tazpy)$_3$](PF$_6$)$_2$ (tazpy = *o*-tolylazopyrdine, **38**) as well as complexes [Ru(azpy)$_2$(bpy)](PF$_6$)$_2$ (**39**) and [Ru(azpy)(bpy)$_2$](PF$_6$)$_2$ (**40**, Fig. 1.18) were synthesised and their cytotoxic activity investigated in order to ascertain whether the remarkably high cytotoxicity displayed by complex **34** is due to its two *cis* chloride ligands. It is suggested that these might be exchanged for biological targets such as DNA nucleotides, thereby enabling a similar mode of action to cisplatin (Section 1.4). It was found that the cytotoxicity of **37** and **38** were still moderate towards a sizeable selection of tumour cell lines. Even without the presence of chloride ligands on the molecule, cytotoxicity was observed, which suggests that these 2-phenylazopyridine ruthenium(II) complexes are able to work through a mechanism other than the DNA-chelation that is characteristic of cisplatin and other platinum(II) drugs.[114]

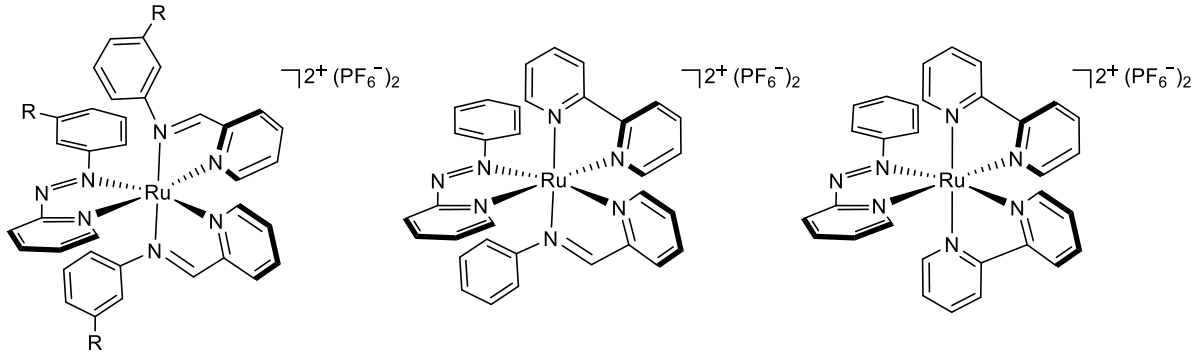

R = H: (37)
R = Me: (38)

(39) **(40)**

Figure 1.18 - Structures of [Ru(azpy)$_3$](PF$_6$)$_2$, [Ru(tazpy)$_3$](PF$_6$)$_2$, [Ru(azpy)$_2$(bpy)](PF$_6$)$_2$ and [Ru(azpy)(bpy)$_2$](PF$_6$)$_2$[114]

1.5.5. Dinuclear Complexes of Ruthenium and Platinum

Polynuclear metal-based complexes represent a relatively novel branch of therapeutic agents. Such complexes are designed with the aim of circumnavigating the problem of both intrinsic and acquired drug resistance without removing any of the active character of an agent, thereby retaining a

therapeutically relevant cytotoxicity profile. This is achieved as such complexes are capable of forming a completely different range of DNA adducts compared to cisplatin and its analogues. Chain length and flexibility, hydrogen-bonding capacity and charge of the linker, as well as the geometry of the chloro-ligand to the linker chain emerge as the key factors in designing polynuclear platinum antitumor drugs. A more challenging extension of the functionalisation of dinuclear complexes is the introduction of a different metal to the coordination sites.[115] Polynuclear complexes have been the subject of a surge of research within the last decade.[109,116,117] A 2016 paper[118] reports the syntheses of a number of dinuclear Ru/Pt complexes (Fig. 1.19), and the cell viability of these complexes investigated via MTT assay against a selection of tumour cell lines. Remarkably, the so-called 'ruthplatins' displayed sub-micromolar and nanomolar cytotoxicities in most of the human cancer cells tested; in nearly all cases exhibiting much lower IC_{50} values than cisplatin. Additionally, in different types of cisplatin-sensitive cancer cells, the ruthplatins showed up to 32-fold increased cytotoxicity compared with cisplatin.

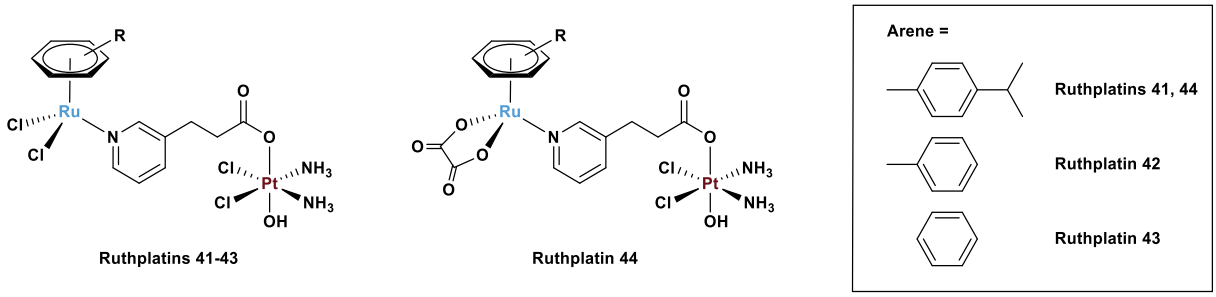

Figure 1.19 - Structures of binuclear complexes prepared by Zhu et al.[118]

1.6. Enzyme Inhibition - Histone Deacetylase Enzymes (HDACs)

1.6.1. An Overview of HDAC Enzymes

The entire human genome is packaged within the nucleus into a macromolecular complex of repetitive nucleosome units; chromatin. Chromatin has four primary functions: (i) to package DNA into a smaller volume to fit the particular cell, (ii) to strengthen DNA in order to facilitate mitosis, (iii) to prevent DNA damage and (iv) control gene expression and DNA replication. A single nucleosomal unit of chromatin is composed of a fragment of DNA (146 base pairs) coiled around a core histone octamer. Histones are small basic proteins that are rich in the amino acids lysine, tyrosine and arginine. They feature accessible sites to undergo various post-translational modifications, including phosphorylation, methylation, and most pertinent to this report, acetylation/ deacetylation. The equilibrium between acetylated and deacetylated histone is regulated by the corresponding enzymes: histone acetylases (HATs) and histone deacetylases (HDACs). The mechanism through which HDACs transform *N*-acetyl-lysine into lysine is highlighted in Figure 1.20.[119] The inhibition of HDACs represents a rapidly developing strategy in human cancer therapy, as these enzymes play a fundamental role in regulating gene expression and chromatin assembly; processes on which the development and accumulation of

cancerous cells rely. Such agents are potent inducers of growth arrest, as well as differentiation and apoptosis of tumour cells.[120]

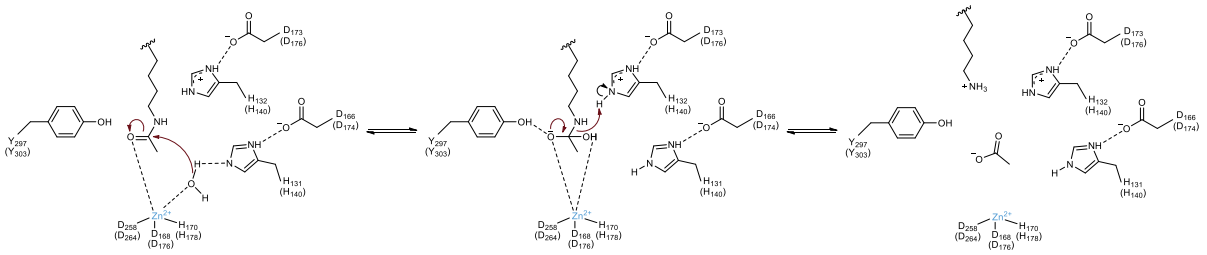

Figure 1.20 - The proposed mechanism for the deacetylation of acetylated lysine. Histone deacetylase-like protein (HDLP) active residues and their HDAC counterparts (in brackets) are labelled. Reproduced / adapted from ref. 20

1.6.2. HDAC Inhibitors

Inhibitors of the histone deacetylase enzymes exist as a relatively wide range of structures, which derive from both natural sources (Fig. 1.21) as well as from synthetic routes (Fig. 1.22). With a few exceptions, they can all be divided into chemical classes including hydroxamic acid derivatives, cyclic peptides, electrophilic ketones, carboxylates and also benzamides.[121]

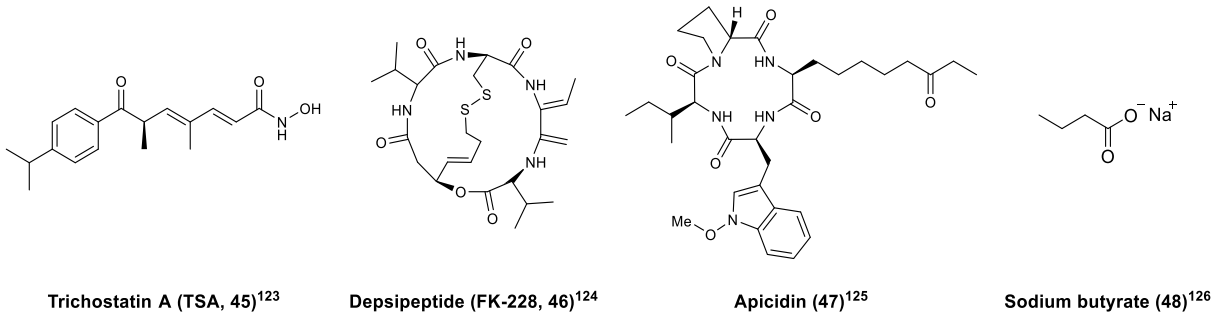

Trichostatin A (TSA, 45)[123] | Depsipeptide (FK-228, 46)[124] | Apicidin (47)[125] | Sodium butyrate (48)[126]

Figure 1.21 - A selection of HDAC inhibitors from natural sources[122]

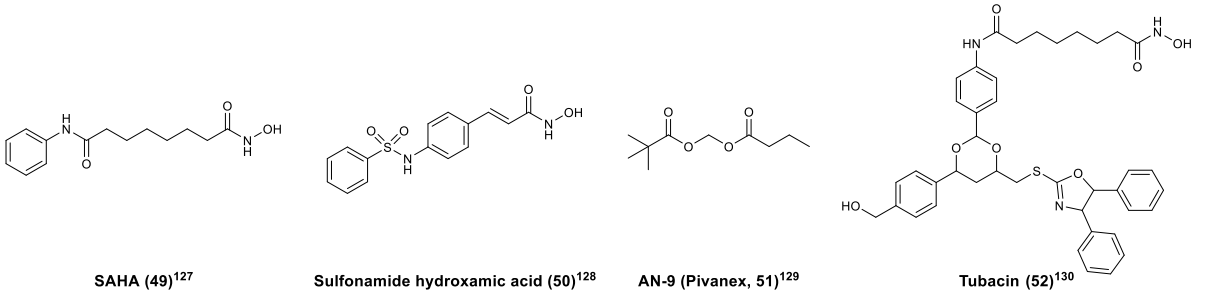

SAHA (49)[127] | Sulfonamide hydroxamic acid (50)[128] | AN-9 (Pivanex, 51)[129] | Tubacin (52)[130]

Figure 1.22 - A selection of synthetic HDAC inhibitors[122]

HDAC proteins are grouped into four classes, based on innate similarities such as subcellular localisation, tissue distribution and substrates. Three of the four classes contain zinc and are known as Zn-dependent histone deacetylases.[130] With successful hydroxamic acid based agents such as

trichostatin A (TSA, **45**), or SAHA **(49)**, the functional hydroxamic acid coordinates to the zinc through its carbonyl and hydroxyl groups, resulting in a penta-coordinated Zn^{2+} (Fig. 1.23). It is proposed that the hydroxamic acid also hydrogen-bonds with both charge-relay histidine residues as well as the Tyr 297 hydroxyl group (Fig. 1.23, right) and replaces the zinc-coordinated water molecule of the active structure with its hydroxyl group.[122]

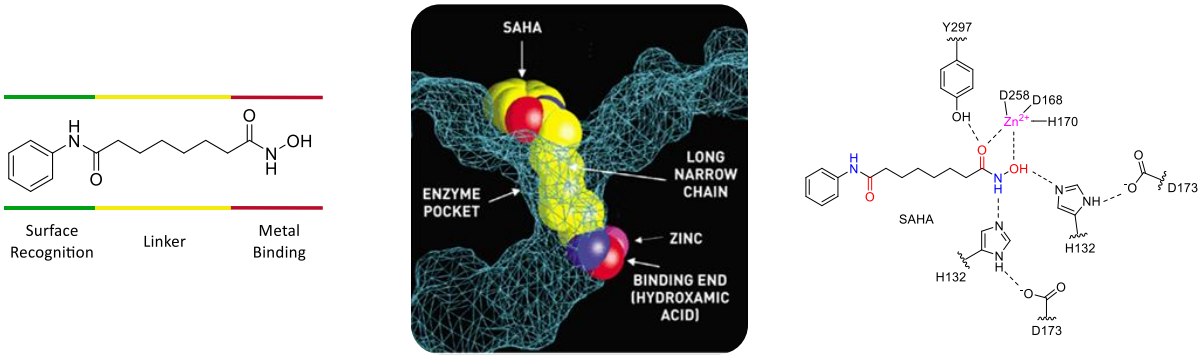

Figure 1.23 - Pharmacophoric schematic of hydroxamic acid derivative HDAC inhibitor structural characteristics (left), space-filling representation of SAHA in the active site pocket, and inhibitor-HDLP enzyme interactions in the active site (right)[122,127]

SAHA, also known as Vorinostat, is a prototypical histone deacetylase inhibiting compound, which was approved in 2006 by the Food and Drug Administration for treatment of cutaneous T-cell lymphoma.[131] SAHA exhibits a 30-fold weaker inhibitory activity than TSA, but the two agents have been observed to bind HDLP similarly. The SAHA hydroxamic acid group makes the same contacts to the zinc and active-site residues, and the importance of these interactions is underscored by the loss of activity of SAHA derivatives lacking the hydroxamic acid group.[132] The aliphatic chain of six carbons of SAHA packs in the tube-like hydrophobic portion of the pocket. Compared to TSA, however, SAHA's aliphatic chain packs less snugly and makes quantitatively fewer van der Waals contacts, which is reported to be in part because SAHA lacks TSA's alkenyl methyl-group branch (Figs. 1.21, 1.22).[122] SAHA also lacks TSA's double bonds in this region, and this may lead to increased flexibility of the aliphatic chain, where rigidity may be a favourable characteristic. Further, the capping group of SAHA consists of a phenyl-amino ketone group. In the crystal structure of a SAHA-inhibited HDLP enzyme, the phenyl group displays weak electron density, suggesting that it may not pack as well as the cap group of TSA. This could be due, in part, to the larger spacial separation between the hydroxamic and cap groups of SAHA than between those of TSA.[122]

1.6.3. Organometallic HDAC Inhibitors

Recently, there has been a surge of research into the design and pharmacological testing of organometallics-based HDAC inhibiting agents. Again, additional features such as variable geometries,

redox potentials as well as easily functionalisable ligands in additional coordination sites around the metal centre(s) make such complexes a very attractive branch of therapeutic chemistry.

The group of Marmion *et al.*[133] report the design and synthesis of a novel multifunctional drug of platinum(II) with DNA binding, histone deacetylase inhibitory activity and enhanced selectivity for cancer cells (**53**). One of the major drawbacks of platinum-based anticancer therapeutics is their non-discriminate toxicity leading to damage to healthy cells. An important asset of histone deacetylase inhibiting agents is their impressive selectivity towards cancer cells. It was therefore theorised that the incorporation of a hydroxamic acid motif with appropriate spacer group may confer selectivity to the drug candidate. Moreover, it was speculated that the additional functionality of the complex may be active against a broader range of cancer lines, in particular those that have acquired cisplatin resistance. While no synergistic effect or improved efficacy towards cisplatin-sensitive or cisplatin-resistant lines were observed, complex **53** did exhibit marked selectivity for cancerous cells over healthy cells, while showing a similar toxicity to cisplatin (IC_{50} value of 9 ± 3 µM vs IC_{50} of 2.9 ± 0.1 µM).

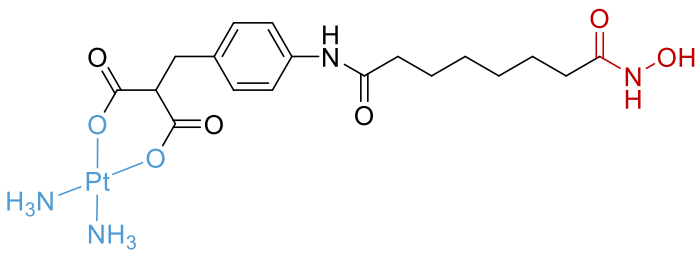

(53)

Figure 1.24 -Bifunctional platinum(II) complex, with DNA-intercalating (blue) and HDAC inhibiting (red) functionalities highlighted[134]

A series of ferrocene-based SAHA analogues were reported by Spencer *et al.*,[134,135] many of which displayed similar, if not better, inhibitory profiles towards zinc-dependent HDACs. JAHA (**54**) and *homo*-JAHA (**55**) both showed such inhibitory profiles, however, only the former exhibited a clinically relevant activity on MDA-MB231 cell lines, representing aggressive human breast cancer (IC_{50} of 8.45 µM at 72 h). While the exact reasoning remains to be discerned, this discrepancy between the JAHA congeners suggests that the additional methylene spacer in *homo*-JAHA has a large effect on its activity in a cellular environment, and highlights the importance of precise and detailed biological characterisation when designing such enzyme inhibitors. A further complex of the JAHA scaffold; ferrocenyl-SAHA (Fc-SAHA, **56**), has been reported to show an IC_{50} value two-fold lower than that of SAHA in an HDAC binding assay, but an IC_{50} value over four-fold higher than that of SAHA when introduced to MCF7 breast cancer cell lines.[136] This suggests that ability as an HDAC inhibitor, while a very good indication of the efficacy of a compound as an anticancer drug, may not be the only relevant factor.

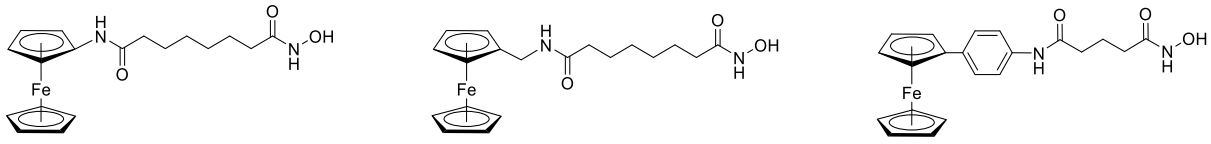

Figure 1.25 - Structures of JAHA and two of its derivatives[135,136]

Recently, the JAHA scaffold has been used in the design of a light-activatable organometallic HDAC inhibitor. This is reported to be the first example of photoactivated release of an organometallic enzyme inhibitor.[136] P-Fc-SAHA (**57**) features a photolabile leaving group about the hydroxamic ester, which, when removed via irradiation, relinquishes the active complex; the hydroxamic acid featuring Fc-SAHA, which has previously been shown to efficiently inhibit HDACs and be highly cytotoxic towards various cancer cell lines. Activating the drug through irradiation allows for spatial and temporal control of the activity of the system. This contributes to the lessening of side effects, as an inactive, relatively benign complex is in transit around the body up to the point of activation at the relevant site. Novel enzyme inhibiting compounds as well as tailored drug delivery are much sought after tools to be developed in modern therapeutic chemistry, and an ever-growing body of literature is incorporating and developing these areas.

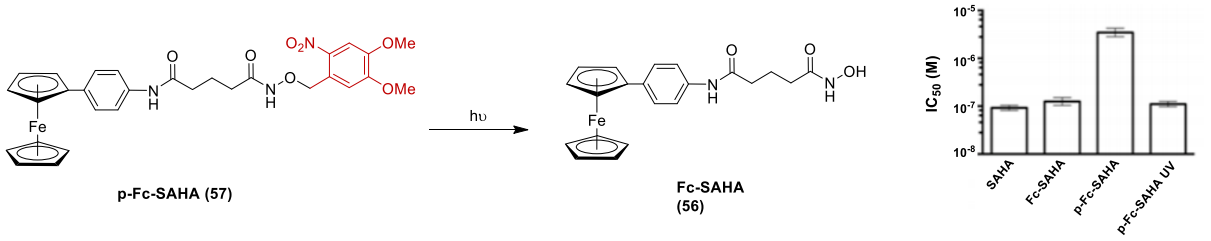

Figure 1.26 - Activation of histone deacetylase inhibiting agent Fc-SAHA by removal of photolabile protecting group (red, left) and inhibitory activity of 51 and relevant derivatives against the HDAC1 enzyme (right)[137]

A phosphorescent rhenium(I) histone deacetylase inhibitor (**58**) has recently been reported (Fig. 1.27, left). Rhenium complexes are suitable scaffolds to be utilized to construct highly effective enzyme inhibitors[137] and recently, a growing number of studies have demonstrated that rhenium complexes can also undergo photodynamic anticancer therapeutic activities.[138,139] While rhenium(I) organometallic complexes have been shown to display potent anticancer activity, some with activity comparable to that of cisplatin, their anticancer mechanism is largely unknown.[140] However, perhaps the most impressive feature of the reported rhenium(I) complexes is their dual function as diagnostic tools as well as therapeutic agents. Complexes of rhenium(I) with relevant intraligand (π - π^*) and metal to ligand (dπ - π^*) charge transfer processes, with long-lived excited states and large Stokes' shifts, express innate imaging capabilities that, when paired with anticancer properties, provide an incredibly useful tool in the monitoring of anticancer activity.[141] Similar complexes of ruthenium(II), featuring this dual "theranostic" action, have also been prepared (Fig. 1.27, right).[142] Complex **58** was tested in comparison to cisplatin and the 'naked' hydroxamic acid-containing ligand, i.e. prior to ligation, against a number

of cell lines. The majority of the selected cell lines show the rhenium(I) complex to have a higher cytotoxicity profile than both cisplatin and naked ligand, while also showing an impressive cytotoxicity towards cisplatin-resistant cells, as well as marked selectivity towards tumour cells. Such complexes represent another example of the direction of anticancer therapy; enzyme inhibiting or otherwise, to fully exploit photodynamic effects in a therapeutic context.

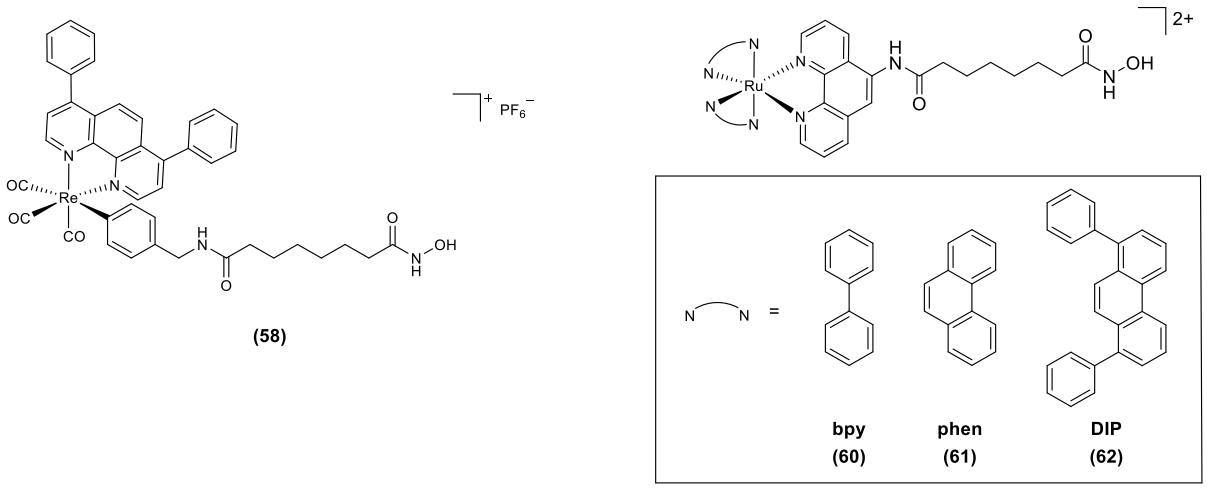

Figure 1.27 - Phosphorescent rhenium and ruthenium-based histone deacetylase inhibitors from Mao *et al.*[142,143]

Project Aims

The primary intention of this project is to expand and diversify the library of known HDAC inhibiting anticancer agents, while investigating the role of metals within anticancer therapeutic chemistry. These intentions will be realised through the following aims:

- A selection of ruthenium(II) sandwich complexes, featuring an η^6-arene capping group, as well as a cyclopentadienyl motif to facilitate the desired hydroxamic acid functionality are to be synthesised. Variations in capping arene, chain length and functionality, and additional functionality about the Cp ring, as well as investigations into the optimum metal centre and counterion are all routes to be explored.
- Ruthenium(II) sandwich complexes with a functionalised η^6-benzene ligand, which confers the active Zn^{2+} binding hydroxamic acid group as well as a cyclopentadienyl capping group are also synthetic targets. The same variations as the first class of sandwich complexes are to be explored in depth.
- Piano stool complexes of ruthenium(II), which utilise *N*-heterocyclic carbene ligands as a binding group to the metal, which facilitates the terminally attached hydroxamic acid on an alkyl spacer chain are also to be synthesised.
- All successfully synthesised complexes are to have their anticancer properties investigated through a series of biological assays.

2. Results and Discussion

2.1. Ruthenium(II) Sandwich Complexes as HDAC Inhibitors

Stark potential has been shown by organometallic HDAC inhibitors - namely the ferrocene-based JAHA and its derivatives, as well as the numerous ruthenium-based enzyme inhibitors discussed in Section 1.6.3 (*vide supra*). This provided the theoretical interest for an investigation into the anticancer properties of novel, functionalised sandwich complexes of ruthenium. Ruthenium complexes with a capping arene group as well as a tether-functionalised cyclopentadienyl motif have been scrutinised by the Walton group in the context of nucleophilic aromatic substitution catalysis.[143] Notably, the catalyst **59** bears structural similarities to JAHA (**54**) in terms of its metallocene framework and long, functionalised alkyl tether (Fig. 2.1). Thus, it was hypothesised that such Ru sandwich complexes could also play a role in HDAC inhibition. Based on this reasoning, the target molecule **60** was designed as a potential candidate for HDAC inhibition.

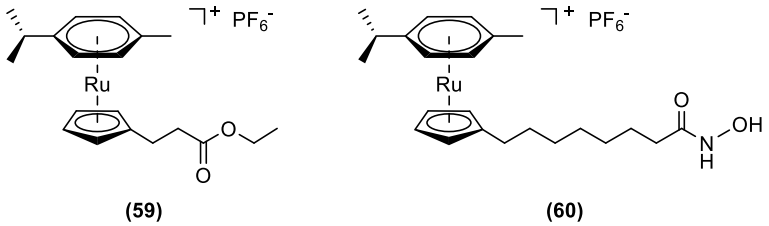

(59) **(60)**

Figure 2.1 - Structures of candidate compound for catalysis 59 and adapted HDAC inhibitor candidate 60

2.1.1. Synthesis

The synthesis of complex **60** is shown in Scheme 2.1. Following the generation of the cyclopentadienyl tether **62**, which is subsequently η^5-chelated to the ruthenium centre via reaction with the dichloro(*p*-cymene)ruthenium(II) dimer to form the sandwich complex **63**, the hydroxamic acid functionality is conferred through reaction of the resulting methyl ester with excess hydroxylamine to produce target molecule **60**.

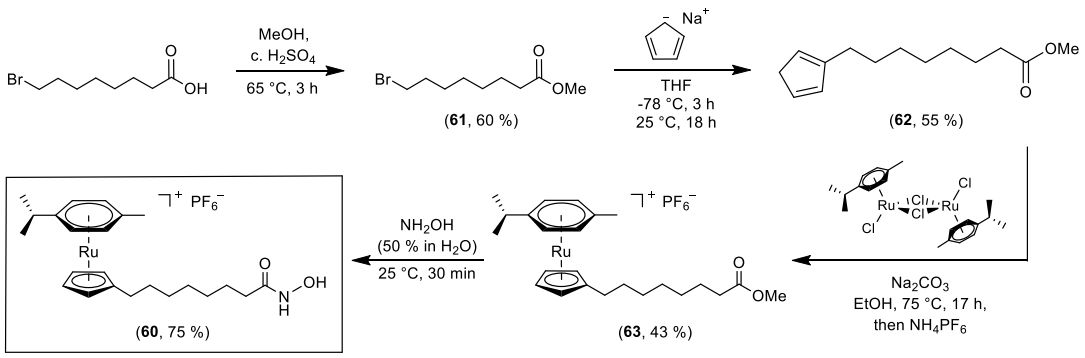

Scheme 2.1 - Synthetic procedure of complex 60

The reaction proceeds in moderate yield for each step, leading to an overall yield of 11 % over four steps for this *p*-cymene derivative. It may be possible, however, to significantly improve the yield of tethered-cyclopentadiene intermediate **62** through the use of a cosolvent, thereby improving the overall yield of target molecule **60**. Mukopadhyay and Seebach[144] report the use of *N,N'*-dimethyl-*N,N*'-propylene urea (DMPU) as an alternative for the commonly used, but carcinogenic, cosolvent hexamethylphosphoramide (HMPT). Both cosolvents are reported to significantly improve the yield of a series of nucleophilic substitution reactions involving anionic, highly reactive nucleophiles. This is achieved as the two cosolvents selectively dissolve cations, thereby accelerating otherwise slow S_N2 reactions by generating more "naked" anions. This modification to the synthesis was, unfortunately, realised following the synthesis itself, but remains an option for the optimisation of syntheses featuring the nucleophilic attack of the cylopentadienyl anion.

The first structural variation to be investigated was decided to be the arene capping group. Changing the sterics and electronics of the capping group could reveal interesting interactions between the molecule and the rim of the HDAC pocket, and a small library of compounds could readily be produced simply by modifying the successful synthesis of **60** to include a different ruthenium dimer. The synthesis of the benzene-capped analogue of **60**; complex **65**, was attempted following the same synthetic method (Scheme 2.2).

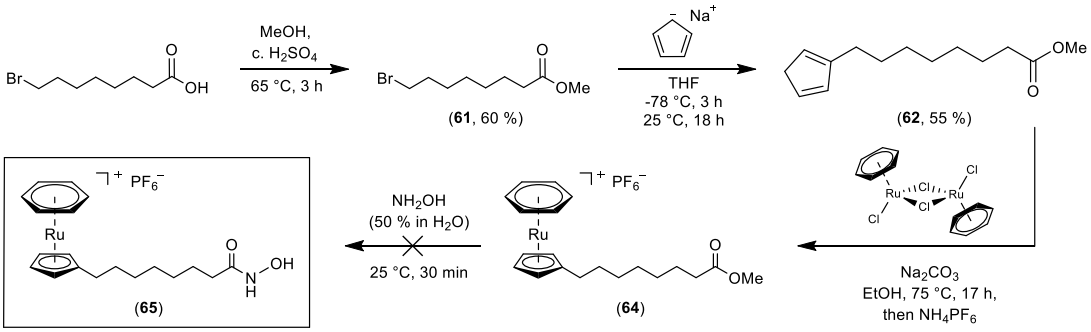

Scheme 2.2 - Synthetic procedure of complex 65

This synthesis was expected to proceed in the same way as that of complex **60**. However, synthetic steps following the introduction of the benzene motif via the ruthenium dimer were observed to proceed more reluctantly than for the *p*-cymene precursor **60**. Complex **64** was isolated as an impure mixture following column chromatography, and the reaction between **64** and hydroxylamine gave no evidence of product having been made. Similar piano stool complexes of ruthenium with both *p*-cymene and benzene capping groups are reported in the literature,[145] and it is commented that the benzene complexes are generally less stable. This is a result of the inductive electron donating effects of the alkyl groups of *p*-cymene contributing to a more electron rich arene which can form a stronger bond to the metal centre. The fact that the metal-arene bond is weaker for benzene than for *p*-cymene might suggest that the arene may exhibit some degree of lability, and it is this that is, at least in part, responsible for the relative reluctance of the benzene-capped molecules **64** and **65** to form in good purity and high yield.

However, the ^{1}H NMR spectrum of the isolated mixture following reaction of **62,** which was acquired following column chromatography (Fig. 2.2), strongly suggests that this is not be the reason for the observed lack of reactivity of **64** in the formation of **65**. Fig 2.2 is shown to be a mixture of two discernible products. There are peaks corresponding to target molecule **64**, and there is also evidence for the presence of the free Cp-tether ligand **63**. This indicates that either the reaction had not gone to completion and the starting material **63** and product **64** pass through the column system (CH_2Cl_2 : EtOH, 0 – 0.5 % in 0.1 % increments) with similar R_f values, or that the product decomposed at some point in the column. The synthesis of complex **65** is likely to have been unsuccessful as a result of this observed lack of purity of **64**.

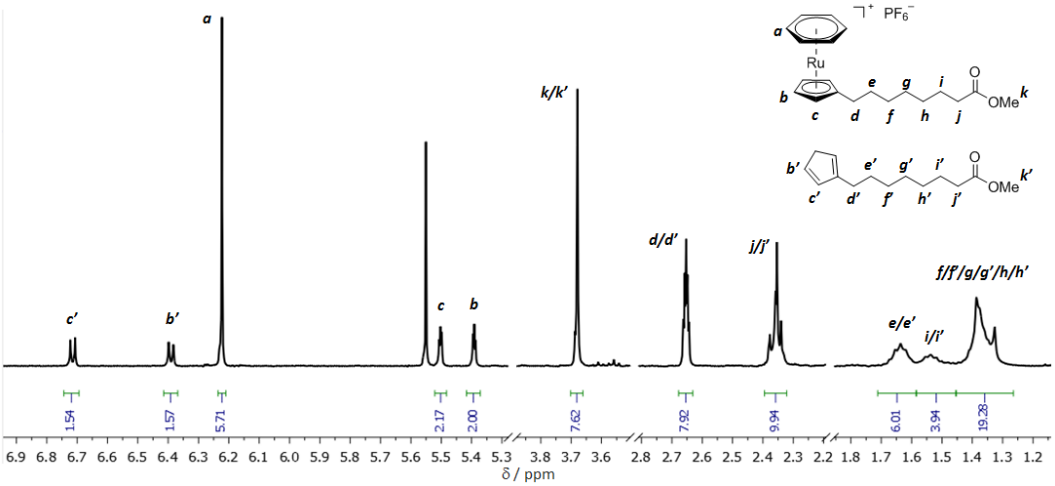

Figure 2.2 - Acquired ^{1}H NMR (methanol-d4, 400 MHz) spectrum of complex 64 with peak integrals shown

The singlet at 6.22 ppm has been assigned as the η^6-benzene protons, as it lies within the relevant region, with a corresponding integral of around 6, relative to the integral of 2 for the protons assigned to be in environment ***b*** on the ruthenium-bound, tethered Cp moiety. Metallocene complexes with a benzene group have been shown in the literature to undergo arene exchange reactions when photolysed.[146] The photolysis of complexes **64** and **65** in an excess of a substituted arene in order to facilitate such arene-exchange reactions was to be investigated had either compound been synthesised in high purity and good yield. This investigation could have allowed for a catalogue of analogues with varying capping groups to be synthesised without the need for a multistep syntheses for each target molecule.

2.1.2. MTT Toxicity Assay

With HDAC inhibitor candidate **60** in hand, an MTT assay could be carried on the non-small cell lung cancer cell line NCI-H460 in order to determine its cytotoxicity. The MTT assay is a quantitative, colourimetric measurement of a compound's toxic effects which operates via the reduction of a tetrazolium dye by NAD(P)H-dependent cellular oxidoreductase enzymes. It is a good quantitative assay, given that MTT is a soluble, yellow tetrazole that is reduced in living cells to the insoluble, purple

formazan. Thus, the generation of formazan and the resultant intensity of colour produced by the molecule gives a quantitative measurement of cytotoxicity, in that the higher the measured absorbance, the fewer cells have been killed by the agent, i.e. the agent is less cytotoxic.[147] In addition to complex **60**, prototypical anticancer agents cisplatin and SAHA were also measured as controls. The results are summarised in Table 2.1 and Figure 2.3. IC_{50} values represent the concentration of an agent required in order to reduce cell viability to 50 %.

Table 2.2 - *In vitro* cytotoxicity of complex 60 and controls cisplatin and SAHA in an MTT assay with NCI-H460 non-small-cell lung carcinoma cell line (3 day exposure) of 200 cells per well

	Cisplatin	SAHA	Complex 60
IC_{50} / μM	0.18 ± 0.02	0.37 ± 0.06	7.4 ± 4.8

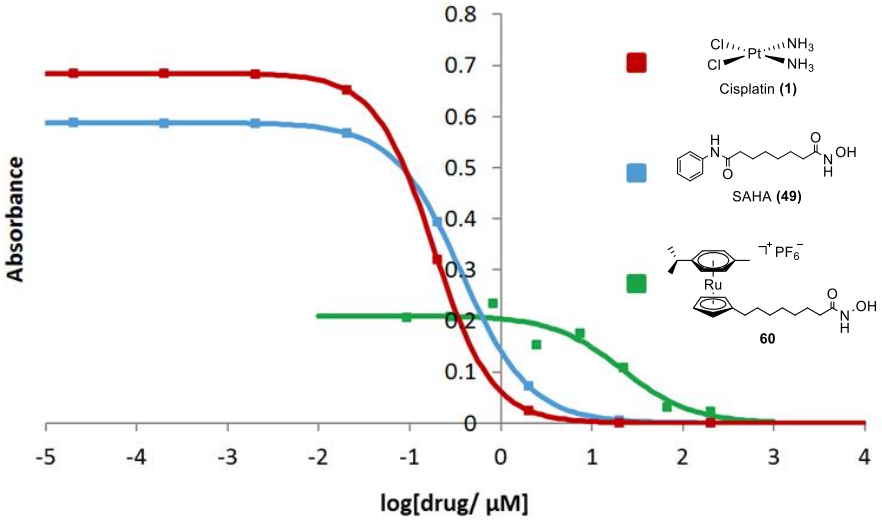

Figure 2.3 - Absorption curves for SAHA, cisplatin and complex 60 from MTT assay. Data processing gives the IC_{50} values shown in Table 2.1

The newly synthesised complex was successful in causing antiproliferative activity against the cancer cells. This is in contrast to many ruthenium complexes, which show no activity against this cell line - often showing IC_{50} values above 200 μM.[148] While it is notable that complex **60** showed toxicity towards the cell line, it has a worse cytotoxicity profile than the clinically approved agents cisplatin and SAHA by over a full order of magnitude, which highlights room for optimisation for this class of compounds. The observed discrepancy between **60** and SAHA can be for a number of reasons. Firstly, complex **60** is a positively charged molecule, which may hamper its passing through a biological medium as well as its entry into the HDAC 'pocket'. As a charged complex, the associated counterion to **60** may cause issues within pharmacological conditions. PF_6 salts are normally relatively insoluble in aqueous solutions, and while the assay was carried out in DMSO, in which the complex was observed to readily solvate, its transit within a cellular environment may be impeded by the counteranion. Hexafluorophosphate is also a sterically large counterion, which may exacerbate its negative effects on

the cytotoxicity profile of **60**. To do a counterion exchange and produce the chloride salt may yield a candidate with higher bioavailability and resultantly a better cytotoxicity, if this reasoning holds true. A second feature of the synthesised complex, which may rationalise its worse antiproliferative ability, is the steric bulk of the head group. Again, the sandwich part of the molecule, featuring the additional steric bulk of the isopropyl and methyl groups of the *p*-cymene capping group, may not facilitate the active, terminal hydroxamic acid to reach the zinc domain at the base of the enzyme pocket. A final discrepancy is the presence of the amide linker in SAHA, which is foregone in the synthesis of **60** due to it significantly complicating the synthesis of the analogue. This linking group is suspected to offer favourable hydrogen-bonding interactions with the amino acids found in the rim of the enzyme pocket as well as to confer a desirable geometry about the head group. Indeed, it has been reported in the literature that in the crystal structure of SAHA bound to the active site of HDAC 8, there is a hydrogen bonding interaction between the amide carbonyl of SAHA and protonated Asp101.[149] Further complexes would need to be tested in order to investigate each of these motifs and truly optimise a ruthenium-based sandwich-molecule HDAC inhibiting agent.

2.1.3. HDAC Assay

In order to ascertain whether the candidate **60** operates through a mechanism of enzyme inhibition, as well as to enforce the cytotoxicity profile gathered through the MTT assay, a fluorometric HDAC assay was also carried out. The assay operates through a substrate and developer combination - when the acetylated lysine side chain on the substrate is deacetylated, it becomes sensitised to the developer such that mixing with the developer generates a fluorescence response. This fluorophore is excited with light of wavelength 360 nm and emits light of wavelength 460 nm, which is detected on a fluorometric plate reader. The intensity of the light emitted corresponds negatively to the extent of enzyme inhibition, i.e. the higher intensity the fluorescence, the more activity of the HDAC enzyme is observed. From this, a measurement relative to a control of a candidate's inhibitory activity can be determined. The control measurement includes just enzyme, substrate, and subsequently developer, with no inhibitory agent. Thus, the maximum possible amount of deacetylated lysine chains are present, generating the maximum possible amount of fluorophore and the highest intensity fluorescence.

In collaboration with Dr. Jason Gill in the School of Pharmacy at Durham University, HDAC fluorometric assays were carried out on complex **60** alongside known HDAC inhibitors trichostatin A (TSA, **45**) and SAHA (**49**). The results of the assay are summarised in Table 2.2.

Table 2.3 - Histone deacetylase activity of TSA, SAHA and complex 60, relative to enzyme / substrate control (mean values, n = 2)

	Control	TSA	SAHA	Complex 60
1 μM	100 %	0.1 %	0.5 %	11.3 %
100 nM	100 %	24.9 %[1]	6.3 %	68.4 %

[1] TSA added at 10 nM final

Complementary to the MTT assay, complex **60** showed a histone deacetylase inhibiting activity of over an order of magnitude lower than that of SAHA, with an IC_{50} value of between 0.1 and 1 μM. TSA, an HDAC inhibitor with higher activity than SAHA, shows marked activity on the 10 nM scale. The fact that the IC_{50} values of **60** and SAHA remain relatively constant across the two assays is a good indication that the cytotoxicity of **60** is due to its enzyme inhibiting capabilities. While it is a positive indication that **60** is shown to display HDAC inhibiting activity, it is not on a therapeutically relevant scale, likely for the reasons discussed for its relatively low cytotoxicity profile, in Section 2.1.2. It is, however, a very positive result for the novel complex **60** to exhibit HDAC inhibition, and as such, **60** remains a relevant starting point for further optimisation of novel, ruthenium-based sandwich molecules. The synthesis of a broad range of possible HDAC inhibiting complexes like **60** can be justified by the fact that it is shown to inhibit the HDAC enzyme, and that there are many parameters to investigate. These include the capping arene, the length and functionality of the alkyl spacer chain, substituents off of the Cp motif as well as investigations into congeners of different metals such as iridium or osmium.

2.1.4. Benzene-functionalised Analogues

Building on the success of complex **60**, the syntheses of two further complexes were attempted. These analogues of complexes **60** and **65** feature reversed functionality: a hydroxamic acid-functionalised benzene head group with a capping cyclopentadienyl derivative (Scheme 2.3).

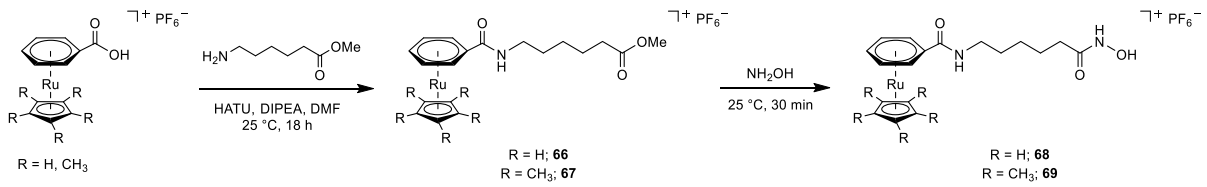

Scheme 2.3 - Synthetic procedure of complexes 68 and 69

Starting from η^6-benzoic acid(cyclopentadienyl)ruthenium(II) hexafluorophosphate, or its pentamethylcyclopentadienyl congener, an amide coupling reaction with 6-aminohexanoic acid was carried out using HATU (1-[bis(dimethylamino)methylene]-1H-1,2,3-triazolo[4,5-b]pyridinium 3-oxid hexafluorophosphate) as the coupling reagent. Evidence of the formation of complexes **66** and **67**

was observed in the mass spectrometry and ^{1}H NMR spectra. The solvent and residual DIPEA were removed by heating the reaction mixture at 80 °C under high vacuum and the crude reaction mixtures were taken through to the final step. Interestingly, at this point, the two mixtures were observed to behave differently in the NH_2OH/H_2O/MeOH mixture. While the crude mixture of Cp* analogue **67** became homogenous in 4 mL solution (2 mL of 50 % by wt. NH_2OH in H_2O and 2 mL MeOH), the crude mixture of Cp analogue **66** had an insoluble precipitate which remained such with even up to 4 mL NH_2OH/H_2O and 8 mL MeOH. This hampered the production of **68**, which required a further 2 mL aliquot of NH_2OH/H_2O solution as well as 2 further days stirring in addition to the conditions required for **69** to form as the only observable product (discernible by ESI^{+} mass spectrometry, Fig. 2.4).

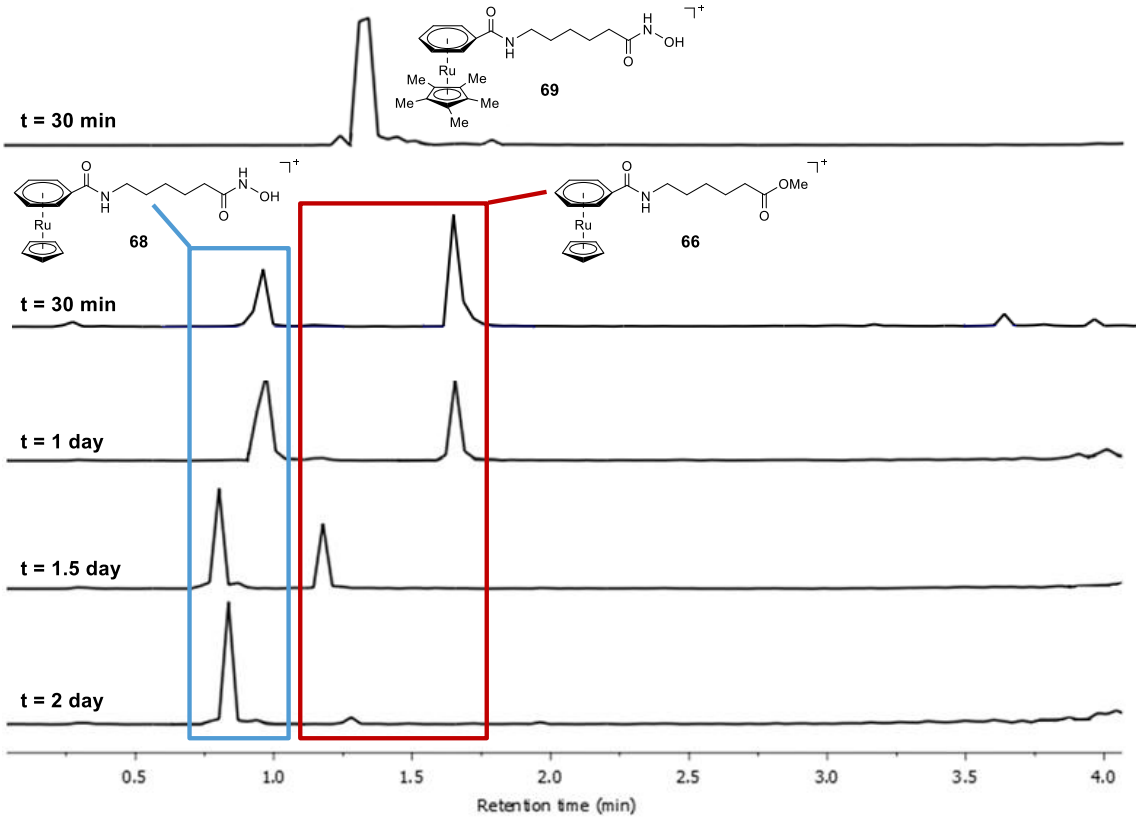

Figure 2.4 - Mass chromatogram between *m/z* = 480-490 (top spectra, *m/z* 67 = 486.1582, 69 = 487.1535) and 410 - 420 (bottom four spectra, *m/z* 66 = 416.07997, 68 = 417.0752) for the two reaction mixtures at varying reaction times. A second aliquot of NH_2OH/H_2O was added to the reaction mixture of 66/68 following the spectra taken at t = 1 day

The observed disparity in the reactivities of **66** and **67** are suspected to be a result of the solubilty of the two complexes in the methanol solvent. The ESI-LCMS (M^{+}) trace showed good separation for both **68** and **69**, and so HPLC was employed as a purification method. However, the results of this purification were not received within the timeframe of the project, but the isolation of complexes **66** and **67** remain ongoing targets for the Walton group.

2.2. *N*-Heterocyclic Carbene (NHC) Complexes of Ruthenium(II) as HDAC Inhibitors

2.2.1. NHC-containing Piano Stool Complexes of Ruthenium

Candidate complexes (**70**, **71**) for HDAC inhibition, featuring the desired functionality through a ruthenium-bound pyridine motif, had been prepared by the Walton group prior to the start of this project (Fig. 2.5). Preliminary studies on these complexes as HDAC inhibitors revealed that the ruthenium-pyridine bond was quite labile, giving rise to a number of challenges. Firstly, the lability of the bond hindered the purification of the complex (high performance liquid chromatography would overcome the energy barrier in order to dissociate the ligand). Further, this feature of the candidates raised questions about their *in vivo* efficacy: i.e., whether physiological conditions would dissociate the pyridine head group from the ruthenium metal, thus leaving the incorporation of the organometallic moiety as a redundant addition to the resultant SAHA analogue.

In order to overcome this setback, the utilisation of an *N*-heterocyclic carbene head group, which exhibits a markedly stronger metal-ligand bond than pyridine, and has the same potential for functionalisation (complex **72**, Fig. 2.5) was designed as an initial, synthetically accessible target.

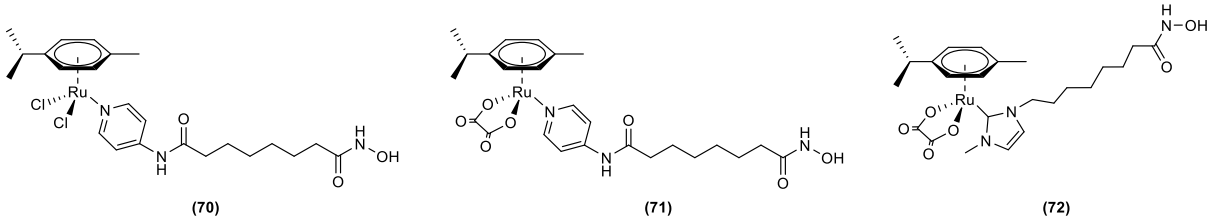

Figure 2.5 - Pyridine-functionalised HDAC inhibitor candidates 70 and 71, and NHC analogue 72

The stronger bonding mode exhibited between an NHC ligand and a metal, with respect to that of an *N*-bound pyridine ligand and a metal, is a result of two effects. The carbene lone pair is situated on a less electronegative atom, in a more reactive sp^2 hybridised orbital, and the nitrogen lone pairs on the heteroatoms adjacent to the carbene carbon can induce further reactivity through a resonant effect (Fig. 2.6, left). These features should lead to a much stronger σ bond between ligand and metal for **72** in comparison to the pyridine in **70** and **71**. Moreover, the empty *p*-orbital on the sp^2 hybridised carbene facilitates π back-bonding from the filled metal *d*-orbitals on the metal (Fig. 2.6, centre). This synergistic bonding mode of concerted σ bonding from ligand to metal as well as π back-bonding from metal to ligand is what, ultimately, leads to the marked stability of the M-L bond for ruthenium and an NHC ligand. As an additional note, if it was a subsequent requirement to further strengthen the metal-ligand bond, the incorporation of electron withdrawing groups with resonant effects on the 3- and 4-positions of the heterocycle have been reported to incur stronger π back-bonding and thus, a stronger overall M-L bonding effect (Fig. 2.6, right).[150]

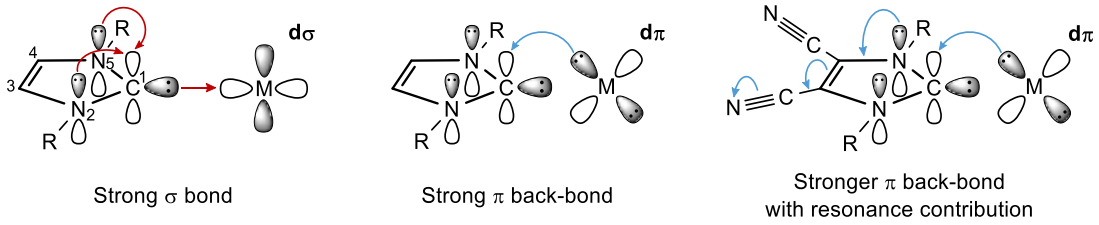

Figure 2.6 - Bonding mode of *N*-heterocyclic carbene when ligated to a metal centre. π back-bonding of NHC with and without resonance contributions shown

2.2.2. Synthetic Route 1

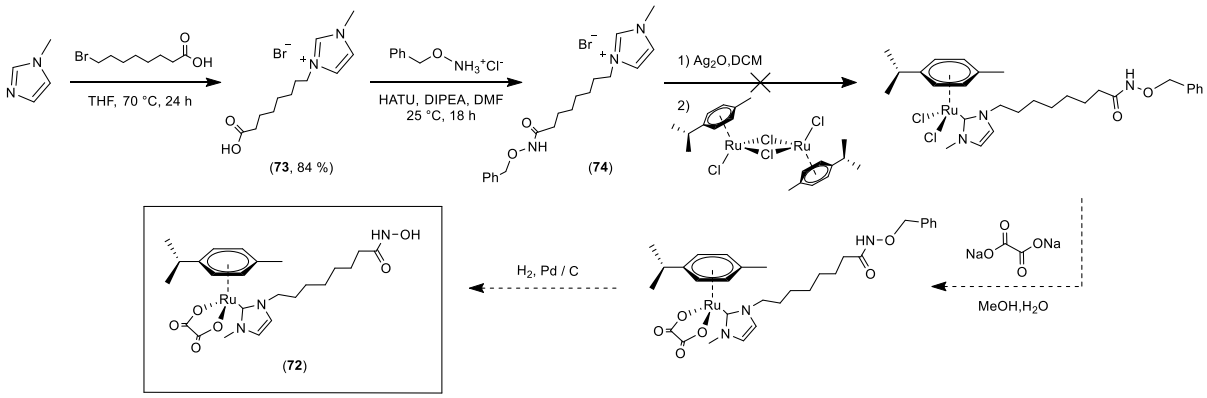

Scheme 2.4 - The first synthetic procedure of complex 72

A retrosynthetic analysis of target molecule **72** broke the compound into its component functional building blocks, and a synthetic scheme was designed (Scheme 2.4). Starting from *N*-methylimidazole, the carbene precursor was alkylated to form *N*-methylimidazole-*N'*-8-octanoic acid, which sees the introduction of the alkyl spacer group of the HDAC inhibitor. Prior to the activation of the carbene, the carboxylic acid group required protection in order to make the imidazolium proton the most acidic proton on the molecule and the generation of the carbene to be the most favourable process upon treatment with Ag_2O. The carboxylic acid was coupled with O-benzylhydroxylamine hydrochloride with the coupling agent HATU to produce the protected carbene precursor **74**. Treatment of such imidazolium salts with Ag_2O activates the carbene and establishes a weak NHC-Ag bond which can then be transmetalated to the Ru-centre. This low bond enthalpy is what makes Ag_2O a good transfer reagent, particularly for transmetalation reactions to form complexes of metals such as Au, Cu, Ni, Pd, Pt, Rh, Ir, as well as Ru. Both the lability of the NHC-Ag bond and the typical insolubility of the produced silver halide are the driving forces for the forward reaction in forming the ruthenium complex. Using this procedure also overcomes the difficulties associated with alternative methods, which typically try to isolate the free carbene, i.e. the use of strong bases, the generation and sustainment of a very inert atmosphere as well as complicated workups.

Imidazolium-based carbene precursors such as **74** are typically ionic liquids, i.e., a salt in which the ions are poorly coordinated, such that the compounds remain liquid at room temperature and pressure. There are inherent difficulties associated with the use of conventional purification methods with ionic liquids. For instance, compound **74** partitioned in a selection of extraction solvents. This happens as the compound features both a hydrophilic, ionic heterocycle as well as a hydrophobic alkyl chain. These binary characteristics within the same molecule also led to a large degree of streaking when column chromatography was attempted. This behaviour was also observed during ESI-LCMS (M^+) experiment. Compound **74** could not be completely purified with any of the following attempted methods: (i) separation in H_2O/ DCM, (ii) recrystallization from MeOH, (iii) column chromatography and (iv) trituration in diethyl ether. An eluent composed of 20% MeOH in toluene showed some degree of separation by TLC but column chromatography did not yield the isolated product **74**. Column chromatography with a second solvent system, the 'magic mix' used in the purification of the [5]catenane olympiadane[151] was also attempted as a proven method of purifying compounds with ionic character. This eluent is a 1:2:7 mixture of CH_3NO_2, NH_4PF_6 and MeOH, however NH_4Cl was used in this case as a cheaper alternative to the phosphorus hexafluoride salt. A yellow/ green oil was collected, which was observed by a ^1H NMR experiment to still be a crude mixture of multiple components. Fine-tuning the relative proportions of this eluent system may still be a worthwhile investigation in order to successfully purify **74** and other ionic liquid precursors.

In the case that **74** had been produced and attached to the ruthenium centre through reaction with Ag_2O and then transmetalation onto the ruthenium, two subsequent steps were to follow. Firstly, a ligand substitution reaction to chelate the more kinetically inert oxalate ligand onto the two chloro-substituted sites of the ruthenium centre, and then deprotection of the benzyl-hydroxamic ester to furnish the active, hydroxamic acid functionalised complex **72**.

A modification to the synthesis was designed, in order to introduce the imidazolium-based carbene precursor as late in the synthesis as possible, and keep the handling of ionic liquids to a minimum (Scheme. 2.5).

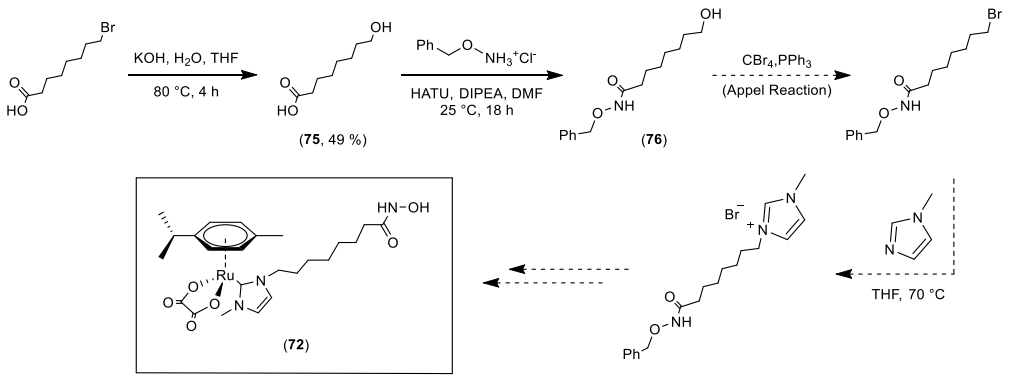

Scheme 2.5 - First synthetic strategy for complex 72, modified to limit the problems associated with ionic liquid intermediates

This modified approach circumnavigates the need for a reactive alkyl halide to be involved in steps concerning other functionalities of the molecule. Further, the only step in which the imidazolium compound would feature would be its coordination to the ruthenium metal, at which point the troublesome binary character of the compound is minimised, as the NHC is established as a ligand.

8-Bromooctanoic acid was reacted with an excess of potassium hydroxide to form 8-hydroxy octanoic acid (**75**). An attempt was made to couple this with the O-benzyl hydroxamic ester protecting group with coupling agent HATU and base DIPEA. Evidence of product **76** was observed by ^{1}H NMR spectroscopy on the crude reaction mixture, following the removal of solvent and DIPEA *in vacuo*. However, product **76** was not isolated in a sufficient enough quantity in order to take the reaction forward.

At the same time, a second modified synthetic route was explored in tandem to the above.

2.2.3. Synthetic Route 2

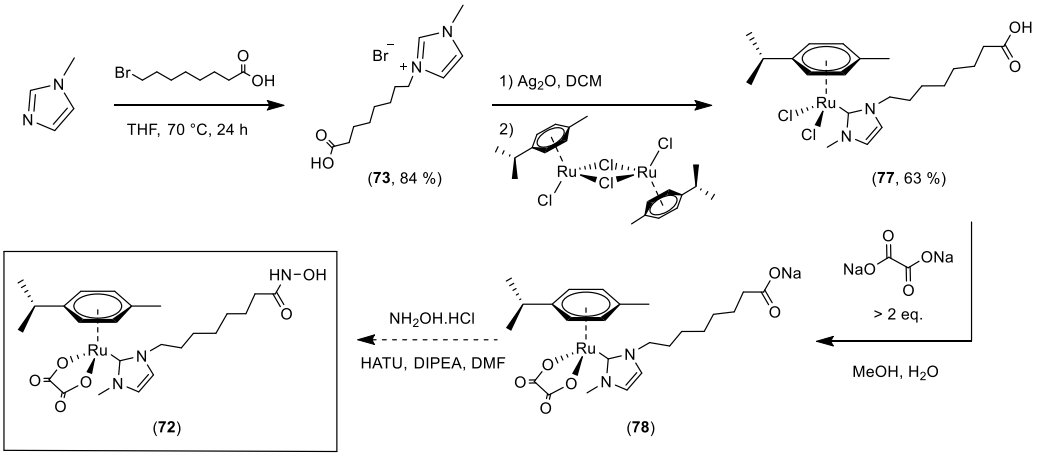

Scheme 2.6 - Second synthetic strategy for complex 72

It was thought that an investigation into the reaction between carboxylic acid **73** and the dichlororuthenium(II) *p*-cymene dimer would be worthwhile, in that if the carbene did bond to the metal, it would remove an unnecessary protection step from the first synthetic method, and perhaps increase the chances of the final product **72** being formed in therapeutically relevant purity and yield. It was surmised that the formation of a very strongly ligated NHC to the ruthenium metal would thermodynamically drive the forward reaction in the formation of **77**, and occur in favour of any side reactions involving the carboxylic acid proton. This was observed to be the case, as **77** was formed in high yield, and was purified from the residual oil when dropped into cold (-78 °C) diethyl ether. The orange solid that crashed out of ether would spontaneously form an oil when exposed to air, and so the isolation of **77** had to be carried out in an inert atmosphere to keep it as an accessible and pure solid. **77**

was taken through with an excess of sodium oxalate in order to undergo a ligand exchange reaction to afford complex **78**. Following purification by addition of DCM, from which the excess oxalate was removed by filtration, the filtrate was observed by TLC to be a mixture of three compounds. At this point, column chromatography could have isolated **78**, however the reaction was on such a small scale at this step that the product would likely have been lost by purification. For future attempts at the isolation of **72**, Synthetic Route 2 remains a relevant strategy with initial evidence of success.

2.2.4. Synthetic Route 3

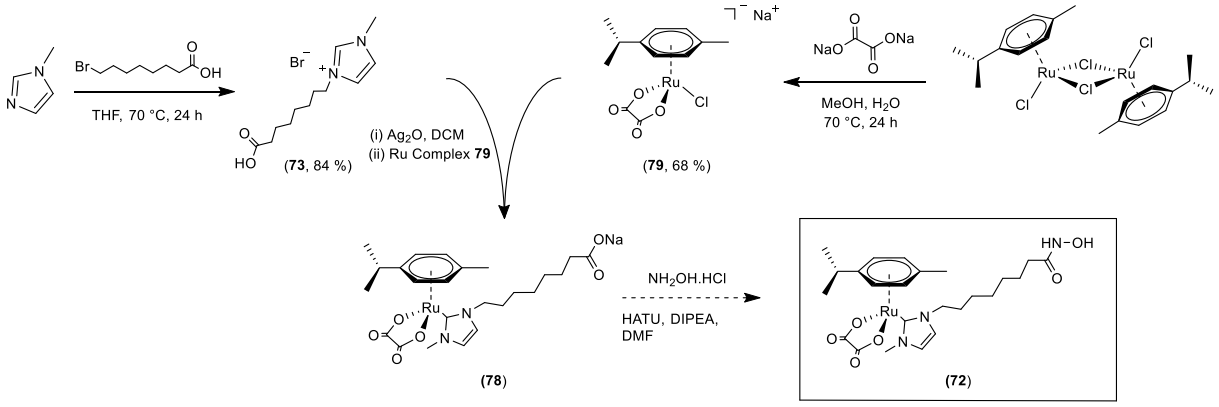

Scheme 2.7 – Third synthetic strategy for complex 72

Having observed the successful chelation of imidazolium intermediate **73** to the *p*-cymene dimer of ruthenium, a synthetic strategy was designed, which has the potential to both simplify the synthesis and be applicable towards the synthesis of many subsequent analogues. Anionic complex **79** represents the organometallic scaffold onto which the active group of target molecule **72** is attached, with one chloro-ligand as an exchangeable ligand for the chelation of the carbene. This convergent synthesis retains the same number of synthetic steps as its straightforward predecessor, however, if **79** was able to be produced in large excess, the synthesis of **72** effectively becomes a three-step synthesis. This method denotes an efficient route of producing congeners of **72**, with potential variation in both chain length and functionalities along the chain, as well as the NHC chelating group. Complex **79** was isolated as an orange solid, and characterised by ^{1}H NMR spectroscopy and mass spectrometry. However, reaction with carbene precursor **73** did not yield the piano-stool complex **78**. Using a vapour deposition method with a small sample of **79** dissolved in the minimum amount of DCM, in a sealed environment with diethyl ether, crystals of **79** were grown and the molecular structure was resolved. The structure had already been resolved in the literature,[152] and so it was not fully refined. Rather, selected bond lengths and angles are lifted from the literature. This data is summarised in Figure 2.7 and Table 2.3.

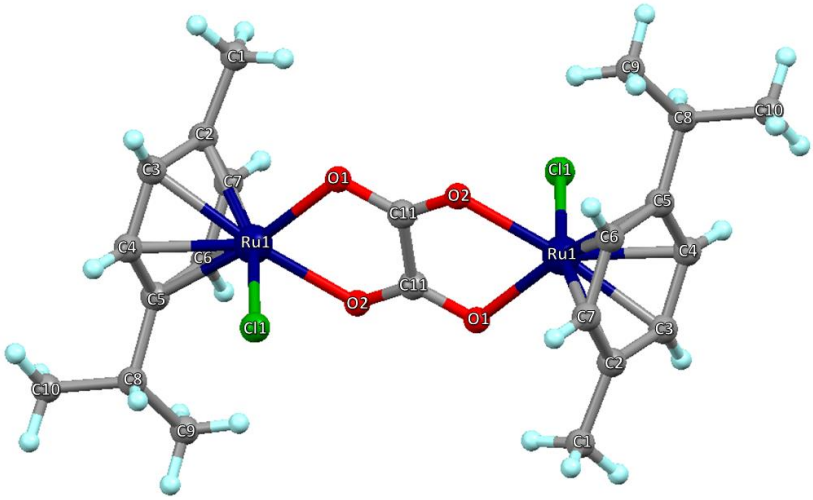

Figure 2.7 – Resolved molecular structure for [Ru(*p*-cymene)Cl]$_2$(η^2-oxalate) (79)

Table 2.4 – Selected bond lengths (Å) and angles (°) for complex 79

Ru(1)-Cl(1)	2.3913(9)
Ru(1)-O(1)	2.128(2)
Ru(1)-O(2)	2.134(2)
C(11)- O(1)	1.255(4)
C(11)-O(2)	1.256(4)
C(11)-C(11b)	1.536(7)
Ru ··· Ru	5.506(5)
O(1)-Ru(1)-O(2)	77.83(9)
C(11)-O(1)-Ru(1)	112.6(2)
C(11)-O(2)-Ru(1)	112.4(2)
O(1)-C(11)-C(11b)	117.1(3)
O(2)-C(11)-C(11b)	117.0(4)
O(1)-C(11)-O(2)	125.9(3)
O(1)-Ru(1)-Cl(1)	83.94(7)
O(2)-Ru(1)-Cl(1)	84.37(7)

The X-ray crystallography showed complex **79** to be a dimeric species, with a bridging oxalate ligand between two ruthenium metal centres. If **79** is indeed the binuclear complex resolved in Figure 2.7, it could offer some explanation to the lack of reactivity between it and imidazolium salt **73**. The dimeric species exhibits an increase in steric bulk about its ruthenium centres. The second, large ruthenium complex blocks the first, and, in particular the bulky, over-arching isopropyl group of the *p*-cymene will hinder the reactivity of a relatively bulky NHC. Moreover, additional scrutiny over the mass

spectrometry readings of the reaction mixture of **73** and **79** revealed no dimeric product with either or both chloride sites replaced with the alkyl-substituted NHC. It is true, however, that such binuclear complexes could degrade in the mass spectrometry electrospray. A mass spectrometry reading of a pure sample of just complex **79** showed mass peaks for both monomeric and dimeric species. Although the definitive structure of **79** can be determined by X-ray crystallography, it does not necessarily give conclusive evidence that this is the identity of the bulk sample. In order to establish a conclusive basis of whether **79** exists as the monomer, dimer or as a mixture of both, infra-red spectroscopy was carried out in order to investigate the asymmetric carbonyl stretch. Calcium oxalate exhibits[153] a strong C=O stretch at just over 1600 cm^{-1}, and it is assumed that chelation to a metal centre will cause the band to drop in wavenumber. Given the lack of alkene and nitrile bonds in the molecule, a peak in the IR spectrum with a wavenumber at around 1550 cm^{-1} would corroborate the oxalate chelated to one metal centre as depicted in Scheme 2.7. The obtained spectrum is shown in Figure 2.8.

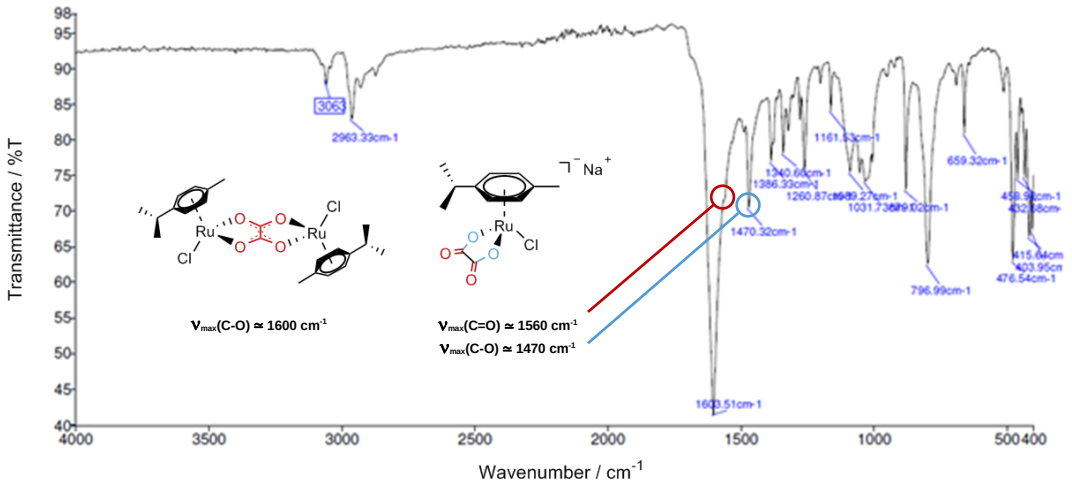

Figure 2.8 – Infrared spectrum of 79, with assigned monomeric C=O and C-O stretches highlighted

There is a large band in the IR spectrum at 1603 cm^{-1}, which likely corresponds to the C-O stretch of the dimer. Each C-O bond in the dimer is equivalent by symmetry and so only one band would be observed for the bridging oxalate motif in the IR. Unfortunately, the size of this band makes it difficult to discern whether there is indeed a monomeric C=O stretch observed with wavenumber of around 1560 cm^{-1}. A small shoulder is observable at around 1560 cm^{-1}, as emphasised in Figure 2.8, which may correspond to the non-bridging oxalate form of **79**. Further, there is a peak of relative intensity at 1470 cm^{-1}, which could correspond to the C-O bond of the terminal oxalate. The IR spectrum suggests a mixture of both the mono- and dimeric forms of **79**. In fact, the seemingly conflicting data gathered from a variety of analytical techniques suggests that **79** exists as the two proposed species in unknown proportions. However, it can be assertively concluded that as a methodology of synthesising a catalogue of **72**-like complexes, going via **79** is a flawed strategy.

2.2.5. Synthetic Route 4

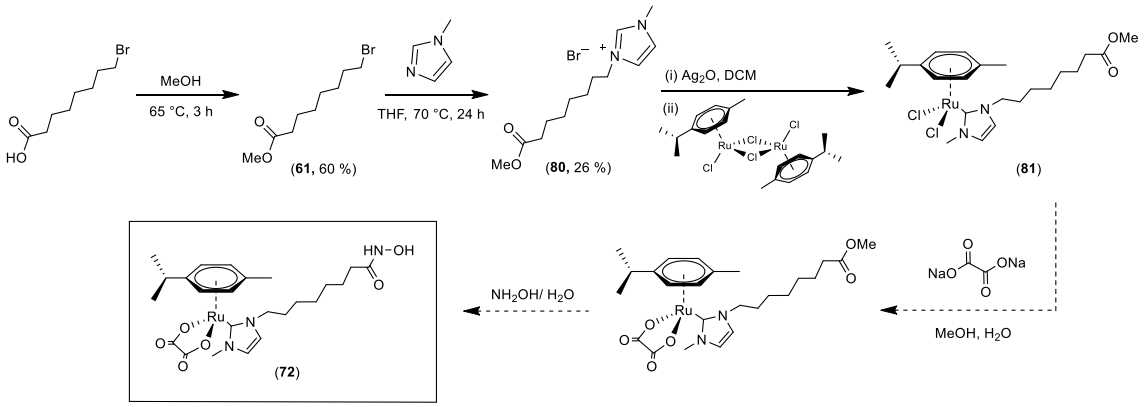

Scheme 2.8 - Fourth synthetic strategy for complex 72

Shifting the focus back to modular, non-convergent syntheses, while investigating whether protecting the carboxylic acid would improve the overall yield of **72**, a fourth synthetic strategy was designed (Scheme 2.8). This method involves the synthesis of the methyl ester of substituted imidazolium **73**: compound **80**, which is manipulated in the same manner as in previous syntheses: (i) ligation to silver by reaction with silver oxide, (ii) transmetalation to ruthenium via addition of the dichlororuthenium(II)(*p*-cymene) dimer. Following a ligand exchange reaction to afford the desired oxalate motif on the two vacant sites on the metal, (iii) the essential hydroxamic acid functionality is conferred to the terminus of the alkyl chain through reaction of the methyl ester with excess hydroxylamine solution. The deprotection remains a single, facile step and this synthesis provides a good indication as to whether the presence of a reactive carboxylic acid motif was hampering the prior syntheses. Methyl ester **61** was isolated in reasonable yield, however the following reaction with *N*-methylimidazole was very low-yielding. This is suspected to be due to the competitive nature of the two nitrogen atoms on the imidazolium ring (Scheme 2.9). The methylated position (2-position in Scheme 2.9a) is the more basic nitrogen as a result of the positive inductive effect of the additional methyl group. As such, it is reasoned that this heteroatom is protonated, before the non-methylated nitrogen atom (position 5) undergoes the desired nucleophilic substitution in the reaction between *N*-methylimidazole and the carboxylic acid (Scheme 2.9a). This suppression of the competition between the two nucleophilic atoms leads to product **73** being isolatable in high yield, as observed in synthetic routes 1-3. However, the absence of a proton acidic enough to protonate the methylated nitrogen in the reaction between *N*-methylimidazole and the methyl ester (**61**) in Scheme 2.9b allows for nucleophilic attack of both nitrogen atoms on the imidazole ring. Such reactions of *N*-methylimidazole and alkyl halides to produce the salt which is alkylated at the methylated nitrogen have been reported in the literature.[154] While this could be behind the observed disparity in the reactivities of *N*-methylimidazole with 8-bromooctanoic acid and its methyl ester, such reasoning is to be approached with caution. The *N*-methyl nitrogen of *N*-methylimidazole is tied up in the molecule's aromatic sextet, and thereby becomes less basic than a typical, non-aromatic, tertiary amine. As a proof of concept, an

equivalent of acid could be added to the reaction mixture of **61** with *N*-methylimidazole, however this was realised in retrospect to the investigation. It is suspected that impurities accumulated following the formation of the methyl ester to also play a role in the different yields of **73** and **80**. It is worth reiterating that the methyl ester required a reaction of formation, while 8-bromooctanoic acid is commercially available, and so the introduction of impurities in this additional reaction also seems to be a likely explanation.

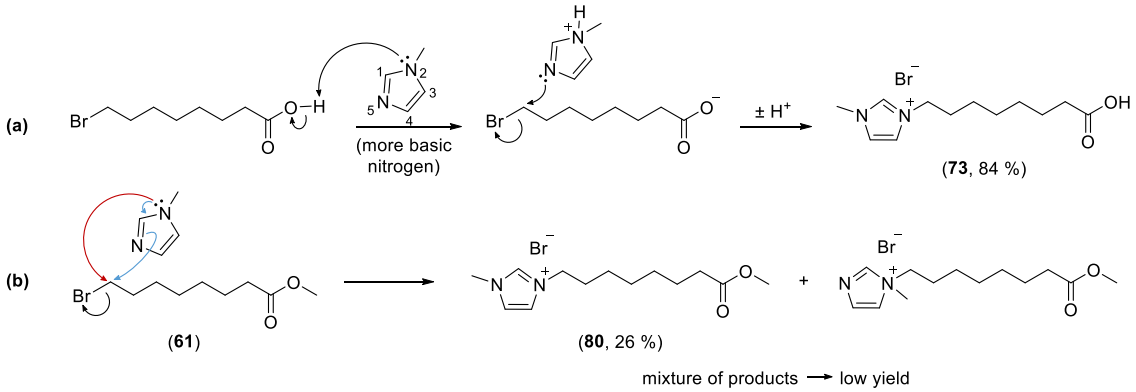

Scheme 2.9 - Proposed mechanisms of the reactions of *N*-methylimidazole with (a) 8-bromooctanoic acid and (b) methyl-8-bromooctanoate

What was isolated of ionic liquid **80** was ligated to the ruthenium centre to form the piano-stool complex **81** (Fig. 2.9, left). The formate complex **82** (Fig. 2.9, right) was observed by ESI^+ mass spectrometry, which provides evidence for the formation of **81**. The formate ligand is introduced by the formic acid present in the mass spectrometer, which displaces the chloride ligands of **81**, producing a positively charged molecule (**82**) with m/z calculated to be 519.55 (**82** requires 520.19).

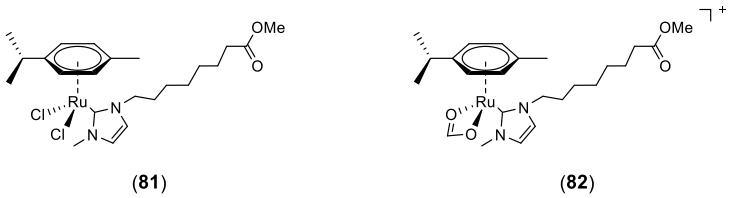

Figure 2.9 – Complex 81 and formate complex 82, as observed in mass spectrometry

Complex **81** was isolated as a crude mixture in an insufficient quantity to proceed with the next step. Due to the low-yielding nature of this synthetic route, it was not taken any further.

2.2.6. The Stabilisation of Organic Carbenes

The direction of carbene chemistry is progressively turning away from the archetypical methodology of weakly coordinating stabilised carbenes to a metal such as silver or gold, and undertaking a subsequent transmetalation reaction. An interesting strategy, that has been the focal point of many

synthetic strategies involving the use of carbenes, is the isolation of free, purely organic carbenic species. In the literature is a wide assortment of imidazole-2-ylidene carbenes that have been stabilised and characterised through their diagnostic ^{13}C NMR chemical shift values for the carbenic carbon, which typically appear between 210-230 ppm.[155,156] A selection of these compounds are shown in Figure 2.10 with their respective ^{13}C NMR carbenic carbon peaks. Compound **86** is the first synthesised air-stable carbene.[155]

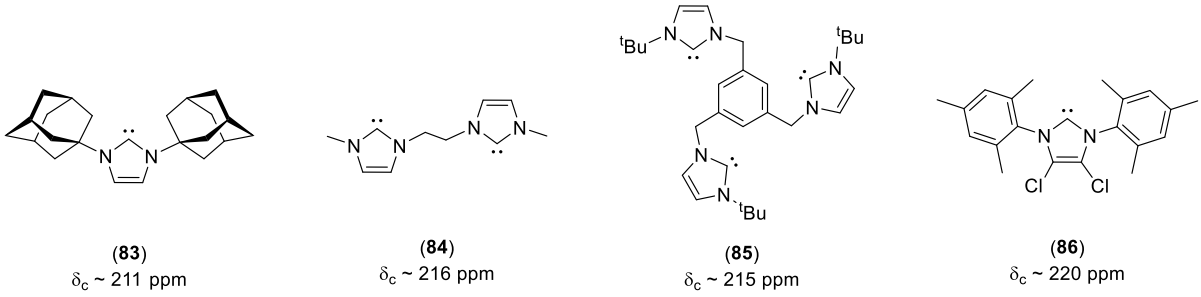

Figure 2.10 – A selection of stabilised NHC compounds from the literature, with characteristic ^{13}C NMR chemical shifts for carbonic carbons

From the reported stability of a variety of sibling NHC compounds in the literature, it was hypothesised that carbene **87** (Scheme 2.10) could potentially be isolated, characterised and used as a reagent to directly bind to a ruthenium centre through reaction with a ruthenium dimer. The carbenes are typically generated through the reaction of the imidazolium salt precursor with a strong Brønsted base such as potassium or sodium hydride, potassium *tert*-butoxide, $MN(SiMe_3)_2$ (*M* = Li, Na, K) or BuLi.[157] Three bases were selected for reaction with imidazolium salt **80**: (i) sodium hydroxide with a catalytic amount of potassium *tert*-butoxide, (ii) potassium bis(trimethylsilyl) amide (KHMDS) and (iii) DBU (Scheme 2.10). The three bases were selected due to their reported pKa values being high enough to remove the imidazolium proton, and the selection providing a variety of nucleophilicities.

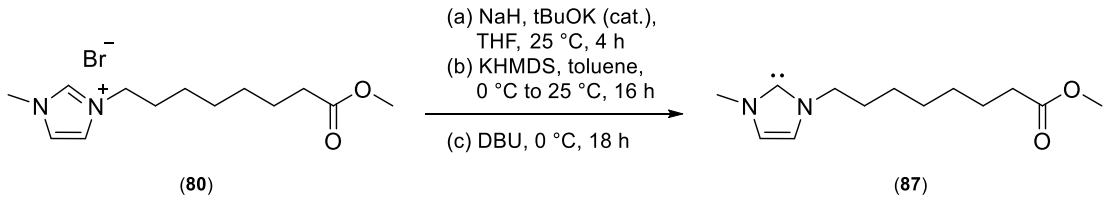

Scheme 2.10 - Reactions of selected bases with imidazole precursor 80 to generate free carbene 87

^{13}C NMR spectroscopy experiments of each of the three reaction mixtures showed no peaks in the relevant region. It has been proposed, and is the subject of much ongoing debate, that for many stabilised carbenes, a chemical equilibrium is established between the carbene itself and its dimer (Figure 2.11, left)[158] - this is known as the Wanzlick equilibrium. While the N-C-N bond angle is shortened in five-membered heterocycles such as **87**, which thermodynamically encourages the formation of dimeric species, compounds such as **88** (Figure 2.11, right) are reported to seldom form without either a Brønsted or Lewis acid catalyst.[159] Nonetheless, if such an equilibrium was established in the attempted

reactions, the dimeric form of **87,** shown in Figure 2.11 (right), would be observed. However, subsequent analysis of the reaction mixtures by mass spectrometry showed no evidence for dimeric compound **88**.

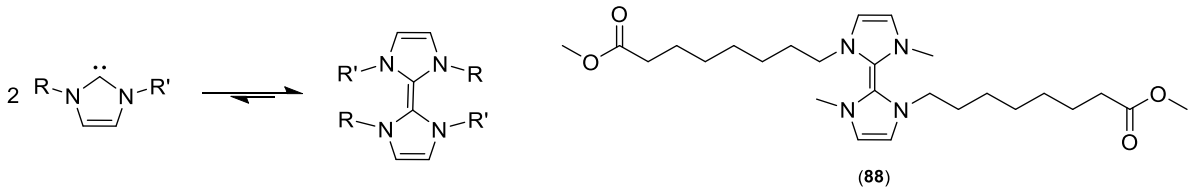

Figure 2.11 - Wanzlick equilibrium of stabilised carbenes (left) and potential dimeric product 88 (right)

Consequently, the reactions were repeated with no spectroscopic analysis, but rather the immediate addition of ruthenium dimer $[RuCl_2(p\text{-cymene})]_2$, in order to create a one-pot synthesis of **81** which removes the handling of what are likely to be air- and moisture sensitive compounds. Through this method, neither **81** nor its formate-featuring analogue **82** were observable by mass spectrometry. The presence of strong bases in the reaction mixture is suspected to hamper this reaction, as competing reactions are introduced.

It is also postulated that carbene **87** may not feature appropriate functionality in order to be stabilised as the free molecule. It is established that for singlet carbenes, electronic effects of the neighbouring heteroatoms plays a dominant role the stability of a carbine compound. However, for triplet carbenes in particular, steric factors are observed to play an important role. In fact, many carbenes reported in the literature are designed as such, to incorporate sterically demanding groups which directly block the carbene functionality. Sterically blocking reactions which may remove the carbenic character from the molecules permits such compounds to be isolated under a broader range of conditions and for longer timescales. The dimeric compound **88**, which has two straight-chain alkyl groups, was hypothesised to be a product as a result of the exposed carbene. It is proposed that this exposure is what leads to a high reactivity of carbene **87**, and resultantly its reluctance to exist as the free carbene. However, there are examples in the literature of somewhat exposed *N*-heterocyclic carbenes that have been stabilised and characterised (**84**, Fig. 2.10), and there are many methodologies left to attempt. For example, an elegant method to generate the free carbene is the reaction of the imidazolium salt precursor with sodium hydride in liquid ammonia. In contrast to many of the other solvents used in such reactions (including THF), liquid ammonia readily dissolves both the imidazolium salt as well as the base (NaH) providing a medium for smooth and effective deprotonation. Further investigations into the stabilisation of **88** represent a worthwhile and justified direction for research in order to further the understanding of the carbene-featuring piano-stool complexes to be synthesised and trialled as HDAC inhibitor candidates.

3. Conclusions and Future Work

A novel organometallic HDAC inhibitor has been designed, successfully synthesised and evaluated to show enzyme inhibition. To the author's knowledge, the *p*-cymene-capped ruthenium sandwich complex **60** is the first HDAC inhibitor of its kind, and opens up several avenues to modify the functionality of the complex in order to achieve an optimal anticancer agent. As alluded to in Section 2.1.3, variations in the length and functionality along the alkyl spacer chain, as well as the arene capping group, adding substituents to the Cp motif, and also an investigation of different counterions and metal centres associated with the complex are all pertinent directions of this research towards the development and optimisation of this class of anticancer agents.

Several synthetic routes were explored for the synthesis of a Ru-based carbene complex (**72**), which increased the understanding of both carbene ligation in general as well as the optimal synthetic method in order to achieve the isolation of complexes of this particular ilk. This furtherance of the understanding of organometallic carbene chemistry within the context of enzyme inhibiting anticancer agents is beneficial for two main reasons. Not only can an optimised synthetic route for **72** be drawn and accomplished from work building on this report, but, again, this class of complexes (which are also believed to be a novel class of anticancer agents) can be the focal point of rigorous and extensive research into modifications of the various functionalities of this group of potential therapeutics.

It is of particular interest to investigate sibling complexes of **60** and **72** with saturated or near-saturated fluorination along the chain. Fluorinated anticancer agents are a rapidly developing branch of medicinal chemistry due to their attractive properties, i.e. stabilising interactions with proteins, the suppression of the adventitious metabolism of a drug within cells due to its increased stability, as well as an improved bioavailability, which is a result of a fluorinated compound's higher lipophilicity and therefore increased cell membrane penetration.[160]

Further, studies into the optimal chain length of such organometallic SAHA-analogues seem to be valid investigations to undertake. The optimal chain length along the spacer group facilitates the strongest binding of the key terminal hydroxamic acid group to the Zn^{2+} cation found at the base of the enzyme pocket. With an idea of optimal chain length, chain functionality can be explored. Trichostatin A (TSA, **45**) features alkene, carbonyl and branching methyl functionalities along its alkyl chain and displays a similar extent of HDAC inhibition at concentrations a full order of magnitude lower than the prototypical HDAC inhibitor SAHA (**49**, experimentally shown in Table 2.2). It has also been shown and discussed in Section 2.1.2 that the amide linker in SAHA exhibits positive interactions with amino acid residues in the enzyme pocket. Surprisingly positive results may arise from the scrutinisation of the exact nature of the HDAC pocket and which functionalities along the spacer group will maximise the inhibition of the enzyme.

Varying the arene capping group of the metallocene sandwich complexes, or the substituents on the Cp motif of these complexes and the NHC of the carbene complexes is another area of potential research stemming from the work carried out herein. It is suspected that the main factors towards an HDAC inhibitor candidate will be the chain length and substituents along the chain. Nonetheless, important realisations concerning the nature of the rim of the enzyme pocket, and the constructive interactions that would increase the efficacy of an HDAC inhibiting agent can be made as a result of studies of this nature. Similarly to research into the optimal counterion for the sandwich complexes, for which the chloride anion is believed to be a suitable starting point, such investigations remain somewhat in the background, but are nevertheless important factors to consider in the development of novel, clinically viable anticancer agents of these types.

As a final note, contributions could be made to the existing library of known, stabilised and characterised carbenes from following the work reported in Section 2.2.6. Preliminary tests have been conducted towards the isolation of **87**, and building on these primary experiments has the potential to produce a ‘naked’, stabilised carbene - both in the interest of the field of carbene chemistry, as well as it being a relevant and convenient synthetic tool for the production of NHC-containing, organometallic HDAC inhibiting agents.

4. Experimental Methods

All reagents were purchased from Sigma Aldrich or Fluorochem and used as received without further purification, unless otherwise stated. Air sensitive reactions were carried out under argon using a Schlenk line.

NMR Spectroscopy. NMR spectra were recorded on a Varian VNMRS-700 spectrometer (^{1}H at 700 MHz, ^{13}C at 176 MHz, ^{31}P at 283.3 MHz) or an Avance-400 spectrometer (^{19}F at 376.5 MHz) at a constant temperature of 298 K, unless otherwise stated, and were processed using MestReNova version 10.0.0. All ^{13}C NMR experiments were proton decoupled. Assignment of the ^{1}H and ^{13}C NMR signals were accomplished by two-dimensional NMR spectroscopy (COSY, NOESY, HSQC, HMBC) where possible. Data are reported as follows: chemical shift; integration; multiplicity; coupling constants (*J* values); and assignment.

Mass Spectrometry. Mass spectrometry data were generated using a Waters QTOF spectrometer. Accurate mass data were processed using Elemental Composition 4.0, part of Masslynx 4.1, Waters Ltd, UK. Mass chromatograms for Figure 2.4 were processed using MestReNova version 10.0.0.

Infra-red Spectroscopy. The infra-red spectrum was produced using a Perkin Elmer FT-IR Spectrum Two Spectrometer. A 5 mg solid sample of the compound was used and the spectrum generated as an average of 16 scans.

Melting Point Measurements. Melting points were recorded using a Gallenkanp (Sanyo) apparatus and are uncorrected.

X-ray Crystallography. X-ray quality crystals of compound **78** were produced by leaving a small, open tube of a solution of compound **78** (dissolved in DCM) in a sealed vial with surrounding diethyl ether. The X-ray single crystal data for complex **78** was produced at 120.0 K with an Agilent XCalibur (Sapphire-3 CCD detector, fine-focus sealed tube, graphite monochromator, λMoKα radiation, λ = 0.71073 Å) diffractometer equipped with a Cryostream (Oxford Cryosystems) open-flow nitrogen cryostat. This data was obtained and solved by Dr. Dmitry S. Yufit of the Single Crystal X-Ray Diffraction service at Durham University.

Cell Cytotoxicity Assay. The MTT assay was run on the H460 cell line. H460 cells are non-small cell lung carcinoma cells derived from primary lung tumour tissue and were obtained from the American Tyoe Culture Collection (ATCC). The cells were maintained as a monolayer in Roswell Park Memorial Institute (RPMI) media, which is supplemented by 10 % fetal bovine serum and 5 % 2 mM L-Glutamine, and incubated at 37 °C in a 5 % CO_2 and 95 % air atmosphere. Using trypsin and

Hank's Balanced Salt Solution (HBSS) to lift the monolayer of cells, a small sample was used for the haemocytometer in order to calculate cell count. The calculated amount of media and cells were transferred to a 96-well plate, with 200 μL in each well, and incubated for 24 h to form a new monolayer of cells inside each well. The concentrations of the cytotoxic agents were made up from a 1 mM stock solution in order to test the concentration range 100 μM to 0.1 nM made by serial dilutions across the plate. These were incubated under the same conditions for 72 h. The supernatant was removed and the MTT solution added (200 μL per well). This solution was removed after 4 h, leaving purple formazan crystals in the wells with surviving cells. The crystals were dissolved in DMSO and the absorbance of the solutions was measured at 550 nm. In the 96-well plates, rows of media, media and cells, as well as media, cells and 0.1 % DMSO were run as controls alongside the serial dilutions of the cytotoxic agents. IC_{50} values were determined as the concentration of compound required to reduce formazan formation by 50%, and are based on quadruplicate assays.

Enzyme Inhibition Assay. The Fluor de Lys® fluorescent assay system was used to carry out this assay. 1 μM and 100 nM solutions of candidate HDAC inhibitor and SAHA in DMSO, as well as 1 μM and 10 nM solutions of trichostatin A were prepared. A commercially sourced solution of HeLa nuclear extract was diluted 30-fold, and a 50 mM stock solution of Fluor de Lys® substrate was diluted to 100 μM. The candidates to be tested with the HeLa nuclear extract solution were dosed onto a 48-well plate and incubated for 15 min at 37 °C. Subsequently, the Fluor de Lys® developer was diluted 20-fold and preserved at 0 °C. 50 μL of the substrate solution was added to each well, and incubated for a further 20 minutes in ambient temperature (~ 25 °C). Lastly, 100 μL of the developer was added to each well. Following a final 15 minutes of incubation at 25 °C, fluorescence readings were taken using a Biotek Synergy™ H4 Hybrid Multi-Mode Microplate Reader reading a wavelength of 460 nm following excitation at 360 nm.

4.1. Synthetic Methods

Methyl 8-bromooctanoate (61)

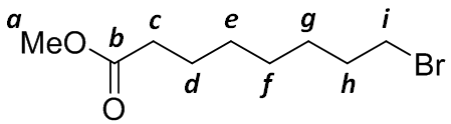

Under an atmosphere of argon, 8-bromooctanoic acid (500 mg, 2.2 mmol) was dissolved in anhydrous MeOH (5 mL). Two drops of concentrated H_2SO_4 were added and the mixture stirred at 65 °C for 3 h. The reaction was monitored by TLC. The reaction mixture was left to cool to room temperature and then the solvent was removed *in vacuo*. The mixture was diluted with EtOAc (5 mL) and washed with H_2O (2 x 10 mL) and a saturated solution of brine (10 mL). The organic fractions were combined, dried

over $MgSO_4$ and the solvent removed *in vacuo* to give the *title compound* as a yellow oil. (320 mg, 60 %) δ_H (700 MHz, methanol-d4) 3.67 (3H, s, H^a), 3.46 (2H, t, *J* 6.5 Hz, H^i), 2.34 (2H, t, *J* 7.0 Hz, H^c), 1.87 (2H, quin, *J* 6.5 Hz, H^h), 1.64 (2H, quin, *J* 4.5 Hz, H^d), 1.47 (2H, quin, *J* 6.0 Hz, H^g), 1.39 - 1.34 (4H, m, $H^{e/f}$), δ_C (176 MHz, methanol-d4) 175.6 (C^b), 51.9 (C^a), 34.7 (C^c), 34.4 (C^i), 33.8 (C^h), 29.9 (C^f), 29.4 (C^e), 29.0 (C^g), 25.8 (C^d). HRMS$^+$ m/z = 237.0490, $[C_8H_{18}O_2{}^{79}Br]^+$ requires 237.0490. R_f = 0.5 (silica, 80 % petroleum ether : 20% EtOAc).

Methyl 8-(cyclopentadienyl)octanoate (62)

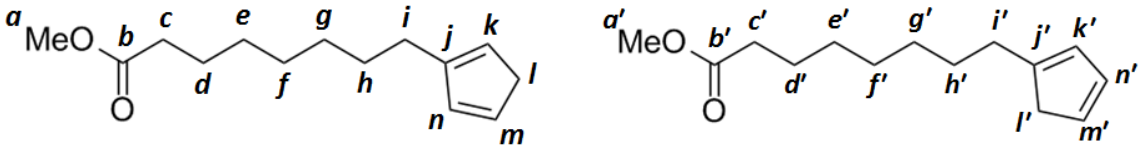

A solution of methyl 8-bromooctanoate (**61**, 1.3 g, 5.4 mmol) in anhydrous, degassed THF (8 mL) was added dropwise to a mixture of sodium cyclopentadienylide solution in THF (2M, 1.7 mL, 5.4 mmol) and anhydrous, deoxygenated (3 x freeze-pump-thaw cycles under argon) THF (16 mL) at -78 °C. The reaction mixture was allowed to reach room temperature and then stirred for a further 18 h. Anhydrous DCM (10 mL) was added to precipitate NaBr, which was removed by filtration. The solvent was removed from the filtrate under high vacuum to give the *title compound*s as a yellow oil, which were used without further purification (0.67 g, 55 %). δ_H (700 MHz, acetone-d6) 6.46 - 6.43 (1H, m, H^n), 6.39 - 6.35 (2H, m, $H^{k/k'}$), 6.22 - 6.19 (1H, m, $H^{n'}$), 6.14 - 6.12 (1H, m, $H^{m'}$), 6.00 - 5.98 (1H, m, H^m), 3.64 - 3.60 (4H, m, $H^{i/i'}$), 3.60 (6H, s, $H^{a/a'}$), 2.90 (2H, q, *J* 1.5 Hz, H^l), 2.86 (2H, q, *J* 1.5 Hz, $H^{l'}$), 2.40 (2H, td, *J* 4.6, 1.5 Hz, H^h), 2.34 (2H, td, *J* 8.4, 1.8 Hz, $H^{h'}$), 2.28 (4H, t, *J* 6.5 Hz, $H^{c/c'}$), 1.58 (4H, quin. *J* 7.0 Hz, $H^{g/g'}$), 1.56 - 1.50 (4H, m, $H^{d/d'}$), 1.36 - 1.28 (8H, m, $H^{e/e'/f/f'}$); δ_C (175 MHz, acetone-d6) 173.1 ($C^{b/b'}$), 134.4 ($C^{n/n'}$), 133.3 ($C^{k/k'}$), 130.1 ($C^{n/n'}$), 126.0 ($C^{m'}$), 125.5 (C^m), 50.5 ($C^{i/i'/a/a'}$), 40.7 (C^l), 42.7 ($C^{l'}$), 33.4 ($C^{c/c'}$), 30.3 (C^g), 29.5 ($C^{g'}$), 29.2 ($C^{e/e'}$), 29.0 ($C^{f/f'}$), 25.0 ($C^{d/d'}$). HRMS$^+$ m/z = 221.1543 [M-H]$^+$ ($C_{14}H_{21}O_2$) requires 221.1547).

Methyl 8-(cyclopentadienyl)octanoate(p-cymene)ruthenium(II) hexafluorophosphate (63)

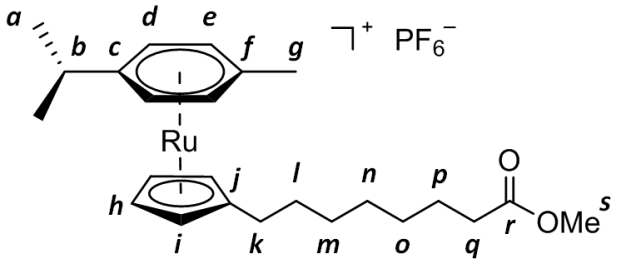

A mixture of methyl 8-(cyclopenta-1,3-dien-1-yl)octanoate and methyl 8-(cyclopenta-1,4-dien-1-yl)octanoate (**62**, 330 mg, 1.50 mmol) was dissolved in anhydrous, deoxygenated (3 x freeze-pump-thaw cycles under argon) EtOH (2 mL). Na_2CO_3 (36 mg, 34 mmol) and $[Ru(p\text{-cymene})Cl_2]_2$ (100 mg, 0.16 mmol) were added and the mixture stirred under argon at 75 °C for 16 h. The reaction was monitored by ESI^+ mass spectrometry. The mixture was left to stir at 25 °C for 2 h before the solution was decanted from residual salts. An aqueous solution of NH_4PF_6 (0.3 M, 2.0 mL) was added to the supernatant and the mixture was extracted with DCM (3 x 10 mL). The organic fractions were combined, dried over $MgSO_4$ and the solvent removed *in vacuo* to give a brown oil. The crude residue was purified by column chromatography (silica, CH_2Cl_2 : EtOH 0 - 0.5 % in 0.1 % increments), giving the *title compound* as an orange oil (180 mg, 43 %). δ_H (700 MHz, acetone-d6) 6.26 (2H, d, *J* 7.0 Hz H^e), 6.24 (2H, d, *J* 7.0 Hz H^d), 5.44 (2H, t, *J* 2.0 Hz, H^i), 5.37 (2H, t, *J* 2.0 Hz, H^h), 3.60 (3H, s, H^s), 2.84 - 2.77 (1H, m, H^b), 2.37 (3H, s, H^g), 2.35 (2H, t, *J* 7.5 Hz, H^k), 2.27 (2H, t, *J* 8.0 Hz H^q), 1.60 - 1.50 (4H, m, $H^{l/p}$), 1.37 - 1.30 (6H, m, $H^{m/n/o}$), 1.29 (6H, d, *J* 7.0 Hz, H^a), δ_C (176 MHz, acetone-d6) 173.2 (C^r), 112.3 (C^c), 103.8 (C^j), 101.1 (C^f), 86.8 (C^e), 84.5 (C^d), 80.9 (C^i), 79.9 (C^h), 50.6 (C^s), 33.3 (C^q), 31.8 (C^b), 30.6 (C^l), 28.8 ($C^{m,n,o}$), 27.3 (C^k), 24.6 (C^p), 22.6 (C^a), 18.8 (C^g); δ_p (acetone-d6) -144.3 (sept, J_{PF} 999 Hz). $HRMS^+$ m/z = 457.1685 $[M\text{-}PF_6]^+$ ($C_{24}H_{35}O_2{}^{96}Ru$ requires 457.1680).

8-(Cyclopentadienyl)octanoic hydroxamic acid(p-cymene)ruthenium(II) hexafluorophosphate (60)

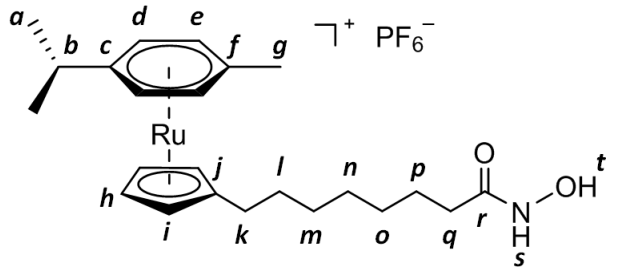

Methyl 8-(cyclopentadienyl)octanoate(p-cymene)ruthenium(II) hexafluorophosphate (**63**, 100 mg, 0.22 mmol) was suspended in a 1:1 mixture of MeOH (6 mL) and 50% NH_2OH solution in H_2O (6 mL). 1M NaOH (0.22 mL, 0.22 mmol) was added and the reaction mixture was left to stir at 25 ˚C for 30 minutes,

at which point the solution was observed to be homogenous. The reaction was monitored by ESI^+ mass spectrometry. The solution was neutralised by the addition of 1M HCl (0.22 mL, 0.22 mmol), and the mixture was extracted with DCM (3 x 10 mL). The organic fractions were combined, dried over $MgSO_4$ and the solvent removed *in vacuo* to give the *title compound* as a brown oil (99.5 mg, 75 %). No further purification was carried out. δ_H (400 MHz, DMSO-d6) 10.33 (1H, s, H^t), 8.64 (1H, s, H^s), 6.17 (2H, d *J* 5.0 Hz, H^e), 6.15 (2H, d *J* 5.0 Hz, H^d), 5.35 (2H, t *J* 2.0 Hz, H^i), 5.28 (2H, t *J* 1.0 Hz, H^h), 2.66 (1H, sept. *J* 6.0 Hz, H^b), 2.23 (3H, s, H^g), 2.19 (2H, t *J* 8.0 Hz, H^k), 1.93 (2H, t *J* 7.5 Hz, H^q), 1.47 (2H, quin *J* 6.0 Hz, H^l), 1.41 (2H, quin *J* 6.0 Hz, H^p), 1.29 - 1.24 (4H, m, $H^{m/o}$), 1.24 - 1.20 (2H, m, H^n), 1.19 (6H, d *J* 7.0 Hz, H^a), δ_C (400 MHz, DMSO-d6) 169.5 (C^r), 111.9 (C^c), 103.6 (C^j), 101.0 (C^f), 86.9 (C^e), 84.6 (C^d), 80.9 (C^i), 80.0 (C^h), 32.7 (C^q), 31.6 (C^b), 30.5 (C^p), 28.9 ($C^{m/n}$), 28.8 (C^o), 27.3 (C^k), 25.3 (C^l), 23.6 (C^a), 19.5 (C^g), δ_p (DMSO-d6) -144.2 (sept, J_{PF} 1005 Hz). $HRMS^+$ m/z = 458.1632 $[M\text{-}PF_6]^+$ ($C_{24}H_{35}O_2{}^{96}Ru$ requires 458.1633).

Methyl 8-(cyclopentadienyl)octanoate(benzene)ruthenium(II) hexafluorophosphate (64)

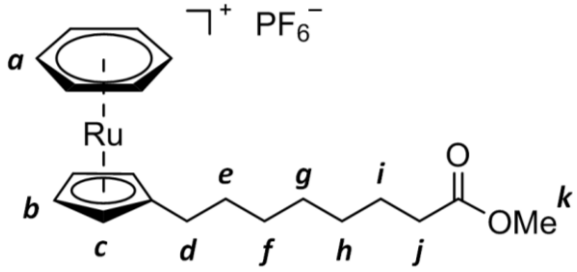

A mixture of methyl 8(cyclopenta-1,3-dien-1-yl)octanoate and methyl 8-(cyclopenta-1,4-dien-1-yl)octanoate (**62**, 400 mg, 1.8 mmol) was dissolved in dissolved in anhydrous, deoxygenated (3 x freeze-pump-thaw cycle) EtOH (2 mL). Na_2CO_3 (36 mg, 34 mmol) and $[Ru(benzene)Cl_2]_2$ (100 mg, 0.16 mmol) were added and the mixture stirred under argon at 75 °C for 16 h. The reaction was monitored by ESI^+ mass spectrometry. The mixture was left to stir at 25 °C for 2 h before the solution was decanted from residual salts. An aqueous solution of NH_4PF_6 (0.3 M, 2.0 mL) was added to the supernatant and the mixture was extracted with DCM (3 x 10 mL). The organic fractions were combined, dried over $MgSO_4$ and the solvent removed *in vacuo* to give a brown oil. The crude residue was purified by column chromatography (silica, CH_2Cl_2 : EtOH 0 - 0.5 % in 0.1 % increments) to give the *title compound* as a brown oil (180 mg, 43 %). δ_H (700 MHz, acetone-d6) 6.22 (6H, s, H^a), 5.50 (2H, t *J* 2.0 Hz, H^c), 5.39 (2H, t *J* 2.0 Hz, H^b), 3.68 (3H, s, H^k), 2.65 (2H, quin *J* 6.0 Hz, H^d), 2.35 (3H, t *J* 6.5 Hz, H^j), 1.71 - 1.59 (2H, m, H^e), 1.58 - 1.49 (2H, m, H^i), 1.43 - 1.29 (6H, m, $H^{f/g/h}$). $HRMS^+$ m/z = 401.1053 $[M\text{-}PF_6]^+$ ($C_{20}H_{27}O_2{}^{96}Ru$ requires 401.1055).

Methyl 6-aminohexanoate

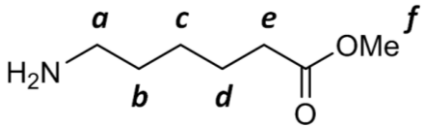

According to a literature procedure[161]; 6-aminohexanoic acid (300 mg, 2.3 mmol) was dissolved in methanol (8 mL). Two drops of concentrated H_2SO_4 were added and the mixture was stirred at reflux (65 °C) for 3 h. The reaction was monitored by TLC. The reaction mixture was left to cool to room temperature and then the solvent was removed *in vacuo*. The mixture was diluted with EtOAc (5 mL) and washed with H_2O (2 x 10 mL) as well as a saturated solution of brine (10 mL). The organic fractions were combined, dried over $MgSO_4$ and the solvent removed *in vacuo* to give the *title compound* as a yellow oil. (180 mg, 51 %). δ_H (400 MHz, methanol-d4) 3.66 (3H, s, H^f), 2.94 (2H, t *J* 7.0 Hz, H^a), 2.35 (2H, t *J* 7.0 Hz, H^e), 1.67 (4H, quin. *J* 7.5 Hz, $H^{b/d}$), 1.42 (2H, quin. *J* 7.5 Hz, H^c). $HRMS^+$ m/z = 145.1103 ($C_7H_{15}NO_2$ requires 145.1103).

Methyl 6-(N-benzoic amide)hexanoate(cyclopentadienyl)ruthenium(II) hexafluorophosphate (66)

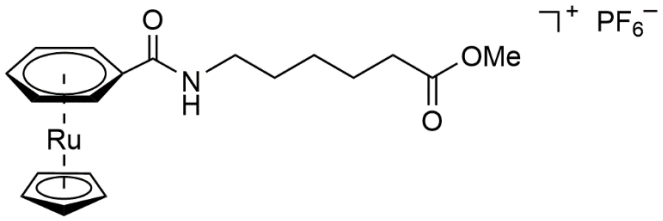

η^6-Benzoic acid(cyclopentadienyl)ruthenium(II) hexafluorophosphate (50 mg, 0.10 mmol) was dissolved in anhydrous, deoxygenated (3 x freeze-pump-thaw cycle under argon) DMF (5 mL) and HATU (60 mg, 0.15 mmol) was added. The mixture was left to stir for 10 min, after which methyl 6-aminohexanoate (23 mg, 0.15 mmol) was added and the mixture left to stir for a further 20 min. DIPEA (0.045 mL, 0.26 mmol) and left to stir overnight. Solvent and volatile reagents were removed *in vacuo* at 80 °C, and remaining residue taken through with no further purification. Evidence of product was observed in the crude spectra of ^1H NMR and MS. A reading of accurate mass was undertaken. $HRMS^+$ m/z = 416.0796 $[M\text{-}PF_6]^+$ ($C_{19}H_{24}NO_3{}^{96}Ru$ requires 416.0800).

6-(N-Benzoic amide)hexanoic hydroxamic acid(cyclopentadienyl)ruthenium(II) hexafluorophosphate (68)

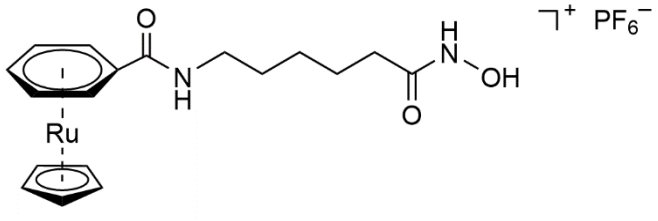

Methyl 6-(*N*-benzoic amide)hexanoate(cyclopentadienyl)ruthenium(II) hexafluorophosphate (**66**, 72 mg, 0.10 mmol) was suspended in a 1:1 mixture of MeOH (2 mL) and 50% NH_2OH solution in H_2O (2 mL). 1M NaOH (0.10 mL, 0.10 mmol) was added and the reaction mixture was left to stir at 25 ˚C for 10 mins, at which point the solution was observed to be homogenous. The reaction was monitored by ESI^+ mass spectrometry. The solution was neutralised by the addition of 1M HCl (0.10 mL, 0.10 mmol), and the mixture was extracted with DCM (3 x 10 mL). The organic fractions were combined, dried over $MgSO_4$ and the solvent removed *in vacuo* and submitted to purification by HPLC, which is currently ongoing.

Methyl 6-(N-benzamide)hexanoate(pentamethylcyclopentadienyl)ruthenium(II) hexafluorophosphate (67)

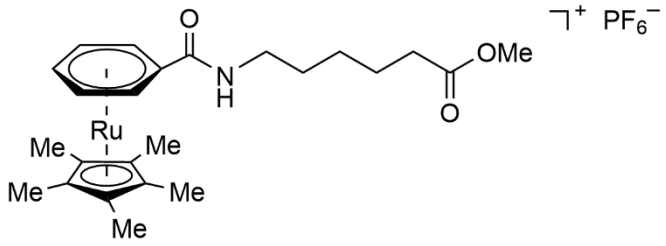

η^6-Benzoic acid(pentamethylcyclopentadienyl)ruthenium(II) hexafluorophosphate (50 mg, 0.10 mmol) was dissolved in anhydrous, deoxygenated (3 x freeze-pump-thaw cycle under argon) DMF (5 mL) and HATU (60 mg, 0.15 mmol) was added. The mixture was left to stir for 10 min, at which point methyl 6-aminohexanoate (23 mg, 0.15 mmol) was added and the mixture was left to stir for a further 20 min. DIPEA (0.045 mL, 0.26 mmol) and left to stir overnight. Solvent and volatile reagents were removed *in vacuo* at 80 °C, and the crude residue was taken through with no further purification. Evidence of product was observed in the crude spectra of ^1H NMR and MS. A reading of accurate mass was undertaken. $HRMS^+$ m/z = 486.1579 $[M\text{-}PF_6]^+$ ($C_{24}H_{34}NO_3{}^{96}Ru$ requires 486.1582).

6-(N-Benzamide)hexanoic hydroxamic acid(pentamethylcyclopentadienyl)ruthenium(II) hexafluorophosphate (69)

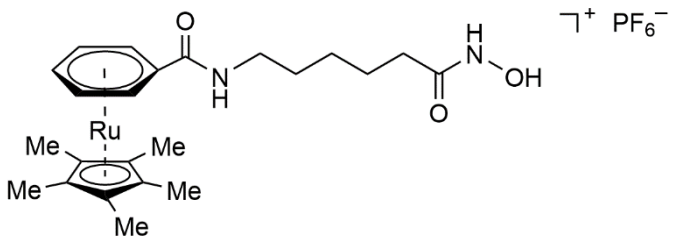

Methyl 6-(*N*-benzamide)hexanoate(pentamethylcyclopentadienyl)ruthenium(II) hexafluorophosphate (**67**, 110 mg, 0.17 mmol) was suspended in a 1:1 mixture of MeOH (2 mL) and 50% NH_2OH solution in H_2O (2 mL). 1M NaOH (0.17 mL, 0.17 mmol) was added and the reaction mixture was left to stir at 25 ˚C for 30 mins, at which point the solution was observed to be homogenous. The reaction was monitored by ESI^+ mass spectrometry. The solution was neutralised by the addition of 1M HCl (0.17 mL, 0.17 mmol), and the mixture was extracted with DCM (3 x 10 mL). The organic fractions were combined, dried over $MgSO_4$ and concentrated *in vacuo*. The residue was submitted to purification by HPLC, which is currently ongoing.

N-Methylimidazolium bromide-N'-8-octanoic acid (73)

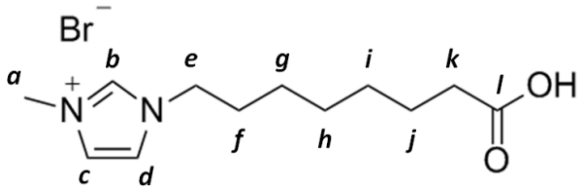

Following a literature procedure[162]; to a solution of *N*-methylimidazole (0.10 mL, 1.3 mmol) in THF (2 mL) was added dropwise a solution of 8-bromooctanoic acid (300 mg, 1.4 mmol) in THF (2 mL). After complete addition, the mixture was heated to 65 °C and stirred at reflux for 18 h. Solvent was removed *in vacuo* and the crude solid washed with diethyl ether (3 x 5 mL) to give the *title compound* as a white solid (320 mg, 84%). δ_H (400 MHz, methanol-d4) 8.97 (1H, s, H^b), 7.64 (1H, d *J* 2.0 Hz, H^d), 7.61 (1H, d *J* 2.0 Hz, H^c), 4.21 (2H, t *J* 7.0 Hz, H^e), 3.93 (3H, s, H^a), 2.27 (2H, t, *J* 7.5 Hz, H^k), 1.89 (2H, quin, *J* 5.5 Hz, H^f), 1.59 (2H, quin, *J* 5.5 Hz, H^j), 1.44 - 1.2 (6H, m, $H^{g/h/i}$), δ_C (151 MHz, methanol-d4) 177.6 (C^l), 124.8 (C^d), 123.6 (C^c), 111.4 (C^b), 50.8 (C^k), 36.4 (C^e), 34.9 (C^a), 31.0 (C^j), 29.8 (C^f), 29.6 (C^i), 27.0 (C^g), 25.9 (C^h). $HRMS^+$ m/z = 224.1600 $[M\text{-}Br]^+$ ($C_{12}H_{20}N_2O_2$ requires 224.1603). Melting point = 118.8 °C (lit. value[161] = 114-116 °C); R_f = 0.3 (silica, 80 % petroleum ether : 20% EtOAc).

8-Hydroxyoctanoic acid (75)

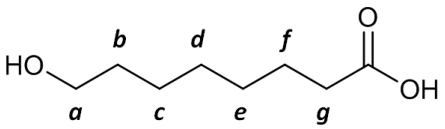

8-Bromooctanoic acid (1.6 g, 7.1 mmol) was dissolved in THF (12 mL) and a solution of KOH (1.00 g, 18 mmol) in H_2O (28 mL) and the mixture was stirred at 80 °C for 4 h. Following acidification with HCl (1M, 17.8 mL), the mixture was extracted with hexane / EtOAc (1:1, 3 x 20 mL). The solvent was removed *in vacuo* and the residue was purified by column chromatography (silica, EtOAc : hexane 5 %) gave the *title compound* as a colourless oil (0.57 g, 49%). δ_H (400 MHz, methanol-d4) 3.46 (2H, t *J* 7.0, H^a), 2.30 (2H, t, *J* 7.0 Hz, H^g), 1.87 (2H, quin., *J* 7.0 Hz, H^b), 1.67 – 1.59 (2H, m, H^f), 1.53 – 1.43 (2H, m, H^c), 1.43 – 1.34 (4H, m, Hz, $H^{d/e}$). $HRMS^+$ m/z = 159.1021 ($[C_8H_{15}O_3]^+$ requires 159.1024).

8-Hydroxy-O-benzyloctanehydroxamate (76)

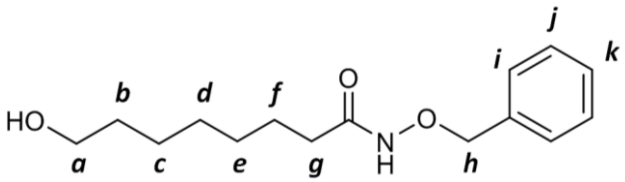

8-Hydroxyoctanoic acid (**75**, 50 mg, 0.31 mmol) was dissolved in anhydrous DMF, and HATU (180 mg, 0.47 mmol) was added. The mixture was left to stir for 10 mins, after which O-benzylhydroxylamine hydrochloride (75 mg, 0.47 mmol) was added. Following a further 20 mins stirring, DIPEA (140 μL, 0.78 mmol) was added and the mixture was stirred overnight. The solvent, as well as residual DIPEA were removed *in vacuo*, and the resultant brown oil was redissolved in DCM and washed with H_2O (3 x 10 mL). Evidence of the *title compound* was observed in the ^1H NMR spectrum. δ_H (400 MHz, chloroform-d) 7.45 - 7.28 (5H, m, $H^{i/j/k}$), 4.99 - 4.83 (2H, m, H^h), 3.48 (2H, t *J* 7.5, H^a), 2.42 (2H, t, *J* 7.0 Hz, H^g), 1.88 (2H, quin., *J* 7.0 Hz, H^b), 1.67 – 1.59 (2H, m, H^f), 1.53 - 1.34 (m, $H^{c/d/e}$).

Dichloro(p-cymene)ruthenium(II) N-methylimidazole-N'-8-octanoic acid (77)

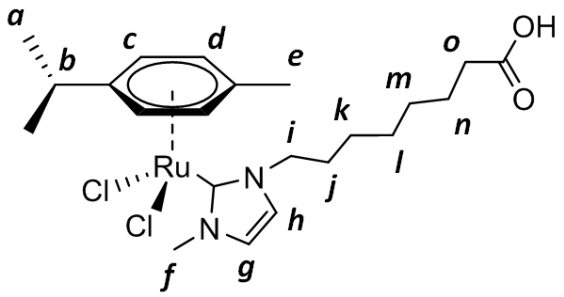

A flame-dried Schlenk tube was charged with molecular sieves, and *N*-methylimidazolium bromide-*N*'-8-octanoic acid (**72**, 9.5 mg, 0.31 mmol) and Ag_2O (37 mg, 0.16 mmol) were added. The mixture was backflashed three times with argon and anhydrous DCM (8 mL) was added. The flask was closed and reaction mixture stirred for 4 h in the dark. A solution of dichloro(*p*-cymene)ruthenium (II) dimer (98 mg, 0.16 mmol) in DCM was added and the solution stirred in the dark overnight. The solution was filtered through Celite® and concentrated *in vacuo*. The orange residue was recrystallised from DCM/ pentane at 4 °C. After a subsequent filtration, the *title compound* was obtained as an orange solid (54 mg, 63 %). δ_H (400 MHz, chloroform-d) 7.09 (1H, d *J* 1.5 Hz, H^h), 7.01 (1H, d *J* 1.5 Hz, H^c), 6.20 (4H, q *J* 5.0 Hz, $H^{c/d}$), 4.21 (2H, t *J* 7.0 Hz, H^i), 3.93 (3H, s, H^f), 2.68 (1H, sep *J* 6.0 Hz, H^b), 2.27 (2H, t, *J* 7.5 Hz, H^o), 1.89 (2H, quin, *J* 5.5 Hz, H^j), 1.59 (2H, quin, *J* 5.5 Hz, H^n), 1.44 - 1.2 (6H, m, $H^{k/l/m}$) 1.25 (6H, d *J* 7.0 Hz, H^a).

Oxalate(p-cymene)ruthenium(II) N-methylimidazole-N'-8-octanoic acid (78)

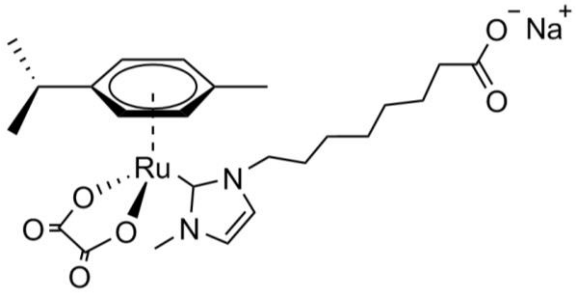

Dichloro(*p*-cymene)ruthenium(II) *N*-methylimidazole-*N*'-8-octanoic acid (**77**, 100 mg, 0.18 mmol) was dissolved in MeOH (10 mL) and a solution of sodium oxalate (74 mg, 0.55 mmol) in H_2O (5 mL) was added. The mixture was stirred for 48 h and reaction was monitored by ESI^+ mass spectrometry. The solvents were removed *in vacuo* and DCM was added in order to facilitate the precipitation of excess sodium oxalate. Following filtration, the filtrate was collected and solvent removed via rotary evaporation to give the *title compound* as a crude brown oil. Three compounds were observable by

TLC; R_f = 0.0, 0.4, 0.6 (silica, 90 % DCM : 10% MeOH. HRMS$^-$ m/z = 541.1419 [M-Na] ($C_{24}H_{33}N_2O_6{}^{96}Ru$ requires 541.1415).

Sodium chloro(p-cymene)(oxalate)ruthenium(II) (79)

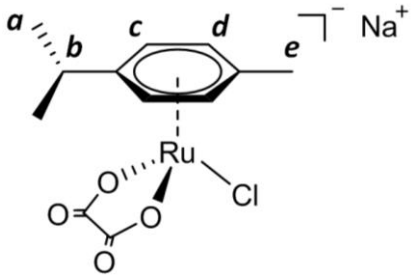

Dichloro(*p*-cymene)ruthenium(II) dimer (50 mg, 0.082 mmol) was dissolved in MeOH (10 mL) and the solution purged with argon. A solution of sodium oxalate (33 mg, 0.27 mmol) in H_2O (4 mL) was added and the mixture was stirred for 24 h. The reaction was monitored by ESI$^+$ mass spectrometry. Solvent was removed *in vacuo* and DCM was added in order to facilitate the precipitation of excess sodium oxalate. Following filtration, the filtrate was collected and concentrated *in vacuo* to give the *title compound* as an orange solid (21 mg, 68%). δ_H (400 MHz, chloroform-d) 5.59 (2H, d *J* 1.5 Hz, H^c), 5.35 (2H, d *J* 1.5 Hz, H^d), 2.89 (1H, sept. *J* 4.0 Hz, H^b), 2.25 (3H, s, H^e), 1.33 (6H, d, *J* 7.0 Hz, H^a). HRMS$^-$ m/z = 325.0019 [M-Na-Cl+H] ($C_{12}H_{15}O_4{}^{96}Ru$ requires 325.0014).

N-Methylimidazolium bromide-N'-methyl-8-octanoate (80)

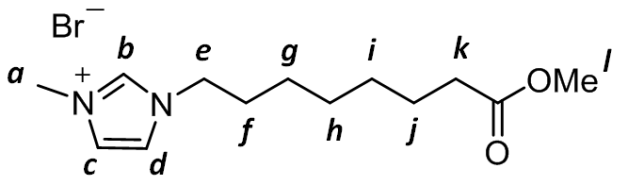

N-Methylimidazole-*N*'-8-octanoic acid (**73**, 540 mg, 1.8 mmol) was dissolved in methanol (5 mL). Two drops of concentrated H_2SO_4 were added and the mixture was stirred at reflux (65 °C) for 3 h. Reaction progress was monitored by TLC, and the solvent removed *in vacuo*. The residue was redissolved in DCM and washed with H_2O (3 x 5 mL). The product was dried over $MgSO_4$ and solvent removed *in vacuo* to give the *title compound* as an orange oil (310 mg, 60%). δ_H (400 MHz, DMSO-d6) 9.13 (1H, s, H^b), 7.78 (1H, d *J* 3.0 Hz, H^d), 7.61 (1H, d *J* 3.0 Hz, H^c), 4.16 (2H, t *J* 7.0 Hz, H^e), 3.86 (3H, s, H^a), 3.58 (3H, s, H^l), 2.29 (2H, t, *J* 7.0 Hz, H^k), 1.78 (2H, quin, *J* 7.0 Hz, H^f), 1.51 (2H, quin, *J* 7.0 Hz, H^j), 1.34 - 1.20 (6H, m, H$^{g/h/i}$). HRMS$^+$ m/z = 238.1760 [M-Br]$^+$ ($C_{13}H_{22}N_2O_2$ requires 238.1760).

Dichloro(p-cymene)ruthenium(II) N-methylimidazole-N'-8-octanoic acid (81)

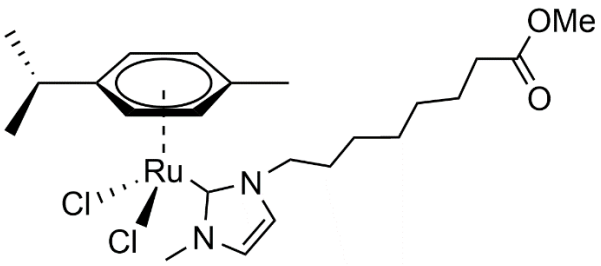

N-Methylimidazolium bromide-*N*'-methyl-8-octanoate (**80**, 250 mg, 0.77 mmol) and Ag_2O (93 mg, 0.40 mmol) were added to a dried Schlenk tube charged with flame dried molecular sieves. The mixture was backflashed three times with argon, and then anhydrous DCM (5 mL) was added. The solution was stirred for 4 h in the dark. Dichloro(*p*-cymene)ruthenium(II) dimer (650 mg, 0.40 mmol) was added and the reaction mixture was stirred overnight. The mixture was filtered through Celite® and the filtrate concentrated *in vacuo* to isolate the *title compound* as a crude mixture. ESI^+ m/z = 519.55 $[M-2Cl+CO_2]^+$ ($C_{13}H_{22}N_2O_2$ requires 520.19).

References

[1] World Health Organization, *World Cancer Report 2014*. 2014, Chapter 1.1
[2] M.J. Lind, Medicine 2008, **36** (1), 19
[3] A. Jemal, F. Bray, Center MM, J. Ferlay, E. Ward, D. Forman, CA: A Cancer Journal for Clinicians. 2011, **61** (2), 69
[4] W. B. Coleman, T. C. Rubinas, Molecular Pathology: The Molecular Basis of Human Disease. Amsterdam: Elsevier Academic Press. 2009, **4**, 66
[5] G. Pawelec, E Derhovanessian, A Larbi, Critical reviews in oncology/hematology. 2010, **75** (2), 165
[6] B. Alberts, A Johnson, J Lewis, *et al*., *Molecular biology of the cell* (4th ed.), 2002, New York: Garland Science
[7] V. N. Anisimov, E. Sikora, G. Pawelec, *Biogerontology* 2009, **10** (4), 323
[8] http://www.bbc.co.uk/news/health-26031748 (Accessed 30/08/2016)
[9] B. Rosenberg, L. Van Camp, T. Krigas, *Nature*, 1965, **205**, 698
[10] J. A. Friederich, J. F. Butterworth, *Anesth. Analg.*, 1995, **81** (1), 152
[11] R. Motterlini, *et al*., *Circ. Res.*, 2003, **93**, e2-e8
[12] R. Motterlini, *et al*., *Dalton Trans.*, **2007**, 4962
[13] W. F. Kean, L. Hart, W. W. Buchanan, *British Journal of Rheumatology*, 1997, **36** (5), 560
[14] R. Alberto, *et al*., *Chem. Eur. J.* 2005, **11** (14), 4089
[15] A. H. White, *et al*., *Dalton Trans.*, 2006, 3708
[16] B. Maher, *Environmental Chemistry* 2005, **2,** (3), 139
[17] S. Gibaud, G Jaouen, *Top. in Organomet. Chem.*, 2010, **32**, 1
[18] I. Kostova, *Curr. Med. Chem.* 2006, **13** (9), 1085
[19] H. Bregman and E. Meggers, *Org. Lett.*, 2006, **8** (24), 5465
[20] W. H. Ang, A. Casini, G. Sava, P. J. Dyson, *Journal of Organometallic Chemistry* 2011 **696** (5), 989
[21] P. J. Sadler *et al*. *Inorg. Chem*. 2007, **46**, 4049
[22] A. L. Noffke, A. Habtemariam, A. M. Pizarro, P. J. Sadler, *Chem. Commun*., 2012, **48**, 5219
[23] S. P. Fricker. *Dalton Trans*. 2007, 4903
[24] E. Meggers, *Chem. Commun. (Camb).* 2009, 1001
[25] K. H. Thompson, C. Orvig, *Science*. 2003, **300**, 936
[26] T. W. Hambley, *Dalton Trans*. 2007, 4929
[27] N. J. Wheate, S. Walker, G. E. Craig, R. Oun, *Dalton Trans.*, 2010, **39**, 8113
[28] E. R. Jamieson, S. J. Lippard, *Chem. Rev*., 1999, **99**, 2467
[29] L. Kelland, *Nat. Rev. Cancer*., 2007, **7**, 573
[30] M. Galanski, V. B. Arion, M. A. Jakupec, B. K. Keppler, *Curr. Pharm. Des.*, 2003, **9,** 2078
[31] M. Galanski, M. A. Jakupec, B. K. Keppler, *Curr. Med. Chem.*, 2005, **12**, 2075
[32] N. J. Wheate, S. Walker, G.E. Craig and R. Oun, *Dalton Trans*., 2010, **39**, 8113
[33] K. R. Harrap, *Cancer Treat. Rev*., 1985, **12**, 21–33
[34] S. Neidle, I. M. Ismail, P. J. Sadler, *J. Inorg. Biochem.*, 1980, **13**, 205
[35] D. Wisher, *Martindale: The complete drug reference*, Pharmaceutical Press, London, 35th ed., 2007
[36] L. Kelland, *Nat. Rev. Cancer*, 2007, **7**, 573
[37] T. Boulikas and M. Vougiouka, *Oncol. Rep.*, 2003, **10**, 1663
[38] J. Kasparkova, M. Vojtiskova, G. Natile and V. Brabec, *Chem.-Eur. J.*, 2008, **14**, 1330
[39] A. de Gramont, J. Cassidy, *et al*., *J. Clin. Oncol*., 2000, **18**, 2938
[40] M. Frezza, S. Hindo, D. Chen, A. Davenport, S. Schmitt, D. Tomco, Q. Ping Dou, *Curr Pharm Des*. 2010, **16** (16), 1813
[41] E. M. Alberto, M. F. A. Lucas, M. Pavelka, N. Russo, *J. Phys. Chem. B*, 2009, **113**, 14473
[42] K. Mross, F. Meyberg, H. H. Fieberg, K. Hamm, U. Hieber, P. Aulenbacher, D. K. Hossfeld, *Onkologie*, 1992, **15**, 139

[43] J. A. Gietema, H. J. Guchelaar, E. G. E. de Vries, P. Alenbacher, D. Th. Seifer and N. H. Mulder, *Anti-Cancer Drugs*, 1993, **4**, 51
[44] A. I. Limited, *Drugs R&D*, 2003, **4**, 369
[45] D.-K. Kim, G. Kim, J. Gam, Y.-B. Cho, H.-T. Kim, J.-H. Tai, K. H. Kim, W.-S. Hong, J.-G. Park, *J. Med. Chem.*, 1994, **37**, 1471
[46] D.-K. Kim, H.-T. Kim, J.-H. Tai, Y.-B. Cho, T.-S. Kim, K. H. Kim, J.-G. Park, W.-S. Hong, *Cancer Chemother. Pharmacol.*, 1995, **37**, 1
[47] D.-K. Kim, H.-T. Kim, Y.-B. Cho, J.-H. Tai, J. S. Ahn, T.-S. Kim, K. H. Kim, *Cancer Chemother. Pharmacol.*, 1995, **35**, 441
[48] J.-W. Lee, J.-K. Park, S.-H. Lee, S.-Y. Kim, Y.-B. Cho, H.-J. Kuh, *Anti-Cancer Drugs*, 2006, **17**, 377
[49] N. K. Kim, T.-S. Kim, S.-G. Shin, Y. L. Park, J. A. Lee, Y.-B. Cho, K. H. Kim, D. S. Heo, Y.-J. Bang, *Cancer*, 2001, **91**, 1549
[50] T. C. Johnstone, K. Suntharalingam, S. J. Lippard, *Chem. Rev.*, 2016, **116**, 3436
[51] G. R. Gale, C. R. Morris, L. M. Atkins, A. B. Smith, *Cancer Res.*, 1973, **33**, 813
[52] S. P. Binks, M. Dobrota, *Biochem. Pharmacol*, 1990, **40**, 1329
[53] R. A. Hromas, J. A. North, C. P. Burns, *Cancer Lett.*, 1987, **36**, 197
[54] S. C. Mann, P. A. Andrews, S. B. Howell, *Cancer Chemother. Pharmacol*, 1990, **25**, 236
[55] J. E. Byfield, P. M. Calabro-Jones, *Nature*, 1981, **294**, 281
[56] D. P. Gately, S. B. Howell, *Br. J. Cancer* 1993, **67**, 1171
[57] J. M. Dornish, E. O. Petterson, R. Oftebro, J. E. Melvik, *Eur. J. Clin. Oncol*., 1984, **20**, 1287
[58] J. M. Dornish, E. O. Petterson *Cancer Letters*, 1985, **29**, 235
[59] J. M. Dornish, E. O. Pettersen, R. Oftebro, *Br. J. Cancer*, 1987, **56**, 273
[60] J. W. Reishus, D. S. Martin Jr., *J. Am. Chem. Soc.* 1961, **83**, 2457
[61] U. Frey, J. D. Ranford, P. J. Sadler, *Inorg. Chem*. 1993, **32**, 1333
[62] A. Junker, R. Farinotti, *Ann*. *Pharmacother*., 2009, **43**, 390
[63] D. P. Bancroft, C. A. Lepre, S. J. Lippard, *J. Am. Chem. Soc.* 1990, **112**, 6860
[64] A. M. J. Fichtinger-Schepman *et al*., *Biochem*., 1995, **34**, 8474
[65] J. M. Woynarowski, W. G. Chapman, C. Napier, M. C. Herzig, P. Juniewicz, *Mol Pharmacol.* 1998, **54** (5), 770
[66] R. C. Todd, S. J. Lippard, *Metallomics*, 2009, **1**, 280
[67] D. Wang, S. J. Lippard, *Nat. Rev. Drug Dis.*, 2005, **4**, 307
[68] M. A. Barry, C. A. Benhke, A. Eastman, *Biochem. Pharmacol*. 1990, **40**, 2353
[69] M. Matsumoto, T. Tsuchida, K. Kawamoto, *Int. J. Oncol*. 1997, **11**, 1209
[70] C. Navarro-Ranninger *et al*., *ChemBioChem*. 2002, **3**, 101
[71] S. Page, Simon (2012). *Educ. Chem*. 2012, **49**, 26
[72] J. Reedijk, *Platinum Metals Review*, 2008, **52** (1), 2
[73] http://www.rsc.org/Education/EiC/issues/2012January/ruthenium-compounds-anticancer-agents.asp (Accessed 20/08/2016)
[74] R. Margalit, H. B. Gray, M. J. Clarke, and L. Podbielski, *Chem.-Bio. Interact.*, 1986, **59** (3), 231
[75] A. Bergamo, G. Sava, Dalton Transactions. 2011, **40** (31), 7817
[76] D. Frasca, J. Ciampa, J. Emerson, R. S. Umans, M. J. Clarke, *Met.-Based Drugs*, 1996, **3**, 197
[77] E. S. Antonarakis, A. Emadi, *Cancer Chemo. Pharmacol.*, 2010, **66** (1), 1
[78] P. C. A. Bruijnincx, P. J. Sadler, *Adv. Inorg. Chem*., 2009, **61**, 1
[79] M.J. Clarke, F. Zhu, D. Frasca, *Chem. Rev.* 1999, **99**, 2511
[80] A.D. Kelman, M.J. Clarke, S.D. Edmonds, H.J. Peresie, *J. Clin.Hematol. Oncol.* 1977, **7,** 274
[81] M. J. Clarke, B.K. Keppler, *Metal Complexes in Cancer Chemotherapy*, Weinheim, 1993, 129
[82] P Schluga *et al., Dalton Trans.*, 2006, 1796
[83] D. Frasca, J. Ciampa, J. Emerson, R. S. Umans, M. Clarke, *J. Met.-based Drugs* 1996, **3**, 197
[84] C. Walling. *Acc. Chem. Res*. 1975, **8** (4), 125
[85] A. Bergamo, C. Gaiddon, J. H. M. Schellens, J. H. Beijnen, G. Sava, *J. Inorg. Biochem*. 2012, **106** (1), 90
[86] G. Sava, E. Alessio, A. Bergano, G. Mestroni, *Topics in Biological Inorganic Chemistry: Metallopharmaceuticals*, 1999, **1,** 143

[87] G. Sava, T. Giraldi, G. Mestroni, G. Zassinovich, *Chemico-Biological Interactions*. 1983, **45** (1): 1
[88] Clarke, M.J., Zhu, F., Frasca, D.R., *Chem. Rev*. 1999, **99**, 2511
[89] V. Brabec, O. Novakova, *Drug Resistance Updates*, 2006, **9**, 111
[90] F. Loseto, *et al*., *Anticancer Res.* 1991, **11**, 1549
[91] M. Brindell, E. Kulis, S. K. C. Elmroth, K. Urbanska, G. Stochel, *J. Med. Chem*. 2005, **48**, 7298
[92] K. Szaciłowski, W. Macyk, A. Drzewiecka-Matuszek, M. Brindell, G. Stochel, *Chem. Rev*. 2005, **105**, 2647
[93] B. K. Keppler, *Metal Complexes in Cancer Chemotherapy*. VCH Verlagsgesellschaft, 1993, 436
[94] M. J. Clarke, F. Zhu, D. R. Frasca, *Chem. Rev*. 1999, **99**, 2511
[95] B. K. Keppler *et al*., *Chem. Biodivers.*, 2008, **5** (10), 2140
[96] N. Cetinbas, M. I. Webb, J. A. Dubland, C. J. Walsby, *J Biol Inorg Chem*, 2010, **15**, 131
[97] J. Amin, M. Buratovich, *Mini-Rev. in Med. Chem.*, 2009, **9** (13), 1489
[98] M. J. Clarke, *Coord. Chem. Rev.*, 2003, **236**, 209
[99] G. Sava, *et al.*, *Eur. J. of Cancer*, 2002, **38**, 427
[100] O. Novakova, P. J. Sadler, V. Brabec *et. al, Chem. Biol.* 2005, **12**, 121
[101] R. E. Aird, J. Cummings, A. A. Ritchie, M. Muir, R. E. Morris, H. Chen, P. J. Sadler, D. I. Jodrell, *Br. J. Cancer*, 2002, **86**, 1652
[102] O. Novakova, H. Chen, O. Vrana, A. Rodger, P. J. Sadler, V. Brabec, *Biochemistry*, 2003, **42**, 11544
[103] O. Novakova, J. Kasparkova, V. Bursova, C. Hofr, M. Vojtiskova, H. Chen, P. J. Sadler and V. Brabec, *Chem. Biol.*, 2005, **12**, 121
[104] A. Bergamo and G. Sava, *Dalton Trans*., 2007, 1267
[105] A. M. Pizarro, P. J. Sadler, *Biochem.* 2009, **91,** 1198
[106] A. Bergamo, A. Masi, P.J. Dyson, G. Sava, *Intl. J. Onc.*, 2008, **33**, 1281
[107] A. Bergamo et al. *J. Inorg. Biochem.* 2012, **106**, 90
[108] P. J. Dyson, C. A. Davey *et al*., *Nat. Commun.*, 2014, **5**, 3462
[109] J. K. Barton, *Science*, 1986, **233**, 727
[110] N. Grover, T. W. Welch, T. A. Fairley, M. Cory, H. H. Thorp, *Inorg. Chem.* 1994, **33**, 3544
[111] G. A. Neyhart, C. C. Cheng, H. H. Thorp, *J. Am. Chem. Soc.* 1995, **117**, 1463
[112] O. Novakova, V. Brabec, et al., *Biochem.*, 1995, **34**, 12369
[113] P. M. van Vliet, O. Novakova, V. Brabec, et al., *Inorg. Chim. Acta* 1995, **231**, 57
[114] A. C. G. Hotze, E. P. L. van der Geer, H. Kooijman, A. L. Spek, J. G. Haasnoot, J. Reedijk, *Eur. J. Inorg. Chem.*, 2005, 2648
[115] N. Farrell, *Metal Ions in Biological Systems*, Marcel Dekker, Inc., New York, Basel, 2004, **42**, 251
[116] A. Bergamo, G. Stocco, B. Gava, M. Cocchietto, E. Alessio, B. Serli, *et al*., *J. Pharmacol. Exp. Ther*. 2003, **305**, 725
[117] V. Brabec, J. Kasparkova, *Metal Compounds in Cancer Chemotherapy*. 2005, 187
[118] L. Ma, R. Ma, Z. Wang, S.-M. Yiua, G. Zhu, *Chem. Commun.*, 2016, **52**, 10735
[119] R. Breslow, N. P. Pavletich *et al.*, *Nature*, 1999, **401**, 188
[120] C. Monneret, *Eur. J. Med. Chem.* 2005, **40**, 1
[121] S. Minucci and P. G. Pelicci, *Nat. Rev. Cancer*, 2006, **6**, 47
[122] T. Vanhaecke, P. Papeleu, G. Elaut, V. Rogiers, *Curr Med Chem*. 2005, **11** (12), 1629
[123] R. Furumai, S. Horinouchi *et al.*, *Cancer Research*, 2002, **62**, 4916
[124] J.-W. Han, H.-W. Lee *et al.*, *Cancer Research*, 2000, **60**, 6068
[125] J. R. Davie, *J. Nutr*. 2003, **133** (7), 2485S
[126] R. Breslow, P. A. Marks et al., *Proc. Natl. Acad. Sci*. 2013, **110** (39), 15704
[127] A. Y. Jeng *et al*., *I. Bioorg. Med. Chem. Lett.* 1998, **8**, 897
[128] P. W. Finn, M. Bandara, C. Butcher, A. Finn, R. Hollinshead, N. Khan, N. Law, S. Murthy, R. Romero, C. Watkins, *Helv. Chim. Act*., 2005, **88**, 1630
[129] S. J. Haggarty, K. M. Koeller, J. C. Wong, C. M. Grozinger, and S. L. Schreiber, *PNAS*, 2003, **100** (8), 4389
[130] P. A. Marks, W. S. Xu, *Journal of Cellular Biochemistry*. 2009, **107** (4), 600
[131] B. S. Mann, J. R. Johnson, M. H. Cohen, R. Justice, R. Pazdur, *Oncologist*, 2007, **12** (10), 1247
[132] V. M. Richon *et al*., *Proc. Natl. Acad. Sci. USA*, 1998, **95**, 3003
[133] D. Griffith, M. P. Morgan, C. J. Marmion, *Chem. Commun*., 2009, **44**, 6735
[134] M. Librizzi, A. Longo, R. Chiarelli, J. Amin, J. Spencer, C. Luparello, *Chem. Res. Toxicol.* 2012, **11**, 2608

[135] J. Spencer, J. Amin, T. D. Heightman *et al*., *ACS Med. Chem. Lett.*, 2011, **2** (5), 358
[136] A. Leonidova, C. Mari, C. Aebersold, and G. Gasser, *Organomet.*, 2016, **35**, 851
[137] D. Can, B. Spingler, R. Alberto *et al*., *Angew. Chem., Int. Ed.*, 2012, **51**, 3354
[138] K. Wähler, A. Ludewig, P. Szabo, K. Harms and E. Meggers, *Eur. J. Inorg. Chem.*, 2014, **5**, 807
[139] A. Leonidova, G. Gasser *et al.*, *Chem. Sci.*, 2014, **5**, 4044
[140] A. Leonidova and G. Gasser, *ACS Chem. Biol.*, 2014, **9**, 2180
[141] R. -R. Ye , C. -P. Tan, Y. -N. Lin, L. -N. Ji and Z. -W. Mao, *Chem. Commun.*, 2015, **51**, 8353
[142] R. -R. Ye, Z. -F. Ke, C. -P. Tan, L. He, L. -N. Ji, and Z. -W. Mao *Chem. Eur. J.* 2013, **19**, 10160
[143] J. W. Walton, J. M. J. Williams. *Chem. Commun.*, 2015, **51**, 2786
[144] T. Mukhopadhyay, D. Seebach, *Helv. Chim. Acta*, 1982, **65** (39), 385
[145] K. H. Büchel *et al*., *Houben-Weyl Methods of Organic Chemistry*, 1995, Vol. E 21d, 4th Ed., 4340
[146] B. M. Trost, C. M. Older, *Organomet.* 2002, *21*, 2544
[147] T. Mosmann, *J. Immun. Methods*. 1983, **65** (1–2), 55
[148] J. M. Cross, J. W. Walton *et al.*, *Dalton Trans*., 2016, **45**, 12807
[149] J. R. Somoza, *et* al., *Protein Data Bank*, 2004, **Structure 12**, 1325
[150] D. Khramov, *et* al., *Organomet.*, 2007, **26** (24), 6042
[151] D. B. Amabilino, P. R. Ashton, A. S. Reder; N. Spencer, J. F. Stoddart, *Angew. Chem. Int. Ed. Engl*, 1994, **33** (12), 1286
[152] H. Yan, G. Süss-Fink, A. Neels and H. Stoeckli-Evans, *J. Chem. Soc., Dalton Trans.*, 1997, **22,** 4345
[153] http://webbook.nist.gov/cgi/cbook.cgi?ID=B6007233&Mask=80 (Accessed 22/09/2016)
[154] T. P. Wells, J. P. Hallett, C. K. Williams, T. Welton, *J. Org. Chem.*, 2008, **73** (14) 5585
[155] A. J. Arduengo; H. V. R. Dias; R. L. Harlow, M. Kline, *J. Am. Chem. Soc.* 1992, **114** (14), 5530
[156] W. A. Herrmann; C. Kocher; L. J. Goossen, G. R. J. Artus, *Chem. Eur. J.* 1996, **2** (12), 1627
[157] O. Kühl, in *Functionalised N-Heterocyclic Carbene Complexes*, 1st edn. John Wiley & Sons Ltd, London, 2010, vol. 1 ch. 1, pp. 12
[158] W. Kirmse, *Angew. Chem. Int. Ed.*, 2010, **49** (47), 8798
[159] R. Alder, M. Blake, L. Chaker, J. Harvey, F. Paolini, J. Schutz, *Angew. Chem. Int. Ed*. 2004, **43**, 5896
[160] C. Isanbor, D. O'Hagan, *J. Fluorine Chem.*, 2006, **127**, 303
[161] F. J. Dekker, M. Ghizzoni, N. van der Meer, R. Wisastra, H. Haisma, *J. Bioorganic and Medicinal Chemistry*, 2009 , **17** (2), 460 - 466
[162] Yuehua C., Huiyong W., Yuanchao P., Jiao R., and Jianji W., *ACS Sustainable Chem. Eng.*, 2015, **3** (12), 3167